Εθνικό Μετσόβιο Πολυτεχνείο
Σχολή Πολιτικών Μηχανικών
Τομέας Γεωτεχνικής

National Technical University of Athens
School of Civil Engineering
Geotechnical Division

Διπλωματική Εργασία

Παπακωνσταντίνου Αρετής

Επιβλέποντες

Καθηγητής Γ. Γκαζέτας

Δρ. Ε. Γαρίνη

ΣΤΑΤΙΚΗ ΚΑΙ ΔΥΝΑΜΙΚΗ ΕΥΣΤΑΘΕΙΑ ΤΟΥ ΠΥΡΓΟΥ ΤΗΣ ΠΙΖΑΣ

STATIC AND DYNAMIC STABILITY OF THE LEANING TOWER OF PISA

Diploma Thesis by

Papakonstantinou Areti

Supervised by

Professor G. Gazetas

Dr. E. Garini

Αθήνα, Αύγουστος 2014

Athens, August 2014

ΠΕΡΙΛΗΨΗ

Στην παρούσα διπλωματική εργασία μελετάται με αριθμητική προσομοίωση πεπερασμένων στοιχείων η ευστάθεια του Πύργου της Πίζας στην Ιταλία, η οποία έχει αποτελέσει μία πρόκληση για την επιστήμη του μηχανικού. Ο Πύργος εδράζεται πάνω σε αδύναμο και αρκετά συμπιεστό έδαφος και η κλίση του αυξάνεται διαρκώς με τα χρόνια μέχρι τη σημερινή του κατάσταση. Η ιστορία της κατασκευής του και της εξέλιξης της κλίσης του είναι σημαντικά για την κατανόηση αυτού του φαινομένου.

Για να προσομοιωθεί η πραγματική κατάσταση του Πύργου χρησιμοποιούνται οι πραγματικές ιδιότητες του εδάφους και της ανωδομής, όπως έχουν προκύψει από επί τόπου μετρήσεις στην ευρύτερη περιοχή του Πύργου της Πίζας, καθώς και στον Πύργο. Χρησιμοποιείται ο κώδικας πεπερασμένων στοιχείων του Abaqus και εφαρμόζονται στατικές και δυναμικές φορτίσεις. Στην παρούσα διπλωματική ερμηνεύεται η σημερινή κατάσταση του Πύργου, όσον αφορά τους μηχανισμούς αστοχίας του εδάφους, καθώς και την επιρροή της ανωδομής. Πιο συγκεκριμένα, γίνεται κατανοητή η επίδραση της αστάθειας λόγω της κλίσης του Πύργου, η οποία όσο αυξάνεται αυξάνει την ροπή ανατροπής που επιβάλλεται στο θεμέλιο (φαινόμενα P - δ). Επιπλέον, χρησιμοποιούνται ποικίλοι καταστατικοί νόμοι για το έδαφος, ώστε να γίνει δυνατή η σωστή προσομοίωση της πραγματικής κατάστασης του εδάφους. Τα αποτελέσματα παρουσιάζονται με τη μορφή καθιζήσεων, στροφής καθώς και τάσεων κάτω από το θεμέλιο, ώστε να ερμηνευτεί η στατική ευστάθεια του Πύργου της Πίζας.

Διερευνάται επιπλέον η σεισμική απόκριση του Πύργου μέσω ρεαλιστικών διεγέρσεων για την ευρύτερη περιοχή, καθώς και με τη χρήση παλμών. Παρατηρείται πως η συμπεριφορά της ανωδομής είναι αποδεκτή, καθώς η επιτάχυνση που φτάνει σε αυτή είναι αρκετά μειωμένη. Αυτό συμβαίνει διότι ο Πύργος είναι υψίκορμος με μεγάλη ιδιοπερίοδο. Ωστόσο, η κλίση του καθώς και η καθιζήσεις αυξάνονται. Τέλος, γίνεται σύγκριση μεταξύ των αναλύσεων 2D και 3D.

ABSTRACT

In this diploma thesis we analyze the stability of the Leaning Tower of Pisa in Italy, which has been a very difficult challenge for geotechnical engineering. The system is modeled with numerical finite elements. The Tower is founded on weak, highly compressible soil and its inclination has been increasing inexorably over the years to the point at which is standing today. The history of its construction and its inclination are significant for the understanding of this phenomenon.

The real state of the Tower nowadays is achieved using the characteristics of the soil and the superstructure as they have measured from the in situ tests in the vicinity of the Tower of Pisa and the Tower as well. The finite element code of Abaqus is used and static and dynamic loading are applied. In the present diploma thesis the current condition of the Tower is interpreted, concerning the bearing – capacity failure mechanisms in the soil and the effect of the superstructure in this phenomenon. To be more specific, the detrimental effect of the leaning instability of the superstructure to increase the overturning moment on the footing as the inclination rises (phenomena P – δ) is also accounted for. Furthermore, various constitutive models are used, in order to achieve the accurate simulation of the behavior of the soil underneath the Tower of Pisa. The results are presented mainly in the form of displacements, rotation and stresses under the footing, so that the static stability of the Tower will be able to become understood.

The seismic performance of the Tower is also explored through realistic excitations for the surrounding vicinity and trough pulses, as well. It is observed that the behavior of the superstructure is acceptable, since the acceleration transmitted to the superstructure is reduced. That is because the Tower is slender with big natural period. However, its inclination and the displacements increase. Finally, comparison between 2D and 3D analyses are made.

Chapter 1

The Tower of Pisa

Historical information

The Tower of Pisa is founded on weak highly compressible soil.
Tower began to build up in 1173. Construction continued until 1178 (3 storeys) when the work stopped for an unknown reason. This interruption saved the Tower from an undrained bearing capacity failure. The work started again in 1272. By this time the strength of the Tower had increased due to a consolidation under the weight of the structure. Once again the work stopped in 1278. As before if it did not have stopped the Tower would have fallen down. In about 1360 the work in the chamber began and completed in 1370.
Another measure that led the Tower to incline more was the catino. In 1838 a walkway was excavated around the foundation in order to expose the column plinths and foundation steps, so that everyone could see them. As a result an inflow of water on the south side was occurred, since the excavation was under the water table.
The internationally accepted conventions for the conservation and preservation pf valuable historic buildings, such as the Pisa Tower since it is one of the best known and most treasured historic buildings, require that their essential character should be preserved.
In 1990, a multidisciplinary body was founded with experts in art, restoration and materials, structural engineers and geotechnical engineers as members. They adopted a controlled removal of small volumes of soil from beneath the north side of the Tower foundation. With this excavation they managed to increase the stability of the Tower softly.

Some characteristics

The foundation is 19,6 m in diameter, the weight is 141,8 MN. The foundation was inclines southwards at about $5{,}5^{0.}$
The form of the construction is a hollow cylinder.
The inner and the outer surfaces are faced with marble and the annulus between these facings with rubble and mortar.

Inclination

The materials to the south of the Tower appear to be more silty and clayey than to the north, and the sand layer is locally thinner (horizon A). This is believed to be the origin of the southward inclination of the Tower.
During the first phase of construction the Tower inclined slightly to the north. The northward lean increased slowly to approximately $0,2^{0}$ during the rest period of 100 years. When construction began again in 1272 after its first interruption the Tower started to move southwards and in 1278 inclination reached at $0,6^{0}$. During the next 90 years the tilt rose to about $1,6^{0}$. After the completion of the chamber the inclination peaked at approximately $4,9^{0}$ .Due to the catino the inclination reached at $5,5^{0}$.

The ground profile
It consists of three distinct horizons.
Horizon A is about 10 m thick and consists of estuarine deposits. At the bottom of horizon A there is a 2 m thick medium dense fine san layer.
Horizon B it consists of marine clay to a depth of 40 m. This is subdivided into 4 (distinct) layers. The upper is a soft sensitive clay (locally known as the Pancone). The next intermediate layer is a stiffer clay. This layer is underlain by a sand layer. The bottom layer is a normally consolidated clay known as the lower clay.
Horizon C is a dense sand which extends to a considerable depth.
Water Table is found in Horizon A between 1 m and 2 m below the ground surface.

Borings
They showed that the surface of Pancone (the upper layer of horizon B) is dished beneath the Tower from which is deduced that the average settlement of the Tower is approximately 3 m.

Leaning Instability
A phenomenon controlled by the stiffness of the soil rather than by its strength.
Edmunds (1993) performed a number of small scale physical tests on a model of Tower resting on a bed of fine sand, in order to understand the effect of underexcavation on a Tower close to collapse for leaning instability.
The model Tower had a diameter of 102 mm and was placed on the top of a very loose sand fine sand bed. It was loaded through a hanger at a height of 126 mm over the base. The ratio 126/102 is approximately equal to the ratio of the height of the centre gravity of the Tower of Pisa to the diameter of its foundation.
The results of the loading was in all cases a settlement w and a rotation α.
Failure occurred by toppling with the lowest edge of the model tower's base sinking into the sand as the Tower rotated.
Later *Potts and Burland* (2000) studied the same problem using Finite Element Analysis. They investigated the differences between the leaning instability and the usual bearing capacity failure.

The model clay was a linear elastic-perfectly plastic Tresca material with undrained shear strength s_u=80 kPa. It is a plain strain problem.
The results showed that the failure occurred abruptly with little warning and that the weight of the Tower at failure is dependent on the shear stiffness of soil.
For the soft soil the mechanism o failure is leaning instability, whereas for stiffer soil is a plastic bearing capacity type mechanism of failure.

Models

1) Simple Linear Models

M_s=stabilizing moment
M_0=overturning moment
α=rotation
The model which could be used for a simple linear Analyses is an inverted pendulum. Soil could be represented as a bed of Winkler type springs or as an elastic half space. The results of this Analyses were that Tower is very close to a state of neutral equilibrium. This state is possible only if the system is a linear one.

2) Non-Linearity

The relationship between Ms and α is certainly non-linear after a certain point and approaches a limiting value of Ms asymptotically.
Centrifuge modeling of the Tower and its subsoil was carried out at ISMES. The results of this modeling discussed by Pepe (1995) and confirmed the elastoplastic character of the restraint exerted by the foundation and the subsoil on the motion of the Tower. Both the rotation and the settlement resulted from this model scaled to the prototype and were in good overall agreement with those of the Tower.
Finite element analysis of the behaviour of the Tower and its subsoil was carried out using a finite element geotechnical computer program developed at Imperial College known as ICFEP (Potts and Gens, 1984). A plain strain approach was used for much of the work and only later was three dimensional analysis used to explore certain detailed features.
The results showed again that any further increase in the final inclination of the tower model would result instability, which proves that the Tower is very close to falling over. Another result was that the cause for the lean of the Tower is the phenomenon of settlement instability due to the high compressibility of the Pancone Clay. The direction of the lean is determined due to the principal effect of the layer of slightly increased compressibility beneath the south side of the foundation rather than its magnitude.

Stabilising measures

If an elasto-plastic model is assumed for the Tower then the relation between load and displacement has to be written in incremental form (*Desideri et al.,* 1997)

The increment in displacement depends on the load increment, the current state of load and the load history. As a result the factor of safety FS depends on the current state of stress and stress history and decreases with increasing inclination.
The centrifuge experiments by *Cherny et al.* (1991) showed that a decrease of inclination leads to increase of the stiffness of the foundation-ground system. This generated the idea that a decrease in inclination increases M_s and FS and can be used to stabilise the Tower
Consequently, the Committee took a temporary safety measure to prevent overturning of the Tower. The northern side of the Tower foundation had been steadily rising for most of the 20th century, so the Committee thought to apply a counterweight on the north side as a temporary measure. A prestressed concrete ring cast was implemented around the base of the Tower for supporting a number of lead ingots. This intervention had resulted a northward inclination of 48'' by the end of July in1994. The factory of safety FS was increased to 59 through this measure.

Underexcavation
There were different possible options for the decrease of inclination of the Tower. The Committee explored them and the underexcavation solution finally selected.
A stainless steel tube with an outer diameter of 6 mm inserted to the soil in order to remove it. The inner tube with an outer diameter of 2,1 mm removes the sand from inside the larger tube without significant disturbance of the surrounding soil.
The conclusions from these underexcavations tests were: Firstly, underexcavation can be used in order to reduce the tilt of the model in a way which can be controlled. Secondly, the movement of the Tower can be controlled by using different probes inserted around the Tower. Thirdly, there is a critical point which exists some 5 m north of the central axis of the model tower, in the ground beneath it, beyond which ground removal aggravates the tilt, but behind which underexcavation produces a decrease in tilt. Finally, if one probe is used repeatedly then it ceases to affect the Tower's tilt significantly.
The finite element model confirms that excavation south of a critical line aggravates the tilt.
When the excavation is in progress, then the rate of change of northward inclination increases, as do the settlements, whereas when the drill is retracted then the rate decreases. Moreover the stress distribution after retraction of the drill is smoother than after insertion.
A trial took place in the Piazza north of the Baptistry with a 7 m diameter eccentrically loaded circular reinforced concrete. This trial was successful and after its completion the cavity formed in horizon A was found to close smoothly and rapidly. Besides, the plinth came to rest and since then it has exhibited negligible further movements. This trial, also confirmed the concept of a critical line.

Preliminary Underexcavation of the Tower
The Commission after the results of the above investigations decided to implement preliminary ground extraction beneath the Tower itself, since the Commission knew that those investigations were not completely representive of the possible response of the Tower affected by leaning instability. With this preliminary ground extraction they wanted to decrease the inclination of the Tower by a small amount , but

enough to confirm that the feasibility of underexcavation as a means of stabilizing the Tower permanently, and to adjust the extraction and measurement techniques. This underexcavation was followed by some measurements so that the Tower should be protected from any unexpected adverse movement. This was achieved with a safeguard structure. The structure consisted of two sub-horizontal steel stays connected to the Tower at the level of the third order and to two anchoring steel frames located behind the building of the Opera Primaziale, to the north of the Tower. Each stay was capable of applying a maximum force of 1500 kN, with a safety factor equal to 2. This underexcavation was carried out between February and June, 1999.
The results were that during the underexcavation period the Tower rotated northwards at an increasing rate, as the extraction holes gradually approached the north boundary of the foundation and penetrated below. Furthermore, after the removal of three of the 97 lead ingots acting on the north side of the Tower, the Tower exhibited negligible further movements. Also, the rotation in the west-east plane was much smaller.

Final Underexcavation
The final under excavation was carried out between February 2000 and February 2001. This time 41 hole were drilled (in comparison to the 12 holes in preliminary underexcavation). The tilt of the Tower decreased by half a degree.

Drainage
The level of the water in horizon A is rapidly and markedly variable, under the direct influence of rainfall. It has been repeatedly observed that peaks of the water level corresponding to intense rainfall events produce small and almost instantaneous southward rotation of the Tower. In order to eliminate or minimize this process (the effects of the fluctuations of the water table) a drainage system connected to the gravel layer was implemented below the bottom of the catino. As a result the tilt was slightly reduced.

Attention to the Tower of Pisa
The sudden and unexpected collapse of the Civic Tower in Pavia in 1989 drew attention to the Leaning Tower of Pisa. The risk of collapse due to brittle failure of the masonry, as in Pavia, was discovered. With the increase of the inclination, the safety against foundation failure progressively decreased, and at the same time the stress in the masonry increased with an increasing risk of structural collapse.
Two scenarios for the future
The first, rather conservative one predicts that the Tower will remain motionless for some decades and then gradually resume a southward rotation, first at a very

reduced way and then progressively accelerating. In this scenario the Tower would reach the value of the 1999 inclination in a time span of at least three centuries.
In a more optimistic scenario, the rotation will cease, apart from small cyclic movements caused by seasonal changes in the water table and by the influence of the generalized subsidence of the whole Pisa plane, which affects the ''Piazza'' and the Tower.

The Leaning Tower

Construction

It was founded in August 1173. Its structure is made up of two parts, the foundations and the elevation. In the middle there is a marble catino which was designed in 1830. The elevation is *externally* divided into eight levels (the base, six ringed galleries and the bell chamber) and *internally* formed of two tubular walls which enclose the long, winding staircase that leads to the ringed galleries or loggia. The monument also has two shorter winding staircases, leading to the bell chamber and the terrace and six bronze bells. Each of the eight orders is adorned by columns (15 for the base, 30 for the loggias and 12 for the belfry), plinths and capitals.

Materials

San Giuliano marble

Filettole dark-grey limestone was used to form the dark band of the façade.

Apuanian marble. A grey variety was used to substitute the Filettole dark-grey limestone, and various architectural elements of the loggias (columns, bases, corbels). It, also, substituted the San Giuliano marble in different periods, since varieties are more homogenous in colour and texture.

Agnano and Caprona breccias were used in the internal and external facing walls of the cylinder body and in the internal staircase.

''Panchina'' calcarenite was found in the internal staircase walls and in some parts of the plastered-over vaults of the loggias.

Other stones were recognised on the Tower, but their frequency and structural significance are less important.

The ''infill'' material of the cylinder structure and foundations is composed of fragments of the same lithotypes that make up the facing walls, and gravel and sand, all of which have been cemented with lime-mortar. The volume ratio of mortar/rubble elements is roughly uniform throughout the masonry body: the mortar content is about 1/3 by volume.

Foundation materials

A coarse sand was used in the foundations, while finer sands were employed in the preparation of mortars for the upper parts of the masonry. The binder mainly consists of fine-grained calcite of a dishomogenous texture.

Origin and development of the inclination

Clue for the tilt

A reliable clue to the history of tilt lies in the adjustments that were made to the masonry layers during construction and in the resulting shape of the axis of the Tower.

Perturbations/Disturbances

The first one was caused by cement grouting in the body of the foundations and the soil surrounding the catino, which was carried out in order to prevent the inflow of the water (the bottom of the catino is well below the groundwater table).
The second was related to the pumping of water from the deep aquifer, which induced subsidence throughout the entire Pisa plain. The closure of a number of wells in the vicinity of the Tower stopped the increase of the rate of tilt.

Structural Aspects

Structure

The Tower is made of solid marble ashlars. The marble ashlars form only thin facings (as in many medieval monuments) that surround a thick infill of poor conglomerate (this is called a three-layer wall). Furthermore, the external facing is weakened by the presence of several large recesses that had been left during the works. Time is working against the stability of the ancient masonry with a mechanism of continuous reduction of its strength.

Critical zone

A ''critical zone'' was identified at the first loggia (the helicoidal stairs and the door that opens onto the loggia considerably reduce the resisting cross-section). A further dangerous point is that where the external marble facing is interrupted at the level of the loggia and presses onto the scarce quality of the conglomerate underneath. After a careful structural survey a number of cracks and damaged zones were reviled. Those are the signs of local compression and of lower strength. Tensile radial stresses were found on the ceiling of the helicoidal stairs and these could explain the existing cracks.

Dynamic characteristics

The effects of wind and earthquakes on the Tower are rather uncertain.
The effects of earthquakes: The region o Pisa is situated among three seismogenetic zones. An earthquake could add to a stress situation to the leaning tower of Pisa that is already close to the ultimate limit under the self-weight of the Tower and the effect of the inclination.

RESTORATION ASPECTS

The decay-conservation state of the building materials was investigated by the international committee, in order to realize a project for the restoration of the Tower surfaces.
Percentages of materials
San Giuliano marble (main original building stone) 60%
Filettole dark-grey limestone 3-14%
Agnano and Caprona 3-5%
Aquanian marble used to replace decayed elements 18-31%
A computer system called AKIRA GIS Server ''Leaning Tower'' was developed and enabled the full extent of all the surfaces and their complex geometrical features.

Analysis of the stabilization measures

Ruling out electro-osmosis (as a possible method to decrease the inclination of the Tower)
A full-scale trial proved that this method would be a total failure. Positive excess pore pressures were induced in the subsoil, and temperature increases and gas generation at the electrodes were experienced. These phenomena were evidence that electro-osmosis had to be ruled out as a suitable means of stabilizing the Tower.
The closure of the cavity (underexcavation)
When the drill was withdrawn to form the cavity, an instrumented probe, located in the hollow stem, was left in place to monitor its closure. A cavity that formed in the Horizon A materials was found to close smoothly and rapidly.

Temporary geotechnical stabilization
Discovery of conglomerate
Drilling through the floor of the catino revealed the existence of a 0.8 m thick ancient concrete (conglomerate) layer. A circumferential gap was found all around the foundations and it was concluded that the conglomerate was not connected to the masonry. Work then started to install the post-tensioned concrete ring.
Freezing (was abandoned)
The major problem with the ten-anchor solution was that excavation was necessary, since they should react against a post-tensioned concrete ring around the Tower foundation. In order to perform safely the excavation it was decided to employ local ground freezing below the catino floor. Freezing was commenced in September 1995 on the south-west and south-east sides of the foundations. At the begging no rotation of the Tower was observed, but when freezing stopped for the maintenance phase the Tower began to rotate southward. There was an uncertainty about the strength of the structural connection between the conglomerate and the masonry formed by the steel grout pipes, so freezing was abandoned.

Leaning Instability

Two major, geotehnically related, failure modes of tower foundations:

a) Bearing capacity failure, due to lack of strength of the supporting soil
b) Instability of equilibrium, due to lack of foundation stiffness, aggravated by progressive rotational creep.

Leaning towers are widespread throughout the Italian peninsula. For all of these towers the fundamental bearing capacity problem was self-evidently solved, but initial imperfections and/ or non-uniform system, have led to their long-term critical conditions.
Progressive increase of tilting can, of course, also produce high compressive stresses in the masonry and consequent structure failure (Heyman, 1992; Federico et al., 2001). For example the San Marco bell tower in Venice suddenly collapsed in 1902, due to the presence of weakened and disconnected masonry, even without tilting.

These problems can be considered as a ‘macro-element’ , which cannot only predict the moment (generated by tilting) at which a tower will collapse, but also provide the rotational stiffness of he soil-foundation system.

Instability of equilibrium: Lack of stiffness

The model of the tower for ‘stability of equilibrium’ analyses is usually represented by a uniform rigid bar (weight W), resting on a support at which the deformability of the system is concentrated.

Notation

M_e: external moment (overturning)
M_r: reaction of the restraint (resisting)
H: the height of the centre of gravity of the structure above its base
θ: the total rotation of the tower from the vertical position
θ_0: the unknown initial tilt (due to an initial inclination developed during construction in the example of Pisa)

$M_e=Wh\sin\theta$

M_r: represents the rotational stiffness of the tower and an initial imperfection, such as θ_0 does not generate a resisting moment. However, M_r is a function of the rotation of the tower relative to the initial tilt: that is, $\Delta\theta=\theta-\theta_0$.

An analysis in the V-θ plane, V being the vertical load is convenient when the aim is to show how the critical load is influenced by the initial imperfection.
In Lancellotta’s (1993) Pisa Tower stability analysis, the stiffness of the non-linear elastic rotational spring at the base of the tower did not depend on the applied vertical, and the critical condition could therefore be defined by the V-θ curve peak.
In a more general case, an equilibrium analysis of a tower is best represented in the M-θ plane, in which M_e and M_r can be plotted together, as first suggested by Cheney et al. (1991).

Curves

M_e is a line with slope Wh, and M_r is a curve related to the stiffness of the foundation.

1)Never possible equilibrium ($k\leq Wh$)

If the initial slope of the M_r curve, k, is equal to or lower than the slope (Wh) of the external moment load path M_e then the M_e and M_r paths will never intersect.

2)If $k>Wh$

a)Stable equilibrium

For a small increase in θ, M_r increases faster than M_e.

b)Unstable equilibrium

For a small increase in θ, M_r increases slower than M_e.

c)Critical equilibrium

The maximum value of M_e than can be resisted occurs when the M_e line is tangent to the M_r curve; the coordinates of the tangent point then define the critical condition for instability of equilibrium.

Any initial rotation will include not only the initial imperfection of the system θ_0, but also any additional rotation due to creep, θ_{0creep}.

Creep

The progressive rotational creep deformation (tilting) determines the long-term safety of many towers.

Bjerrum (1967) introduced the attractive assumption that the change in the void ratio developed during creep in confined compression is entirely equivalent to the same point having been arrived at by virgin loading and unloading process.

Rotational creep, unlike vertical creep under constant vertical load, affects the load state of the tower foundation.

The final component of a complete tower displacement prediction model is the rate at which the rotation of a tower (and, ideally, also its vertical displacement) will increase over its lifetime until collapses.

In order to take creep into consideration a rotational creep function was introduced, together with a tertiary creep process under which tilt and the consequent moment load increase rapidly to failure.

Stability analysis of the Pisa Tower

The possibility that bearing capacity will occur first has been excluded, since the long-term footing response of the Pisa Tower is clearly of a continuously hardening type.

General tower properties

Weight: W=142 MN

Diameter of foundation: 2R=19m

Height of the centre of gravity: h=22,6 m

Overall depth of the foundation: d=3m

Depth of the water table below ground level: h_w=3m

The mean soil properties are:

Effective shear stress angle: $\phi' = 26^0$

Saturated soil unit weight: γ_{sat}=20kN/m³

Dry soil unit weight: γ_{dry}=15 kN/m³

A good fit to the M-θ curve, derived by the model output with θ measured in degrees is the next equation:

$M_r = 517{,}5(1-e^{-0{,}55(\theta-\theta 0)}) + 10{,}7(\theta-\theta_0)$

The output of this analysis is not very sensitive to the parameter θ_0.

A *prediction* of the tower's tilt using the next equation:
$\theta(t)=(1+Wh/k_\theta)[\ln(1+t/t_0)-c\ln(1-(t-t_2)/t_1)U(t-t_2)]+\theta_0$
using $\theta_0=0{,}50$, $t_0=5$ years, $c=0{,}08$ and $k_\theta=\infty$
reproduces the historical data rather well.
This prediction also shows that the rate of increase is after 2269 so high that the rotation becomes infinite in 2270. This is a crucially important outcome of tertiary creep process, implying that disaster could strike long before the stability failure are approached.

Pisa Dynamic Microtremor

Introduction
Determining the dynamic characteristics in advance and increasing durability of ground and structures beyond the seismic force is a fundamental for preserving the historical structures. The real danger for the safety of the Pisa is the possibility of earthquakes and there is no detailed study about the dynamic structural behavior of the tower which will be directly related with its damage during the earthquakes. Microtremor is the easiest and cheapest way to understand the structural behaviors without causing any harm to the structure. In a short period of time it provides several information including natural frequency, amplification and vibration characteristics of structures at different frequencies.

Results
Rocking vibration and center of this vibration
There are results for the ratio provided the combined predominant frequency and amplification factor of entre tower together with ground. There are several peaks showing the different modes of the structure in longitudinal and transversal components. First mode frequency is about 0.98 Hz inns and 1.06 Hz for EW direction. This shows the rocking vibration frequency of the tower. One reason of higher frequency in EW direction thought to be the weight of 830 tons of lead that is placed on the south of the tower. However, the only reason seems to be the softer ground characteristics in NS direction. Also, in EW direction amplification is higher than NS direction, this shows that tower has a tendency to move in EW direction, too.
Center of the vibration is located at the south of center line almost under the bottom of foundation in NS direction. The depth is about 1.5 m in EW direction. In NS direction the center of rocking vibration is quite shallow (almost under the bottom of foundation) and generally having a deeper rocking center is better.
Vertical vibration frequency (for entire tower)
A peak at 1 Hz represents rocking vibration. And a peak around 2 Hz appears at each floor shows a vertical vibration frequency for entire tower.

Vertical vibration frequency for entire tower is 3 Hz.
Clear identification of vertical vibration frequency is quite important since it gives an opportunity to calculate spring coefficient K_v that will be helpful to calculate ground bearing capacity. Bearing capacity has been calculated at 1-1.3 kg/m^3 for 2.2 Hz and 2.5 Hz vertical vibration frequencies, respectively for the area that tower is located.

Chapter 2

Free Field Analyses

2.1 Linear Elastic Analyses with SHAKE

The analyses have been carried out using SHAKE2000 (Schnabel, Lysmer & Seed, 1972), which is a program referred to geotechnical engineering. SHAKE carries out an equivalent linear elastic analysis for the accelerogram which takes as an input. In simple terms, the input motion is represented as the sum of a series of sine waves of different amplitudes, frequencies, and phase angles. A relatively simple solution for the response of the soil profile to sine waves of different frequencies (in the form of a transfer function) is used to obtain the response of the soil deposit to each of the input sine waves. The overall response is obtained by summing the individual responses to each of the input sine waves. The analyses, which we have carried out, take into account the next considerations: The excitations are vertically propagating shear waves. This assumption is necessary since SHAKE analyzes problems based on the one dimensional wave propagation analysis. This means that the soil layers are considered as horizontal, extending indefinitely. Furthermore, the excitations take place in the Free Field, which is the soil without the presence of the superstructure.

The nonlinear and inelastic behavior of soil is well established in geotechnical engineering. The nonlinearity of soil stress-strain behavior means that the shear modulus of the soil is constantly changing. The inelasticity means that the soil unloads along a different path than its loading path, thereby dissipating energy at the points of contact between particles. Rigorous analysis of

the mechanical response of soils to any type of loading, dynamic or otherwise, would require that the stress-strain behavior of each element of soil be tracked directly in the time domain. The method of analysis used in SHAKE cannot allow for nonlinear stress-strain behavior because its representation of the input motion by a Fourier series and use of transfer functions for solution of the wave equation rely on the principle of superposition - which is only valid for linear systems.

As a result, SHAKE utilizes an equivalent linear analysis to approximate the actual nonlinear, inelastic response of soil. In this equivalent linear approach, linear analyses are performed with soil properties that are iteratively adjusted to be consistent with an effective level of shear strain induced in the soil. In the equivalent linear approach, the shear modulus is taken as the secant shear modulus which, as shown in figure 2.36, approximates an "average" shear modulus over an entire cycle of loading. As the level of shear strain increases, the secant shear modulus decreases. The relationship between secant shear modulus and shear strain amplitude can be characterized by means of a modulus reduction curve. The nature of this curve, which has an ordinate of modulus ratio (= G/G_{max}) and an abscissa of log (shear strain), has been well established for many soils. The solution algorithm used in SHAKE assumes viscous soil damping which it represents using a complex shear modulus. Viscous damping implies behavior that would be characterized by elliptical stress-strain loops. Because actual stress-strain loops are seldom elliptical, an equivalent damping ratio is used – the equivalent damping ratio is equal to the damping ratio that would be computed based on the area within the hysteresis loop, the secant shear modulus, and the maximum shear strain. The relationship between this equivalent damping ratio and shear strain is characterized by means of a damping curve. The nature of this curve, which has an ordinate of damping ratio and an abscissa of log (shear strain), has been well established for many soils, too. In an equivalent linear analysis, the first iteration is performed using shear modulus and damping ratios that correspond to some initially estimated level of shear strain. While the equivalent linear approach allows the most important effects of nonlinear, inelastic soil behavior to be approximated, it must be emphasized that it remains a linear method of analysis. However, the equivalent linear approach has been shown to provide reasonable estimates of soil response under many conditions of practical importance.

The analyses for the Tower of Pisa carried out using SHAKE have the soil properties (maximum shear modulus G_{max}) plotted in figure 2.37, which are the same with those underneath the Tower of Pisa. Moreover, the curves which are necessary for defining the behaviour of the soil are taken from the libraries of SHAKE (built – in models).To be more specific,we have initially used the Vucetic and Dobry curves for sand (PI = 0) and Clay (PI = 30). Afterwards, we also used the Vucetic and Dobry curves for sand (PI = 15) and Clay (PI = 50) with higher PI due to the measurements underneath the Tower of Pisa for the plasticity index PI (This soil property in relation with the depth z is plotted in figure 2.41). This change affected minimally the final results. The above mentioned curves are plotted in figure 2.38-2.40. [Vucetic and Dobry (1991), building on the work of Kokoshu (1980) in an investigation motivated by the performance of Mexico City clay in the 1985 Michoacan earthquake, showed clearly how modulus and damping behavior are influenced by soil plasticity. Vucetic and Dobry developed families of modulus reduction and damping curves as functions of plasticity index]. These curves are representative for the soil properties underneath the Tower of Pisa. In addition, it is obvious from the curves plotted in figure 2.40 that the greater the PI is, then the behavior of the soil is more elastic in than soil with smaller PI.

We, also, need to mention that the last layer of the soil is above a dense sand. Consequently, in SHAKE we have taken into consideration this boundary with an option (within instead of outcrop) used for this occasion. In other words, the lower boundary takes into account that the layer underneath the last defined layer is not necessarily rock.

The accelerograms which we have used are in short AQP and Shinkobe. The first one is from an aftershock of L'Aquila in 2009 in Italy with M_w = 5.5, while the second is from the earthquake in Kobe, Japan in 1995. Both of these excitations have peak ground acceleration equal to 0.10 g. In the first case (AQP) this is the real peak acceleration, whereas in the second case (Shinkobe) the accelerogram is reduced in order for the peak acceleration to reach this value. In both analyses, the accelerograms are applied at the bottom of the soil. Moreover, we have studied the same accelerograms amplified, so that their peak ground acceleration are threefold, which means equal to 0.30 g.

The results extracted from SHAKE are the following:

1) The accelerograms at the top of the first layer and the accelerogram at a depth equal to 9.5 m. This depth is equal to the radius of the footing of the Tower of Pisa ($z = R_{footing} = 9.5$ m). These accelerograms with the accelerogram applied at the bottom of our soil are plotted for its excitation in figures 2.42-2.45 with their peak ground acceleration marked on them.

2) The above accelerograms lead to the elastic response spectra (damping, $\xi = 5$ %) plotted in figures 2.46-2.48for each excitation. These figures represent the spectra for three different depths according to the accelerograms above (0 - 9.5 – 40 m, top – intermediate depth – bottom repsectively).

3) The amplification function between the top and the bottom elastic response spectra as extracted from SHAKE for each excitation. These data are plotted in figure 2.49.

4) The predominant period of the given subsoil profile. The predominant period is the period corresponding to the maximum value of the Fourier spectrum. In our case,it is equal to 0.64 sec and it is the same for each excitation (does not depend on the excitation, but only on the characteristics of the soil). In our case this period would be difficult to be calculated by hand, since the soil underneath the Tower of Pisa is multi-layered. Thus matrixes are necessary in order to be calculated analytically.

5) The distribution of peak shear stress and strain with depth for each excitation. Figures 2.51 represent these data.

The above mentioned figures refer to the curves Vucetic and Dobry for sand (PI = 0) and Clay (PI = 30). However, a calibration was made by using different values for PI (for sand (PI =15) and Clay (PI = 50)), so different curves. This choice was taken in order to lend more validity to the results of SHAKE for the subsoil underneath the Tower of Pisa. The comparison of the above results is shown in figures 2.52-2.55 for the excitation of AQP with peak acceleration equal to 0.10 g. Besides these results, the elastic response spectra for this excitation for the top of the first layer (UP) extracted by a non-linear inelastic method using Abaqus and Seismosignal (as the previous procedure in 2.1) is plotted in figure 2.53, so that a full comparison can be made

between these two different approaches of the same problem. To be more specific, the red line represents the result of the non-linear inelastic method (Abaqus), the green line shows the results taken by SHAKE for the initial used curves (Vucetic and Dobry for sand (PI = 0) and Clay (PI = 30) - Shake Initial) and the blue line shows the respevtive results for the calibration curves (Vucetic and Dobry for sand (PI = 15) and Clay (PI = 50) - Shake Calibration). Finally, the above mentioned results for AQP (peak aground acceleration equal to 0.10 g for the new curves are plotted in figures 2.52-2.55.

Conclusions for SHAKE

- It can be concluded that SHAKE gives use a good insight for the behavior of the subsoil of the Tower of Pisa. However, these results need further investigation, due to the fact that the analysis is linear – elastic, while the soil behaves nonlinear – inelastic. Consequently, a non-linear inelastic analysis is necessary. This analysis has been made using the finite element code Abaqus.
- In our comparison between these two analyses we deduce that the non-linear inelastic analysis gives increased values of the spectra for periods that the most common structures have (0.4-0.8 sec), while for bigger values of the period the two analyses are close to each other.
- It can been seen that for both excitations the peak acceleration has increased at the top of the soil in comparison to the same value at the bottom, except for 3AQP. This phenomenon can be fully explained due to the curves G/G_{max} and damping with strain γ used. The explanation is given later, after the analysis with Abaqus, which simulates better th real behavior of the soil. Moreover, for 3Shinkobe excitation the increase in the peak acceleration at the top in smaller than for Shinkobe excitation.The explanation is the same.
- The two excitations analyzed in SHAKE have different characteristics concerned their spectra. More precisely, Shinkobe presents a plateau for bigger periods than AQP. This is dangerous for the structures, since structures have in general periods close to these of the plateau. On the other hand, AQP's spectra begins to reduce for smaller periods.

Furthermore, the peak of the two excitations are close. These differences is the reason why we chose these excitations for our analyses.

- The figures of the accelerograms at various depths show that as the waves travel from the bottom to the top, their frequency content (συχνοτικό περιεχόμενο) changes. In other words, the accelrograms become more long – period at the top in comparison with those at the bottom. This feature can been seen from the elastic response spectra plotted in the same diagram in figures 32-34, too. It is obvious that for Shinkobe excitation the peak of the spectra has moved to larger periods (probably due to resonance). This result however is not obvious for AQP excitation. Nevertheless, this does not mean that our conclusion about the spectra is wrong. If we observe better the spectra, we can see that the second biggest peak appears at bigger periods. The figures which can prove better our point are the amplification spectra (ratio of the acceleration spectrum due to the excitation at the bottom to the same values for the excitation – accelerogram at the top). It can been seen that the smallest ratio SADOWN/SAUP appears in a bigger period than the period that the spectra for the accelerogram at the bottom has its peak. In other words, not only the period is important, but also the value of the elastic response spectra on which the amplification will take place. To be more specific, in AQP the biggest period of the accelerogram at the top gives a smaller peak at the respective spectra, due to the fact that the value of the spectra for the excitation at the bottom is small. However, this amplification can be seen in the amplification spectra.
- From the figures 32-34 which represent the distribution of maximum strain with depth we can conclude that there is an increase in its value for depths between approximately 10 and 22 m. This is a quite important conclusion, since these depths correspond to the layer called Pancone, which was mentioned in chapter 2.1. This layer is a high compressible clay layer, which has a strong effect on the stability of the Tower. From this free field analysis it can been deduced again that this layer can cause stability problems to the superstructure above the soil concerned to excitations.
- As far as for the calibration of our analyses by using different curves for G/Gmax and damping with strain γ, so that they will be closer to the real problem, we can observe that

results have slightly change, with a small increase in the values of the elastic response spectra for the new curves.

2.2 Non-Linear Inelastic Analyses with Abaqus

As mentioned in the previous chapter the non-linear inelastic analyses for the free field soil is necessary. For this reason, we have carried out free field analysis using the finite element code of Abaqus and Seismosignal. The procedure of the Analysis is the following: First of all, we run a finite element analysis of the soil without the presence of any superstructure and apply an excitation at the bottom using Abaqus. Afterwards, we extract data and have the excitation at the top of the soil as a result. These accelerograms are put as input data at Seismosignal. Consequently, the Elastic Response Spectra and the Fourier Spectra for each accelerogram are produced. The excitations which have been utilized, so that we will be able to evaluate the seismic performance of the subsoil profile of Pisa are the following:

1) Record L'AQUILA - V. ATERNO - M. PETTINO (AQP - component EW) from the aftershock of L'Aquila 2009, M_w 5.5, Italy.
2) Record Sannicandro Garganico (SNN – component NS) from the shock of Molise 2002, M_w 5.7, Italy
3) Record Atina (component EW) from the earthquake of Lazio Abruzzo 1984, M_w 5.8, Italy
4) Record Cascia (component NS) from the earthquake of Norcia 1979, M_w 5.9, Italy
5) Record Gilroy (both components: 0^o and 90^o - Gilroy0 and Gilroy90 respectively) from the shock of Loma Prieta 1989, M_w 6.9, California
6) Record San Rocco (component 270^o) from the shock of Friuli 1976, M_w 6.5, Italy
7) Record Sturno (component 0^o) from the earthquake of Irpinia 1980, M_w 6.89, Italy

8) Record AegionRock from the earthquake of Greece 1995, M_w 6.2 (this is an altered motion data)

The selected records cover a wide range of seismic motions which could appear in the vicinity of the Tower Pisa, since most of them are from earthquakes in Italy and they are records of medium intensity. Except from these records there are two accelerograms which represent more dangerous motions for the Tower of Pisa. These are the two Gilroy components. Despite the fact that these records are not realistic to appear in the vicinity of the Tower of Pisa, here we have examined them , in order to take into account the worst case scenario. All of the examined records have peak fround acceleration between 0.07 g and 0.16 g (we have scaled down of course the Gilroy record without affecting the frequency content of the record, but only the values of the acceleration). Finally, the AegionRock is an altered record from the earthquake of Greece in 1995 from the record of Aegion. Although, it is not a record in Italy,it is a realistic scenario for the Tower of Pisa, since it is a record from Greece, which is close to Italy. The analyses have been carried out not only to these excitations, but also to the same but with twice accelerations and the same frequency domain. In other words we have scaled up all the records, in order to achieve the desired peak accelerations between 0.14 g and 0.32 g. These excitations are referred with the name of the above and multiplying factor in front of them. This factor is equal to 2 for all the records, except for SNN in which is equal to 6. This happens because SNN has 0.03 g as peak acceleration, so 3SNN has the desired peak acceleration of 0.10 g. As a result, we can have an upper boundary for our analyses, since from the literature for the dynamic evaluation of the Tower of Pisa the maximum acceleration tested is equal to 0.07 g. In addition, two records are examined for smaller peak accelerations equal to 0.03 g and 0.05 g (SNN and AQP/2 respectively).

The results presented in the figures of this chapter are the following:

1) Figures 2.1-2.10 illustrate the accelerograms at the top and at the bottom of the subsoil profile underneath the Tower of Pisa with the peak acceleration marked on them. The red line presents the accelerogram at the bottom and the blue one the accelerogram at the top.

2) The elastic response spectra and the amplification spectra for each record are shown in figures 2.11-2.30. The notation concerned the colour of the lines is the same as mentioned before. The amplification spectra is the ratio of the spectra acceleration for the accelerogram at the top to the spectra acceleration for the accelerogram at the bottom. The comparison of these spectra in one graph is shown in figures 2.31-2.35.

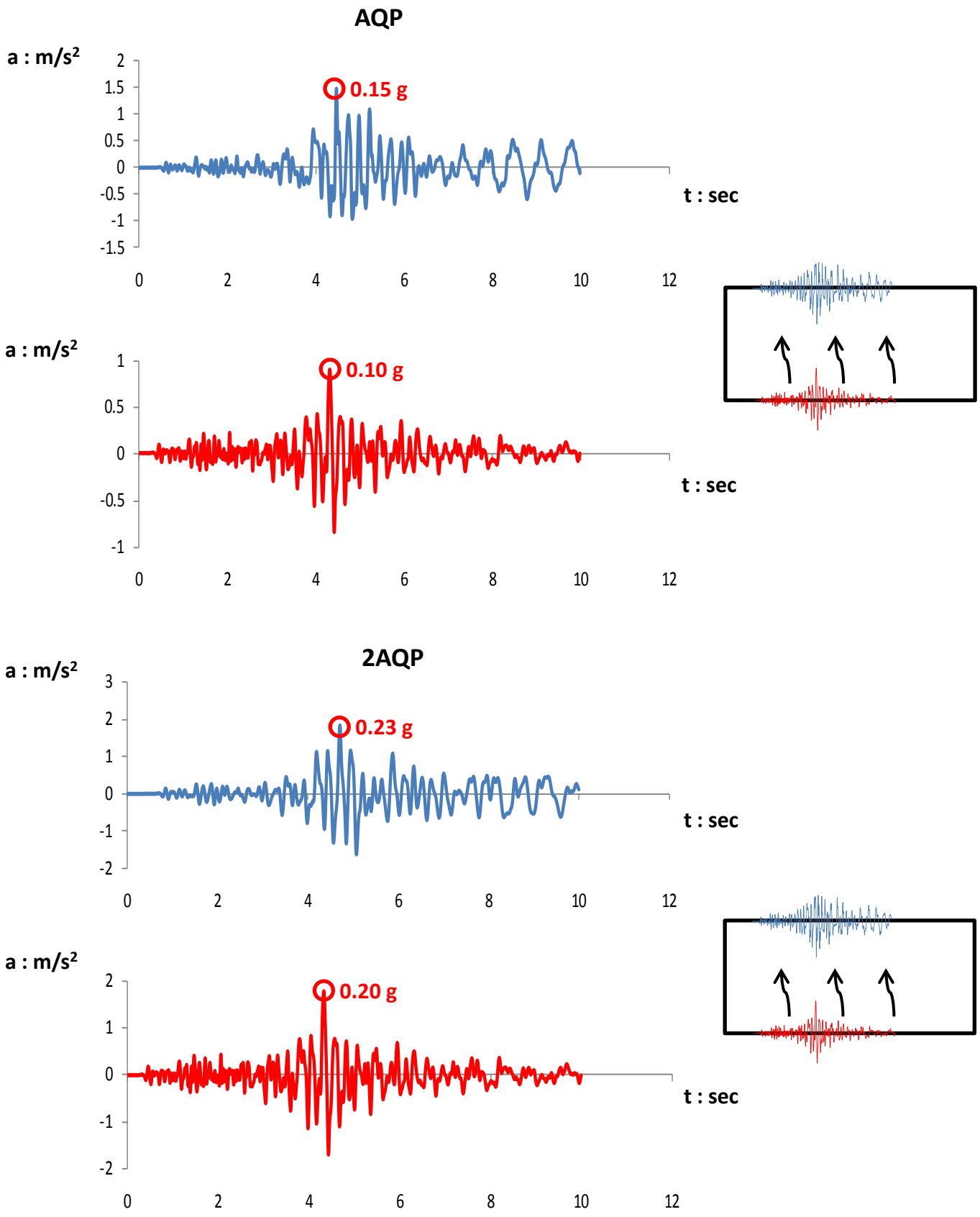

Figure 2.1 Accelerograms Free Field UP and DOWN for L'AQUILA – V. ATERNO – M. PETTINO (AQP) M_w = 5.5, Italy

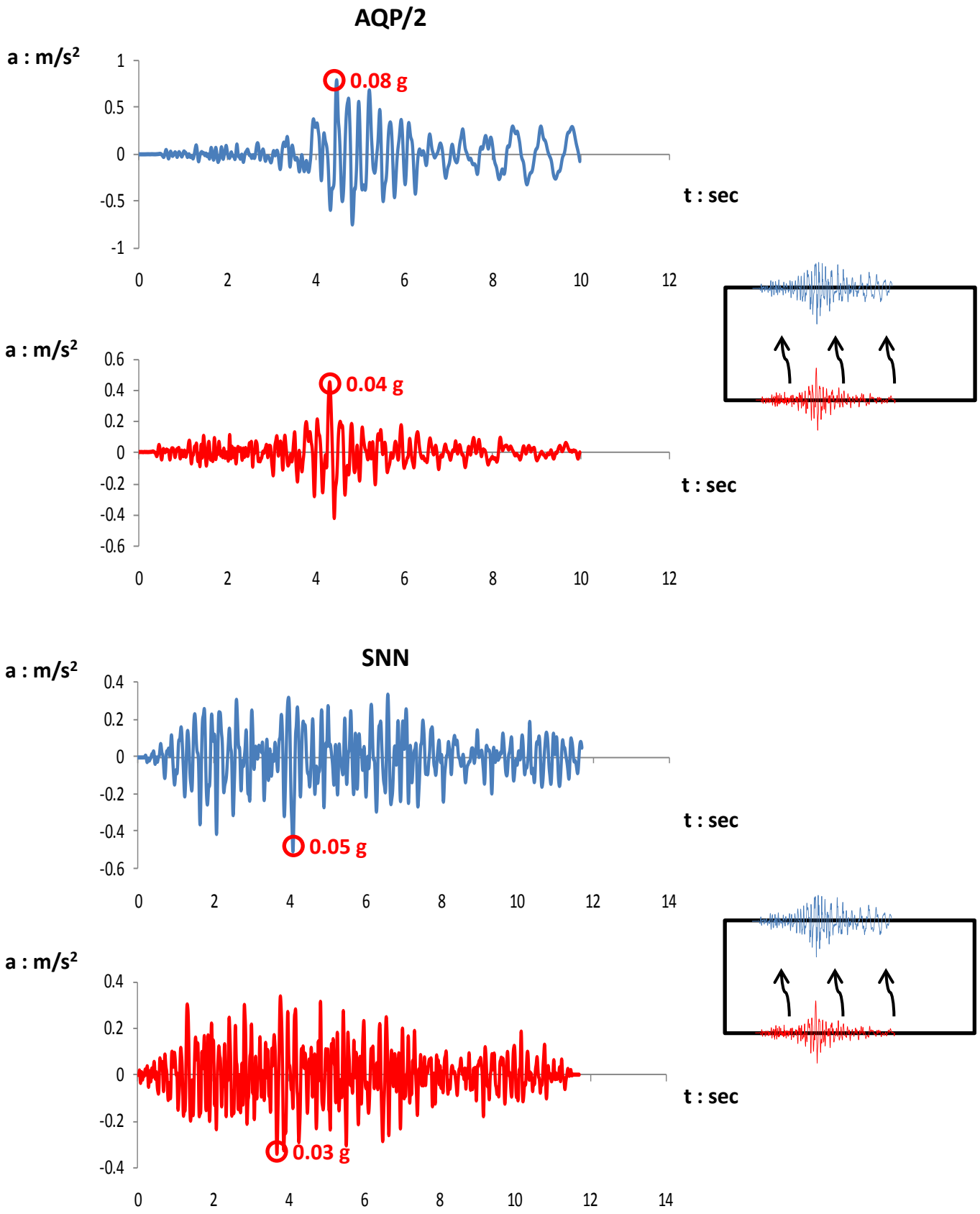

Figure 2.2 Accelerograms Free Field UP and DOWN for L'AQUILA – V. ATERNO – M. PETTINO (AQP), M_w = 5.5, Italy and Sannicandro Garganico (SNN), M_w 5.7, Italy

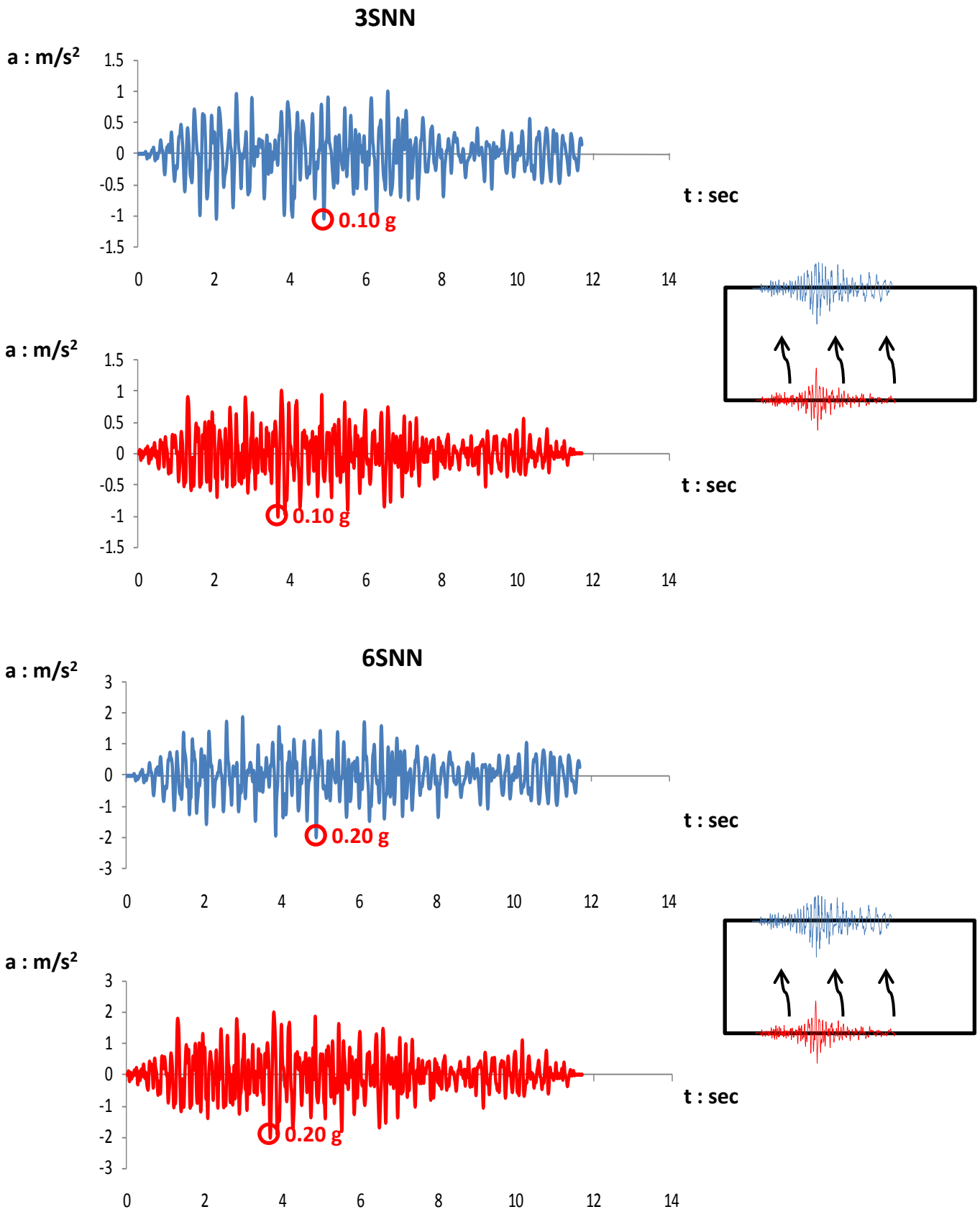

Figure 2.3 Accelerograms Free Field UP and DOWN for Sannicandro Garganico (SNN), M_w 5.7, Italy

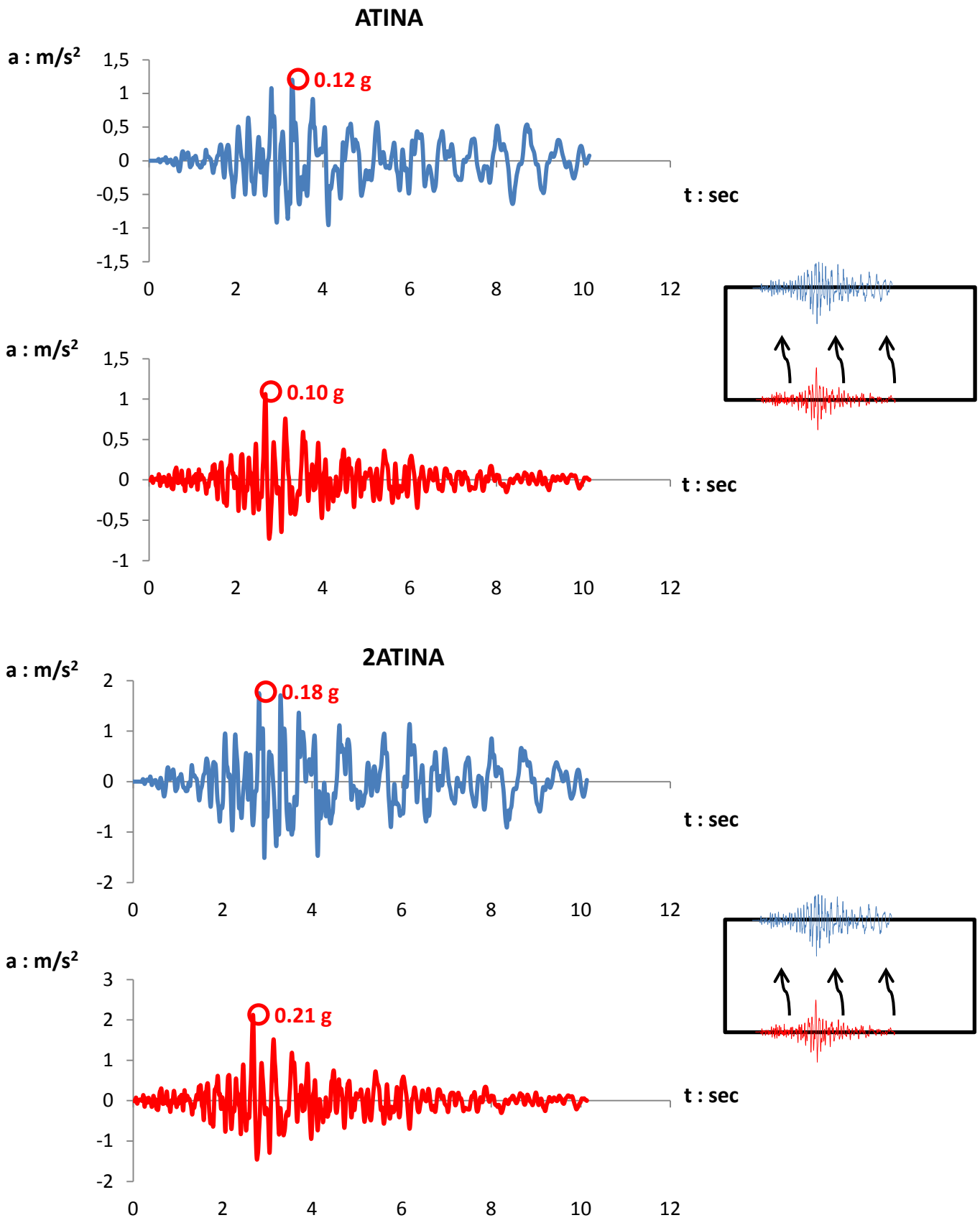

Figure 2.4 Accelerograms Free Field UP and DOWN for ATINA M_w 5.8, Italy

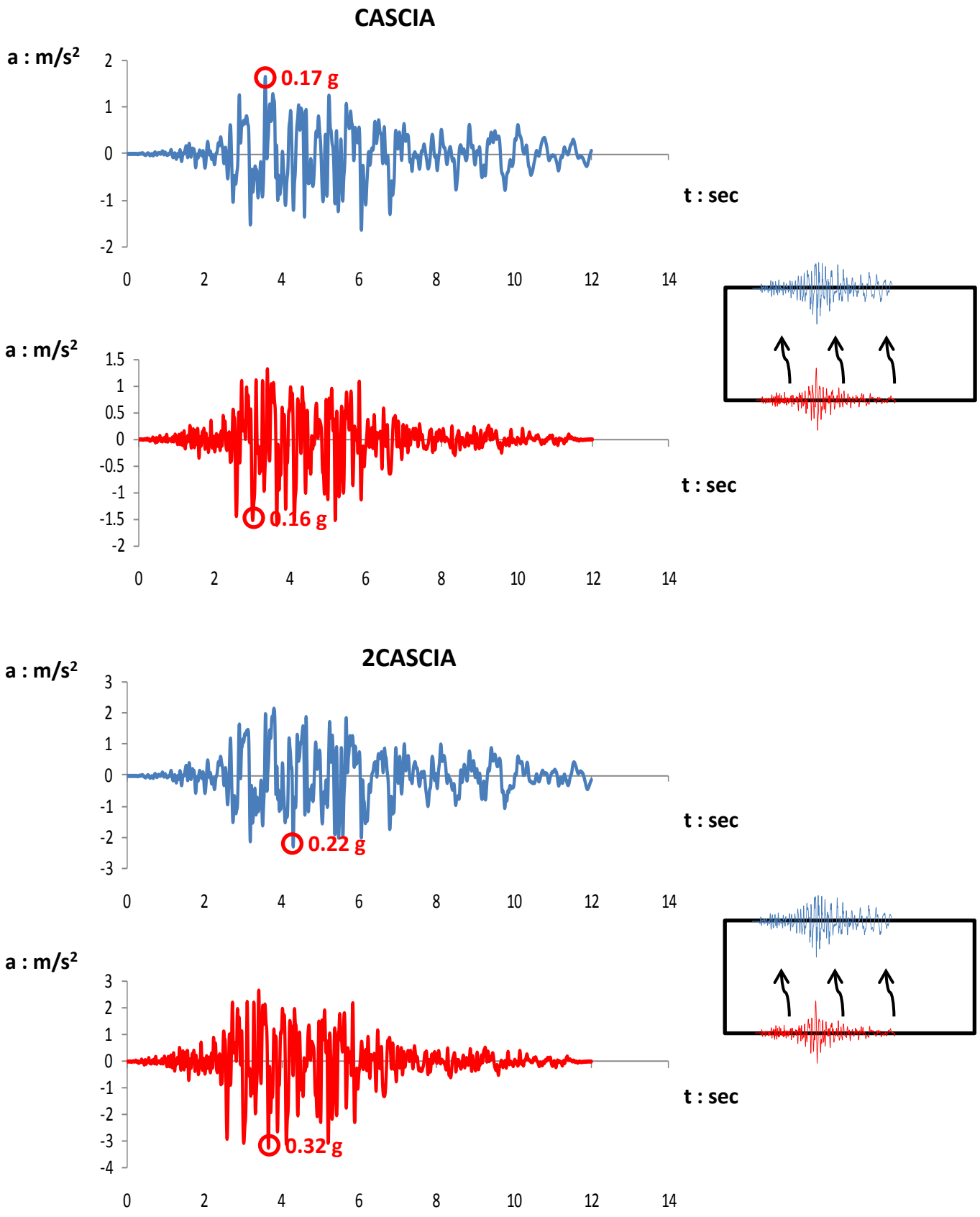

Figure 2.5 Accelerograms Free Field UP and DOWN for CASCIA, M_w 5.9, Italy

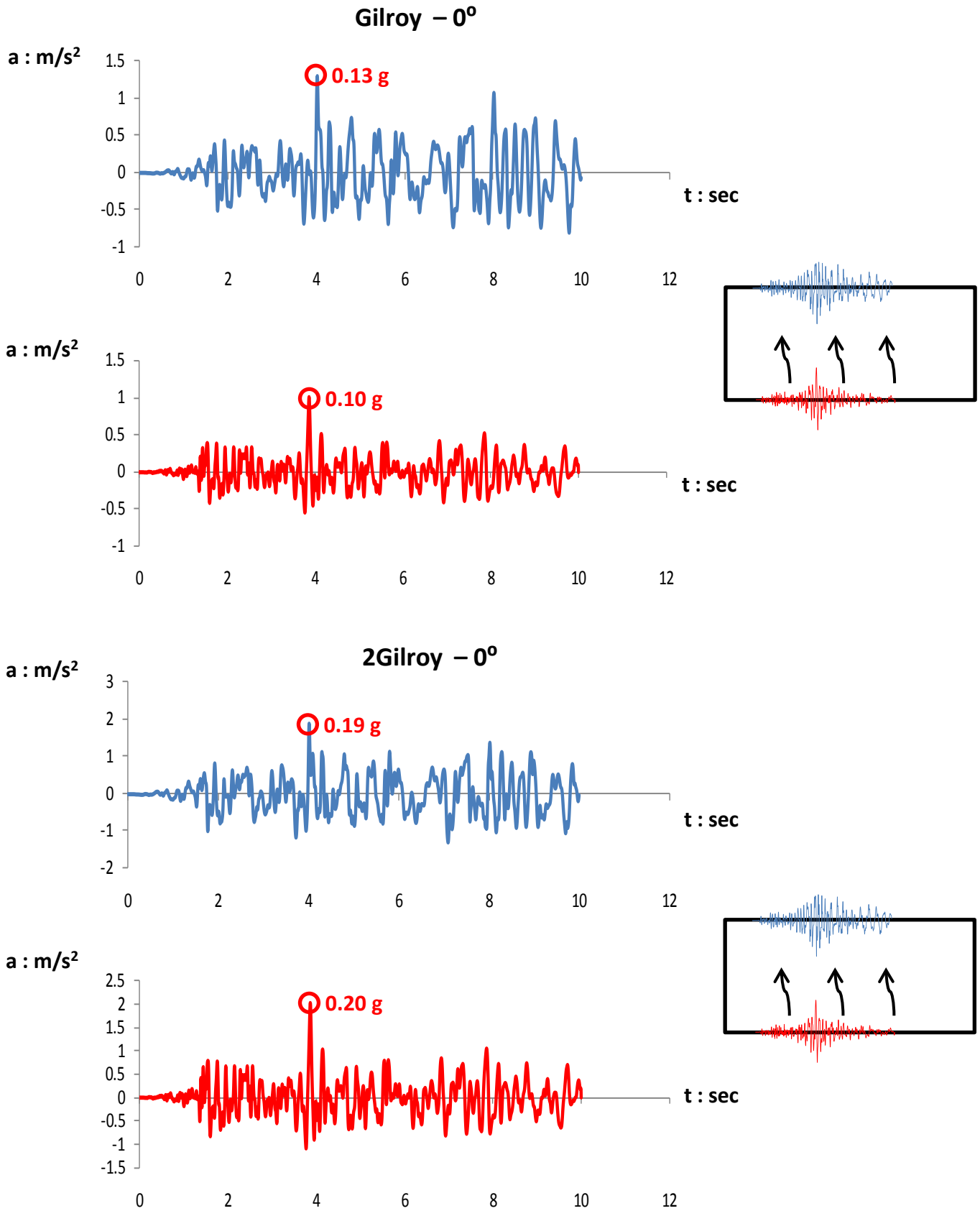

Figure 2.6 Accelerograms Free Field UP and DOWN for Gilroy (0^0), Mw 6.9, California

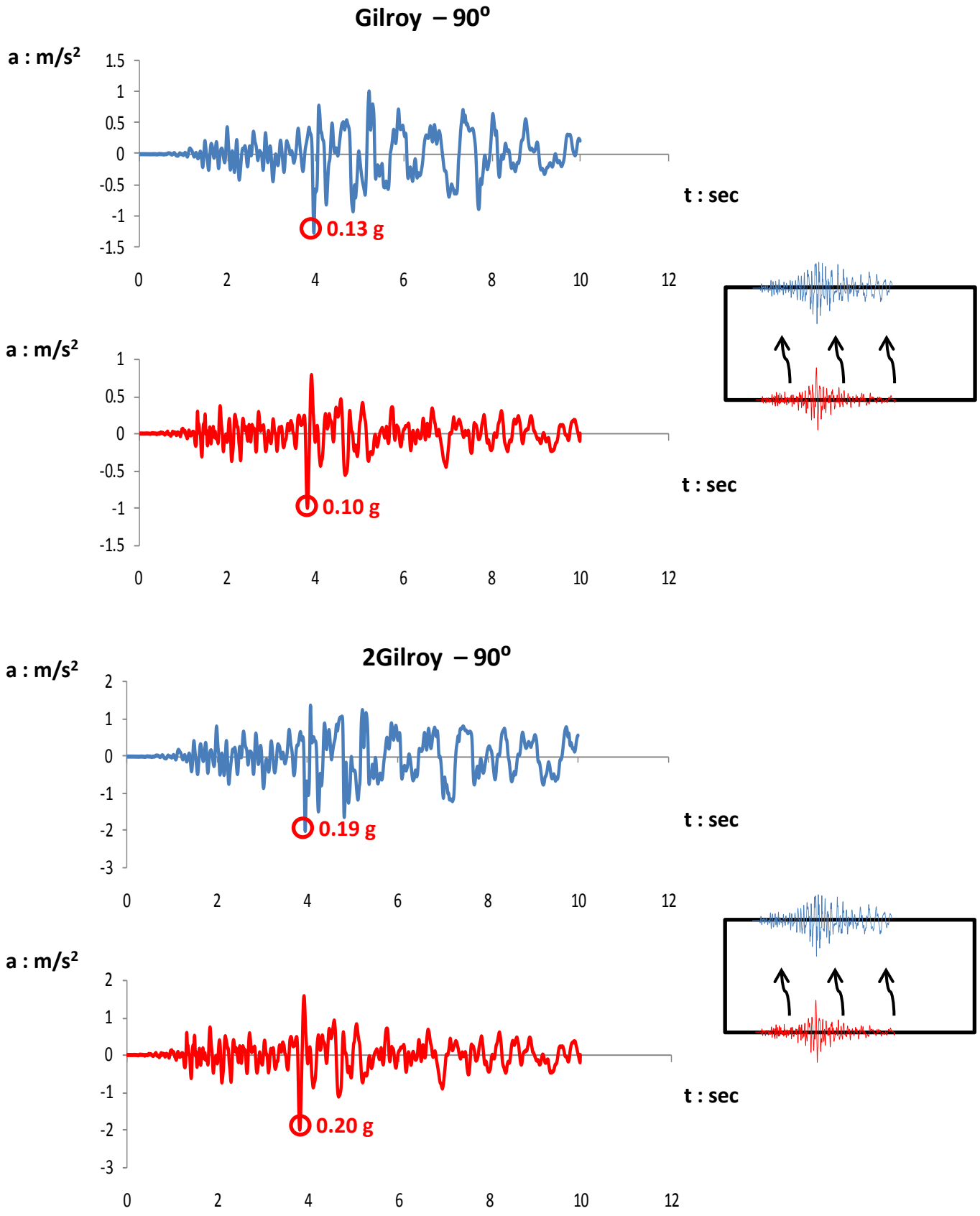

Figure 2.7 Accelerograms Free Field UP and DOWN for Gilroy (90^0), Mw 6.9, California

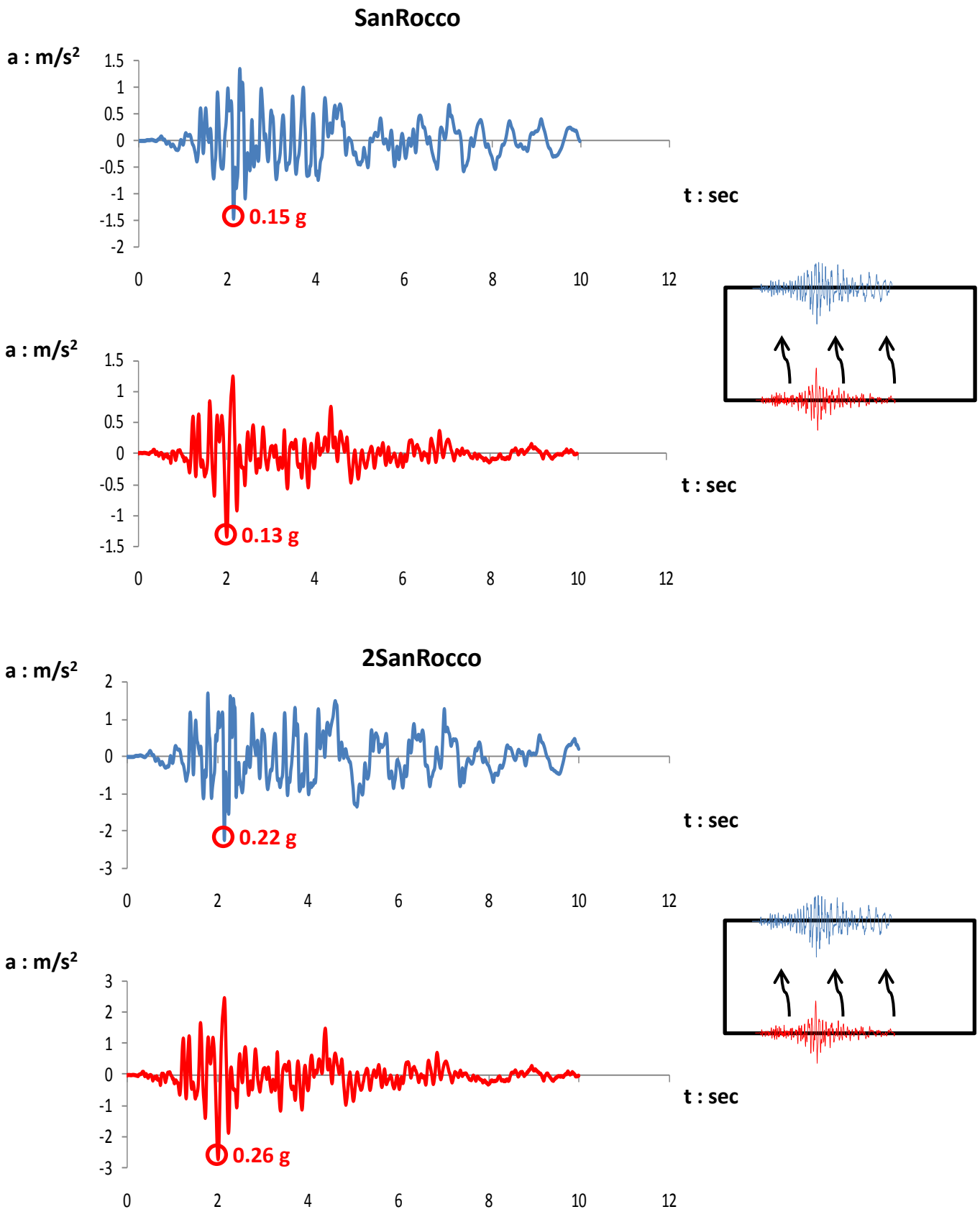

Figure 2.8 Accelerograms Free Field UP and DOWN for SanRocco, M_w 6.5, Italy

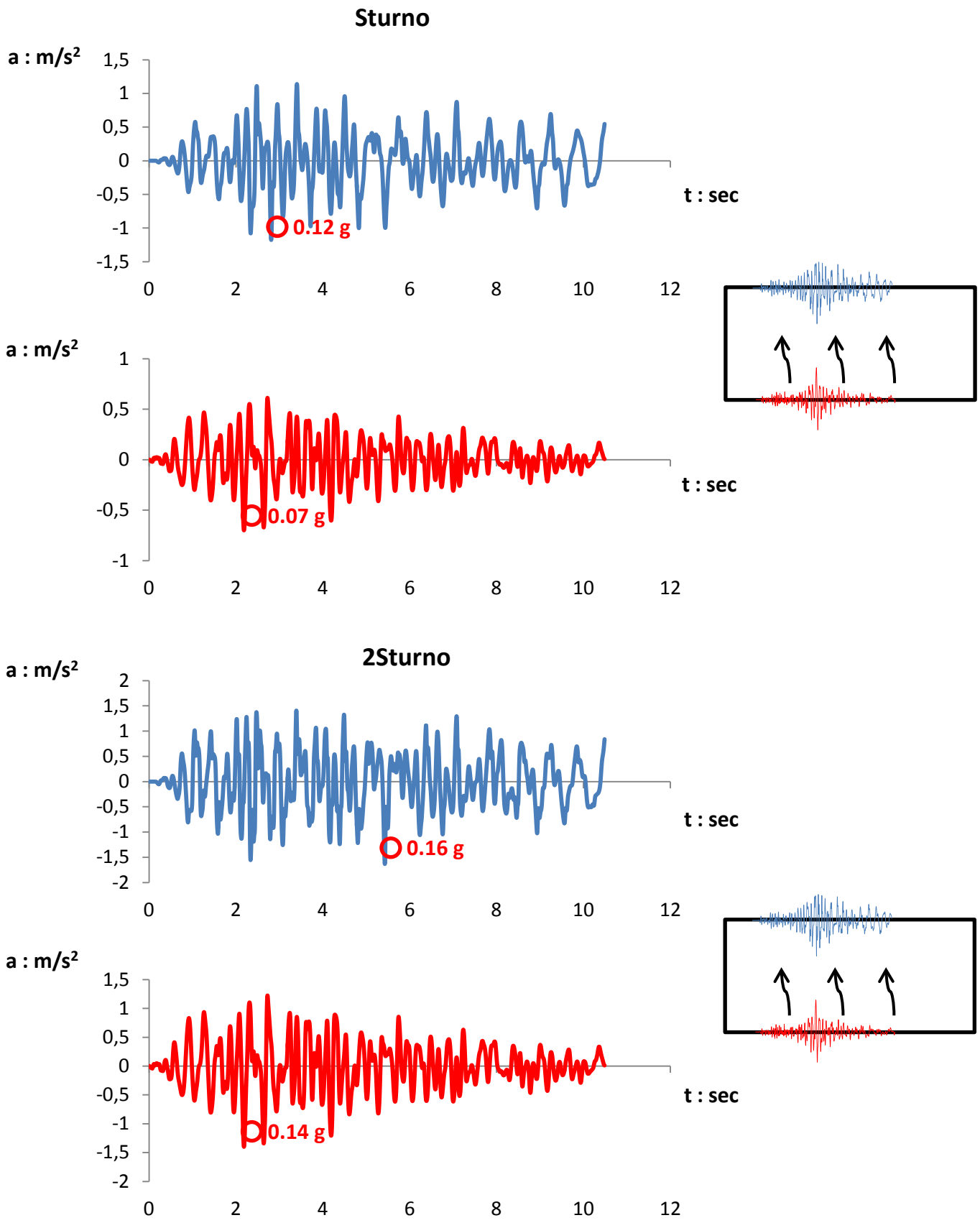

Figure 2.9 Accelerograms Free Field UP and DOWN for Sturno, M_w 6.89, Italy

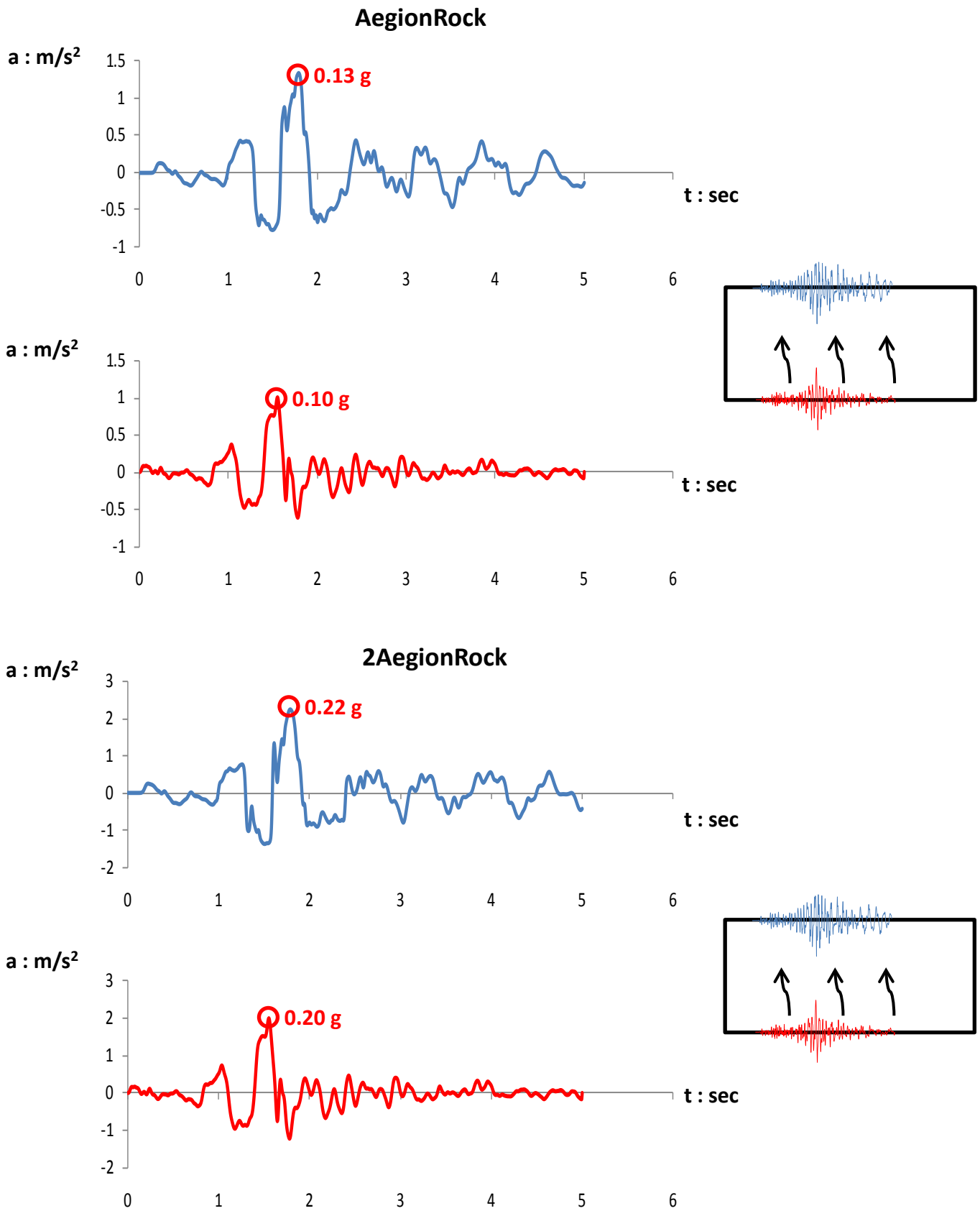

Figure 2.10 Accelerograms Free Field UP and DOWN for AegionRock, Greece

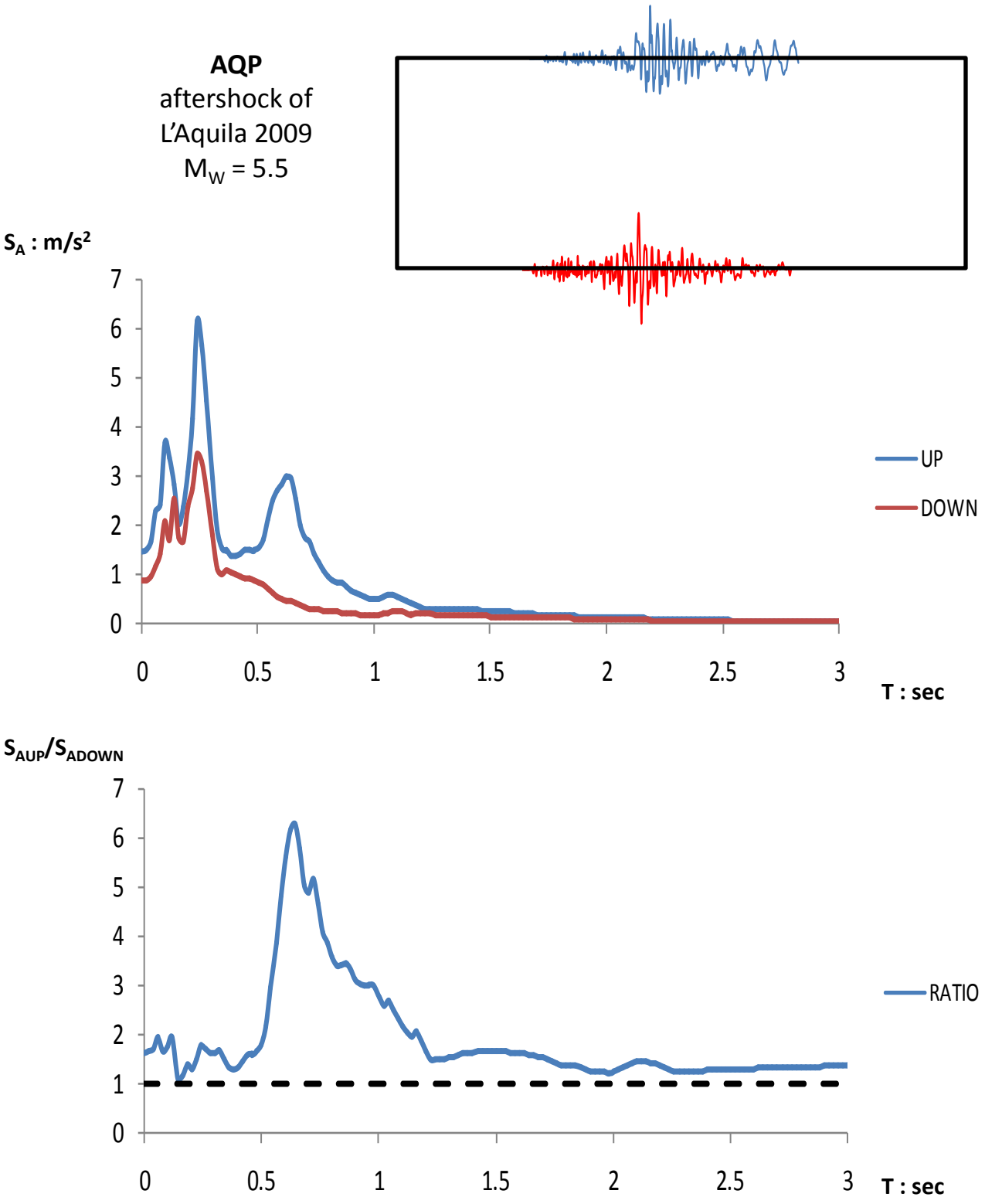

Figure 2.11 Elastic Response Spectra (ξ = 5 %) Free Field UP and DOWN for AQP

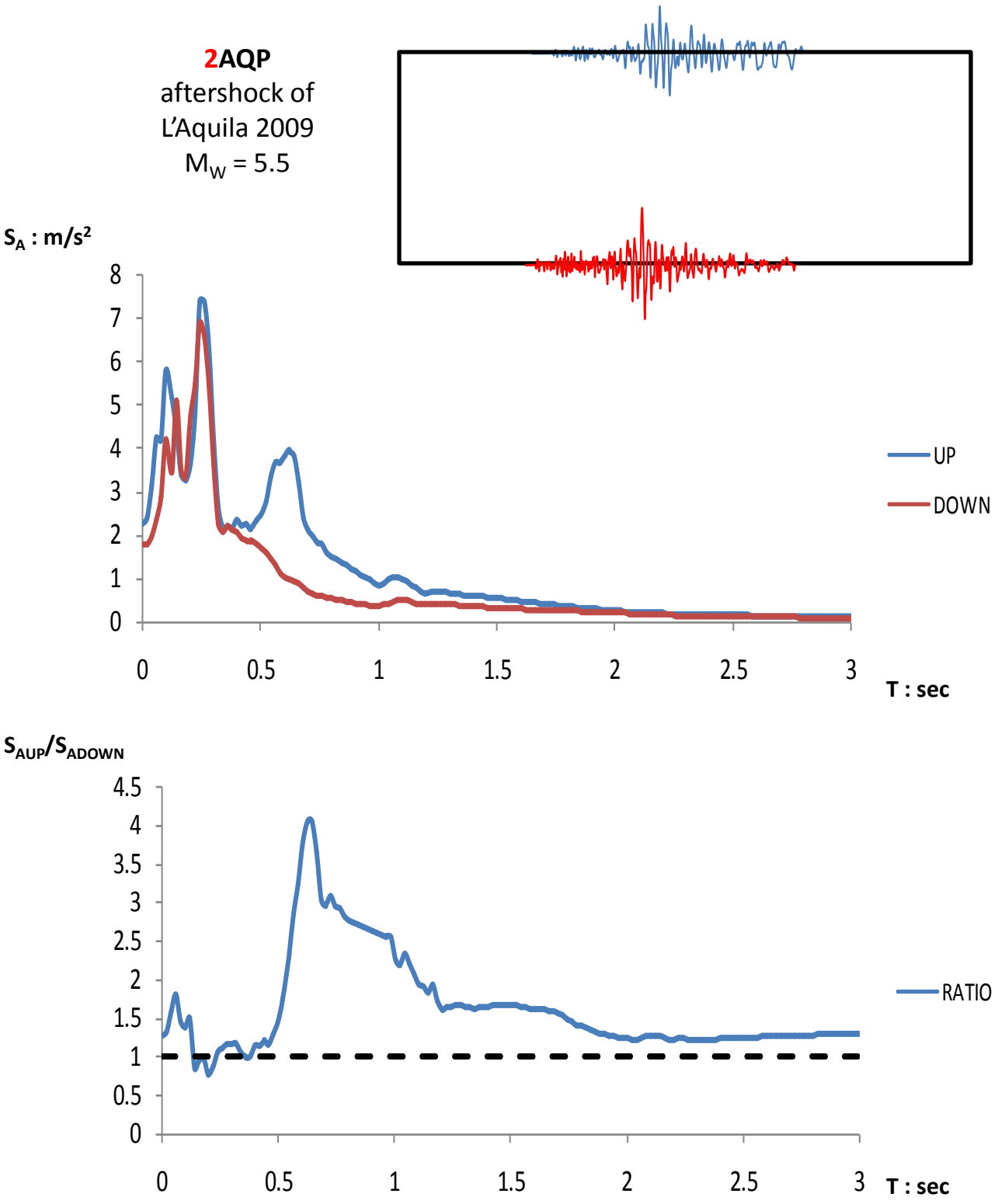

Figure 2.12 Elastic Response Spectra (ξ = 5 %) Free Field UP and DOWN for 2AQP

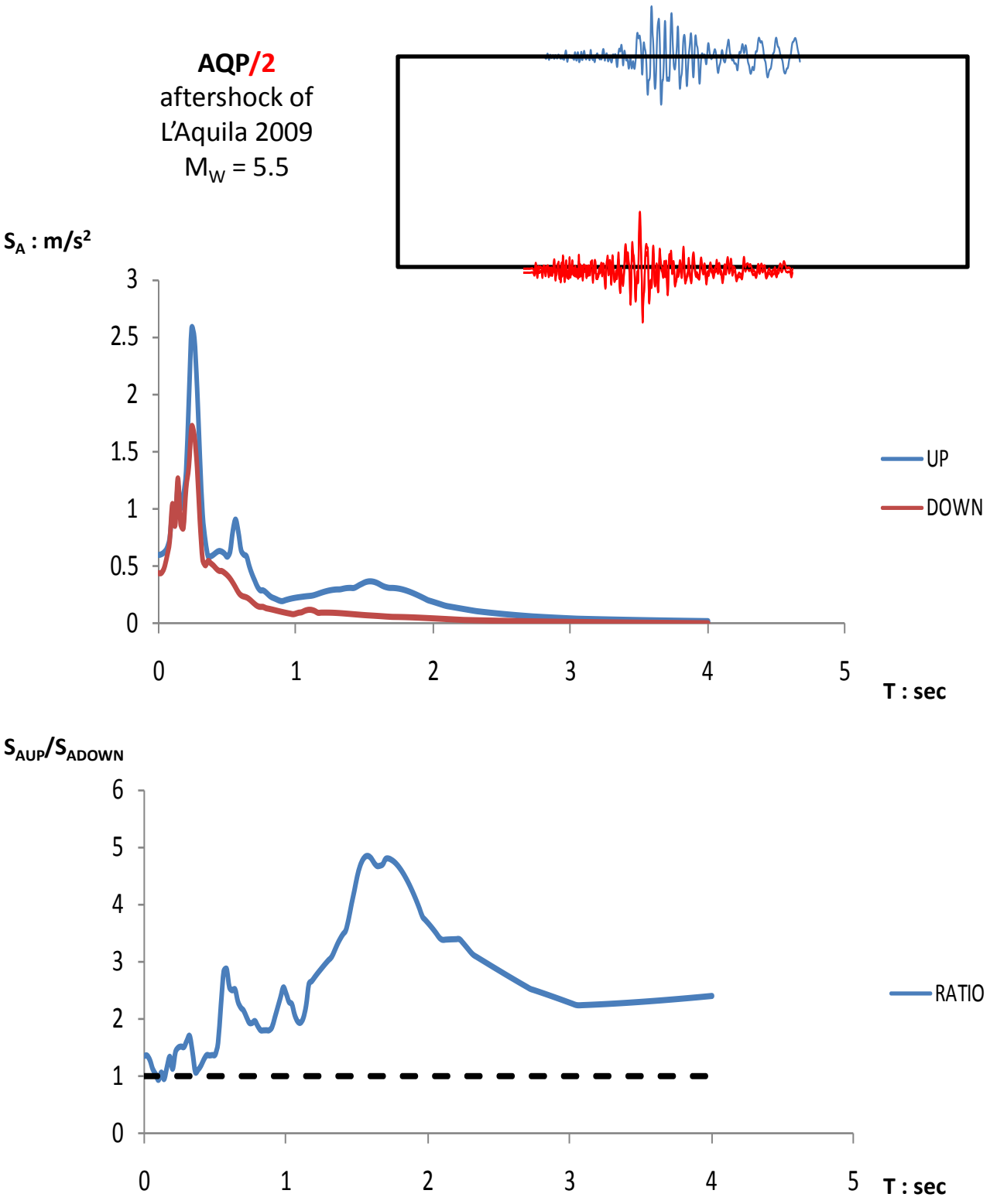

Figure 2.13 Elastic Response Spectra (ξ = 5 %) Free Field UP and DOWN for AQP/2

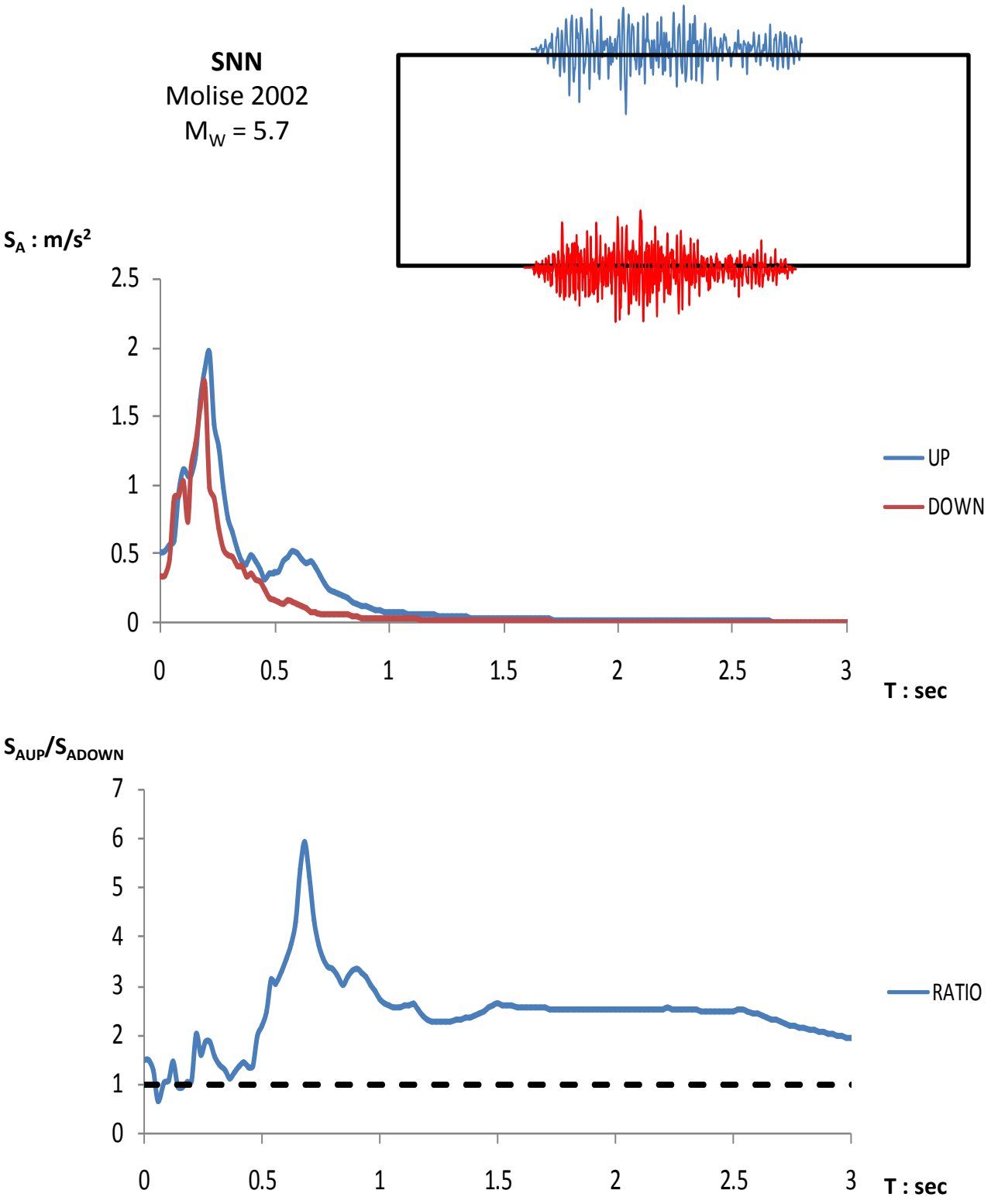

Figure 2.14 Elastic Response Spectra (ξ = 5 %) Free Field UP and DOWN for SNN

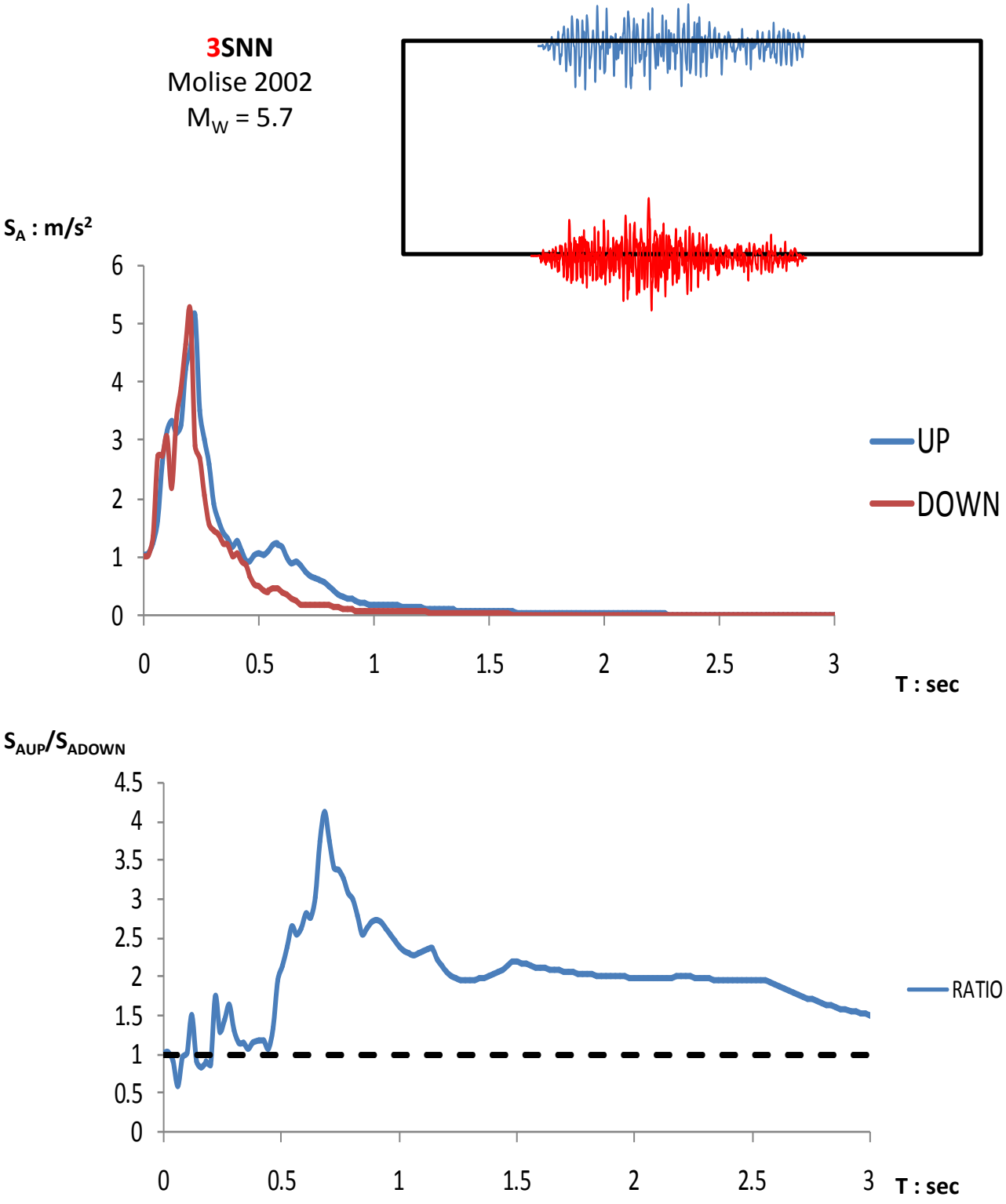

Figure 2.15 Elastic Response Spectra (ξ = 5 %) Free Field UP and DOWN for 3SNN

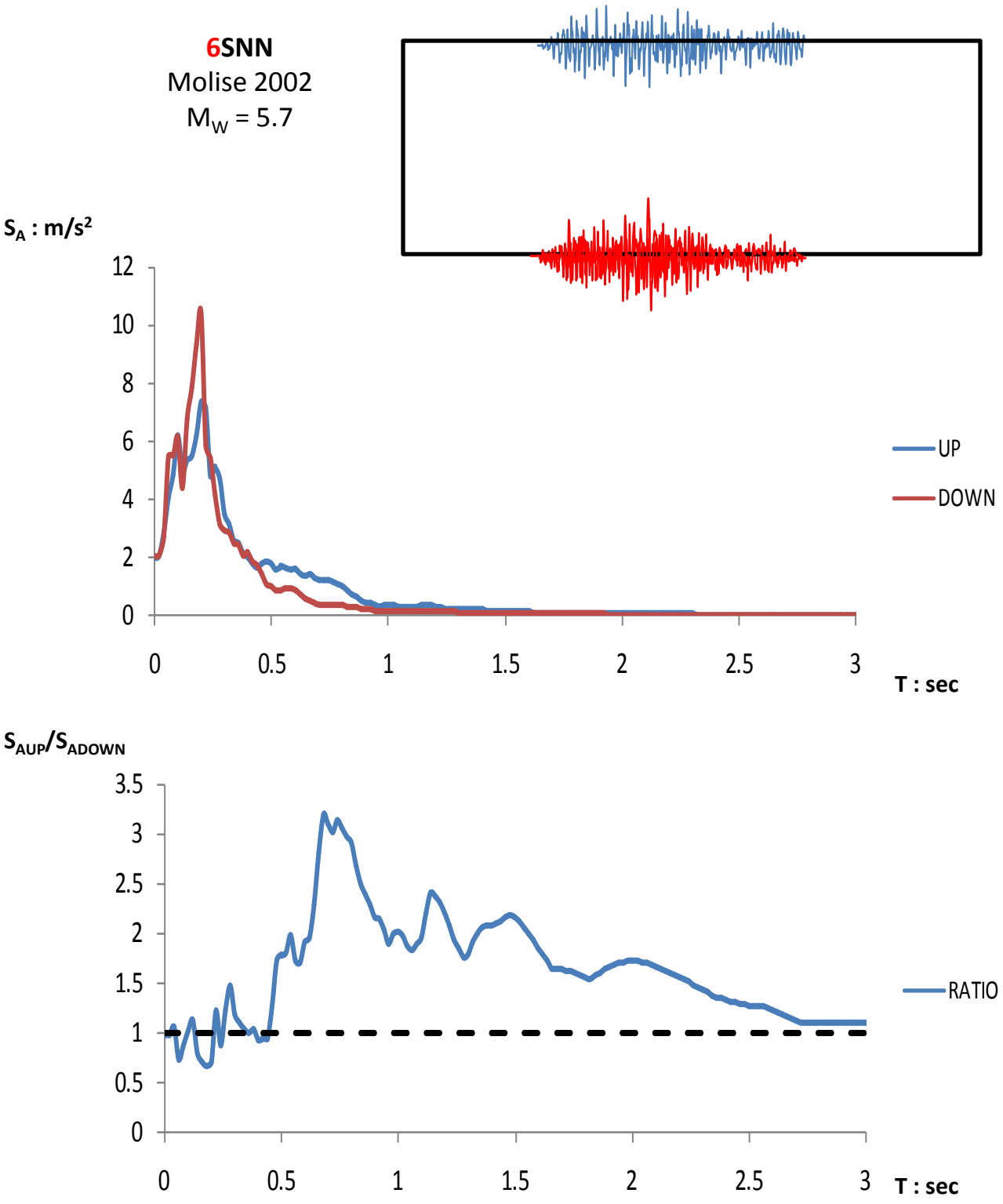

Figure 2.16 Elastic Response Spectra (ξ = 5 %) Free Field UP and DOWN for 6SNN

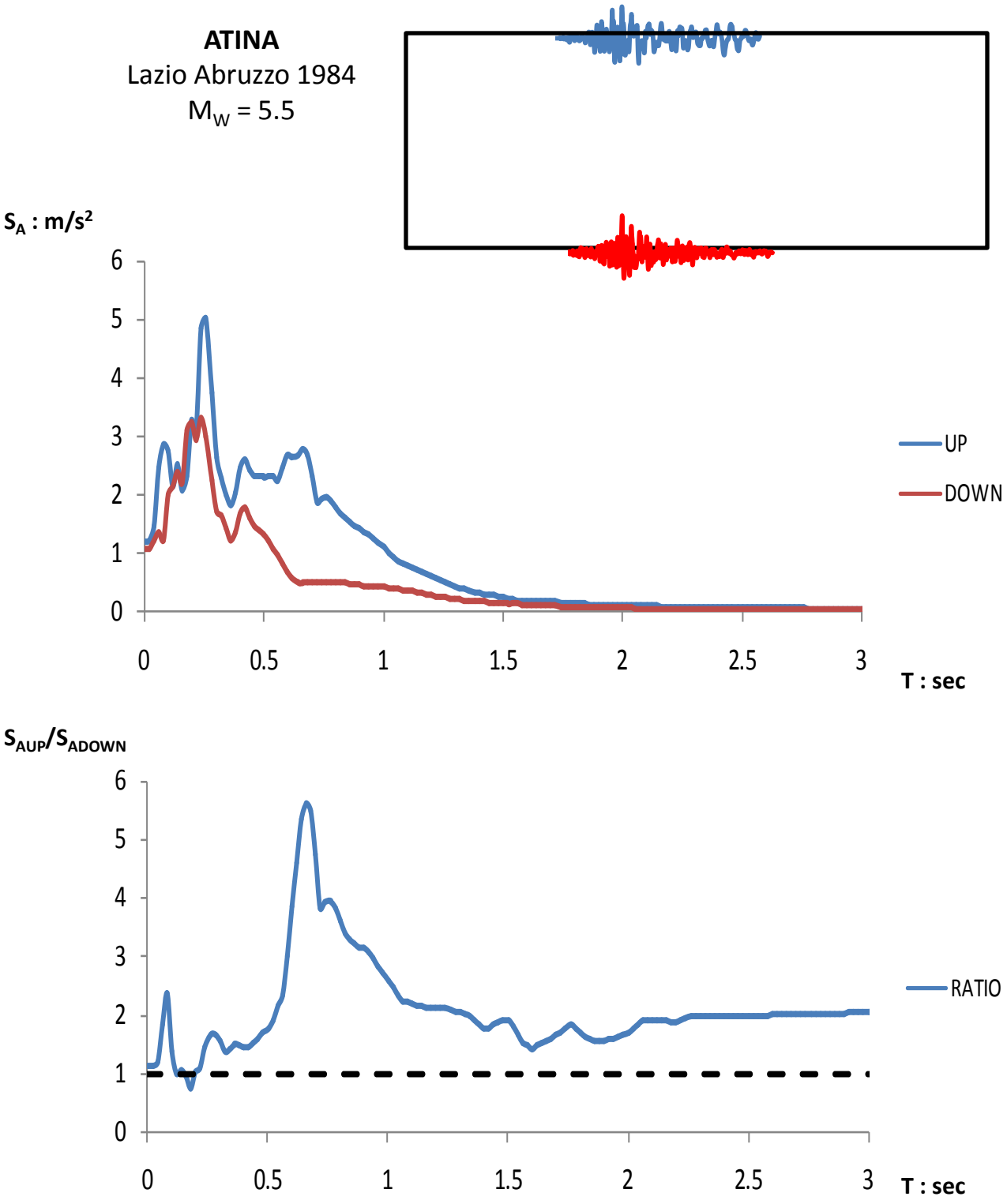

Figure 2.17 Elastic Response Spectra (ξ = 5 %) Free Field UP and DOWN for ATINA

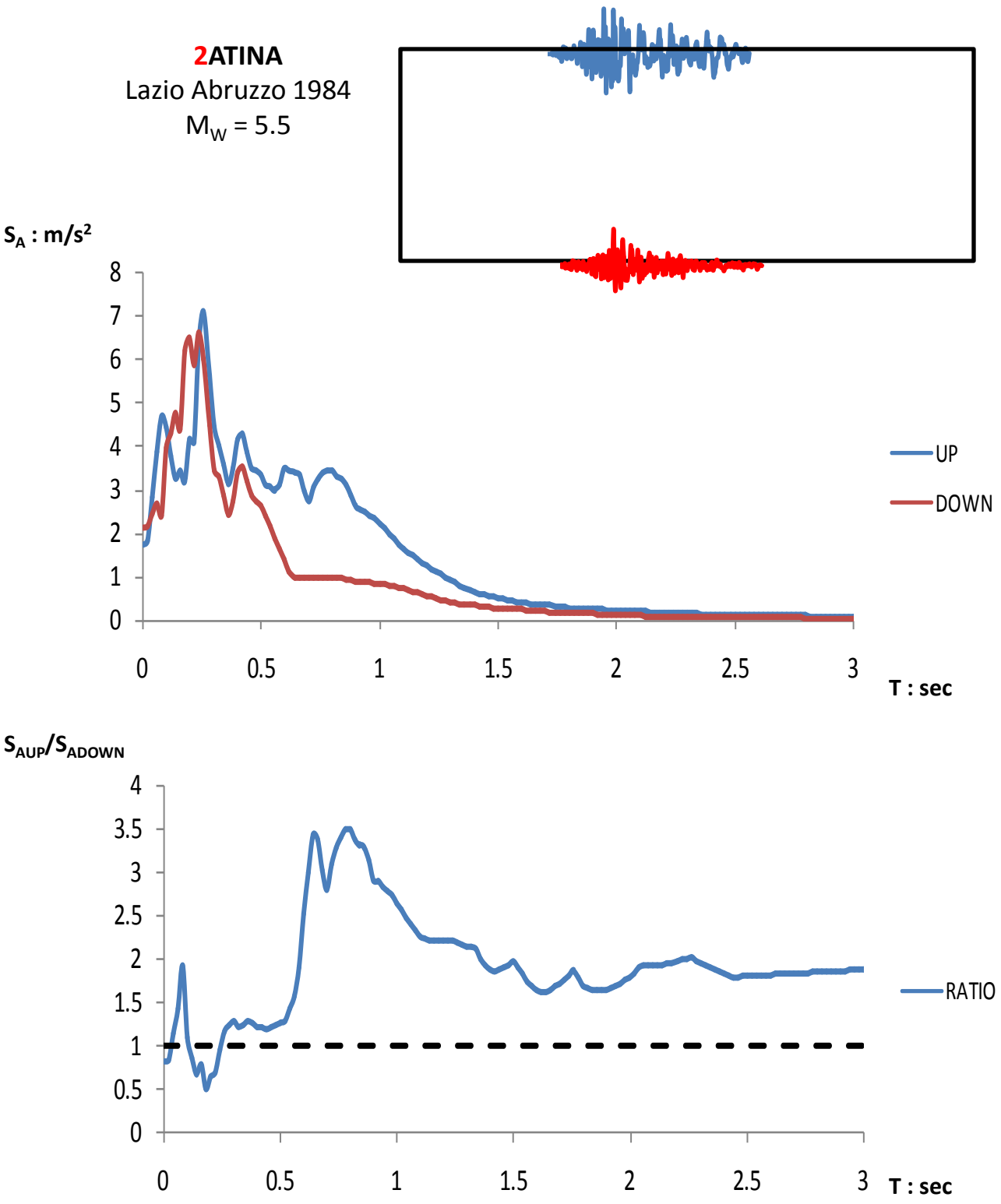

Figure 2.18 Elastic Response Spectra (ξ = 5 %) Free Field UP and DOWN for 2ATINA

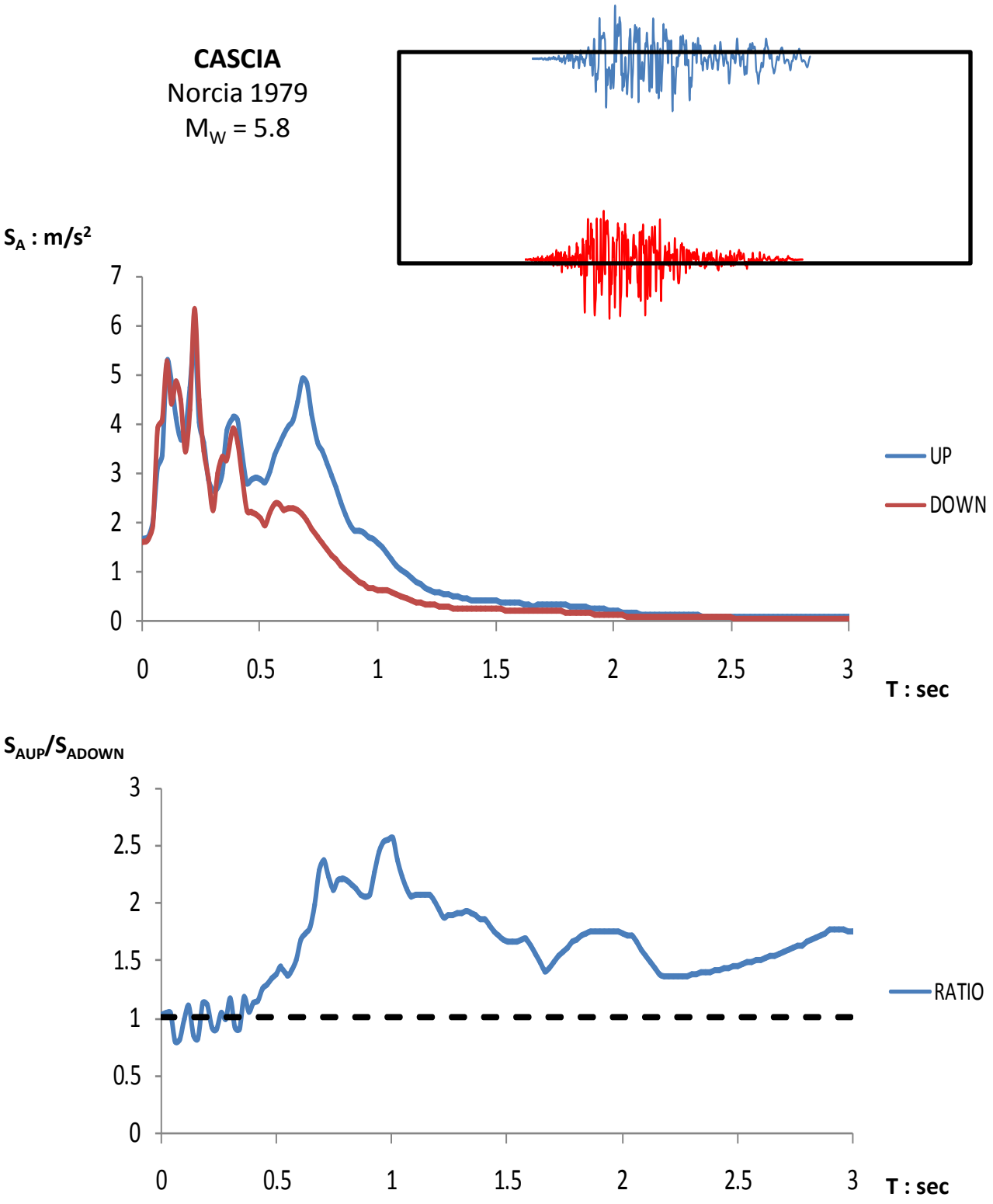

Figure 2.19 Elastic Response Spectra (ξ = 5 %) Free Field UP and DOWN for CASCIA

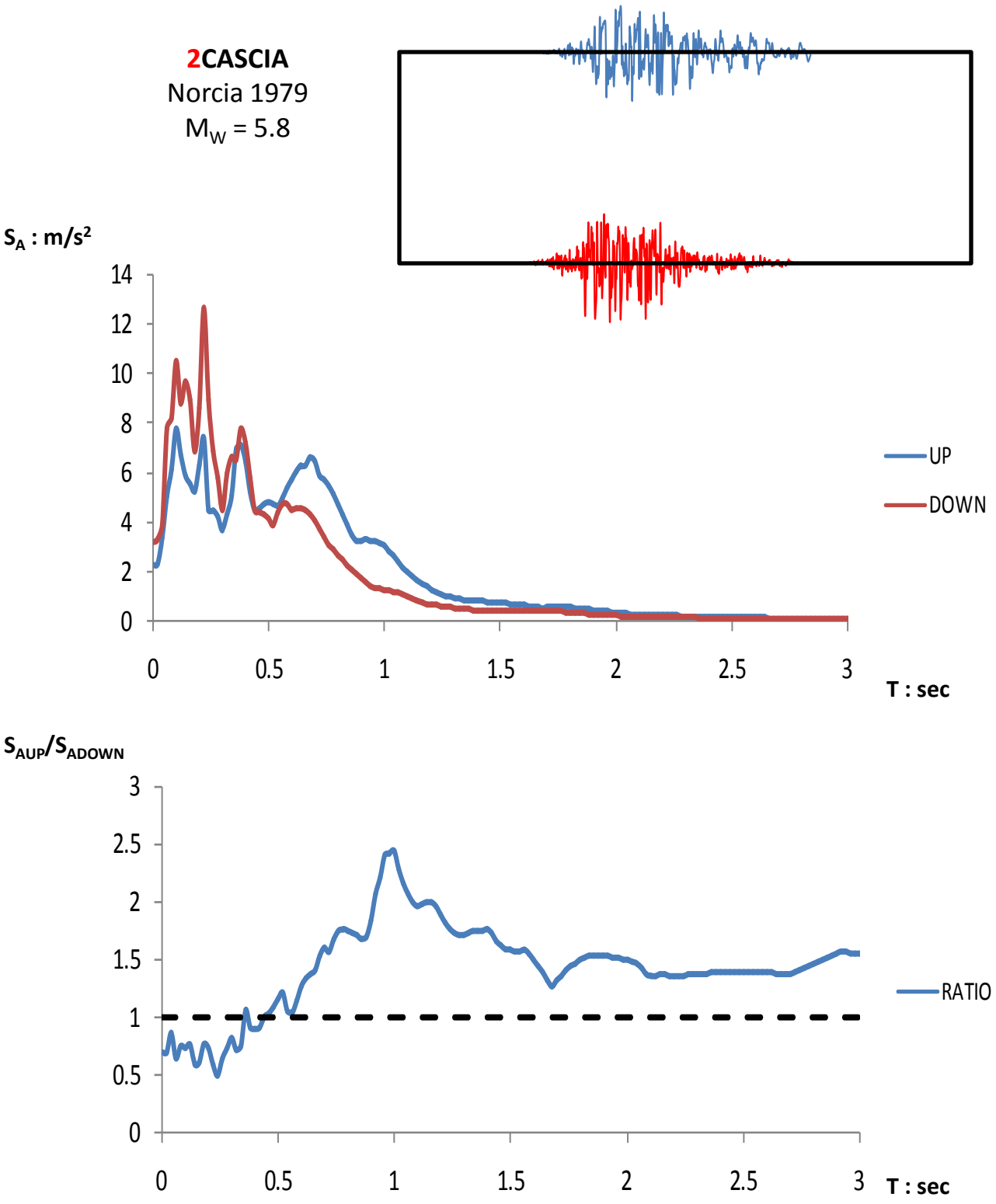

Figure 2.20 Elastic Response Spectra (ξ = 5 %) Free Field UP and DOWN for 2CASCIA

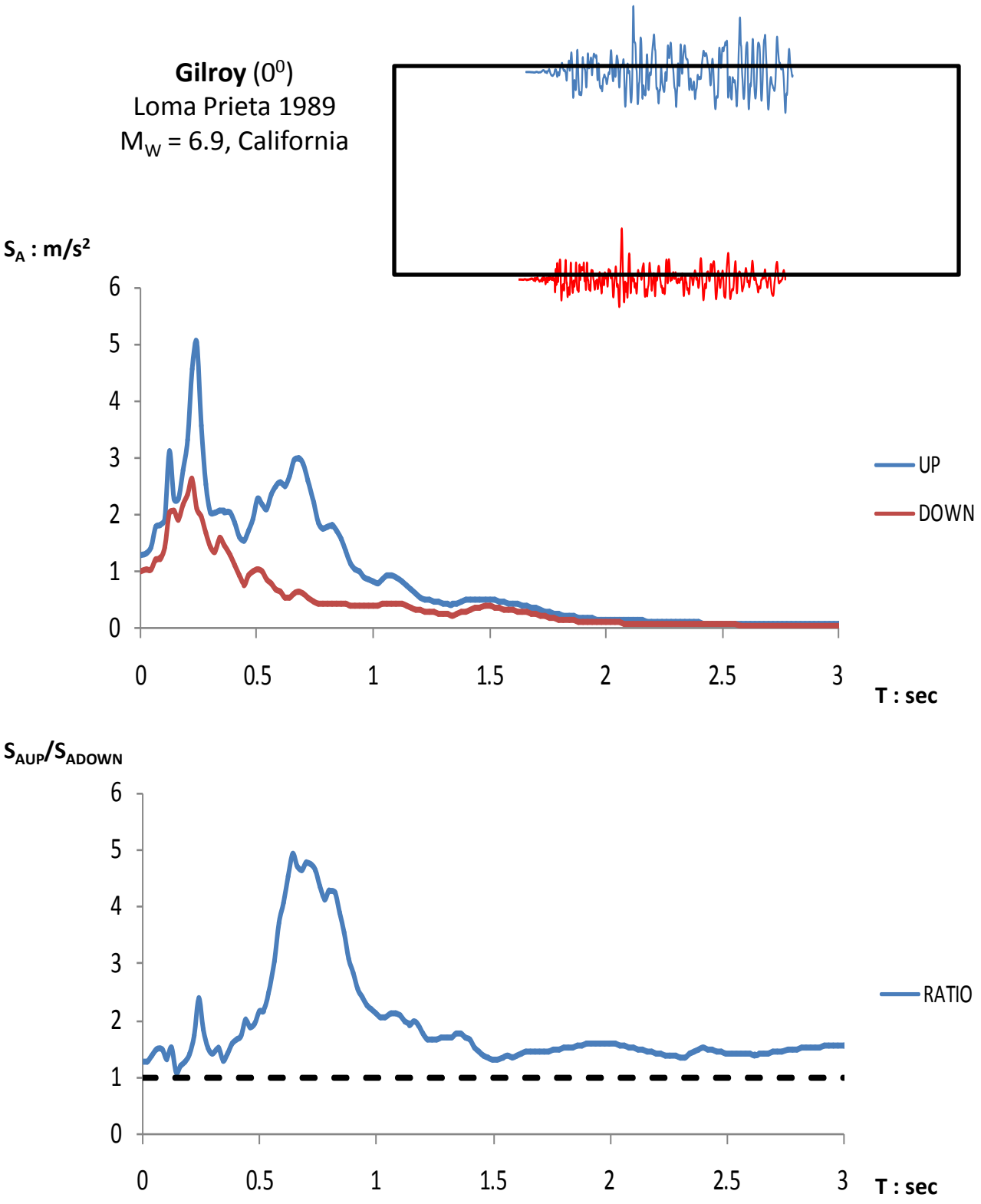

Figure 2.21 Elastic Response Spectra (ξ = 5 %) Free Field UP and DOWN for Gilroy (0 °)

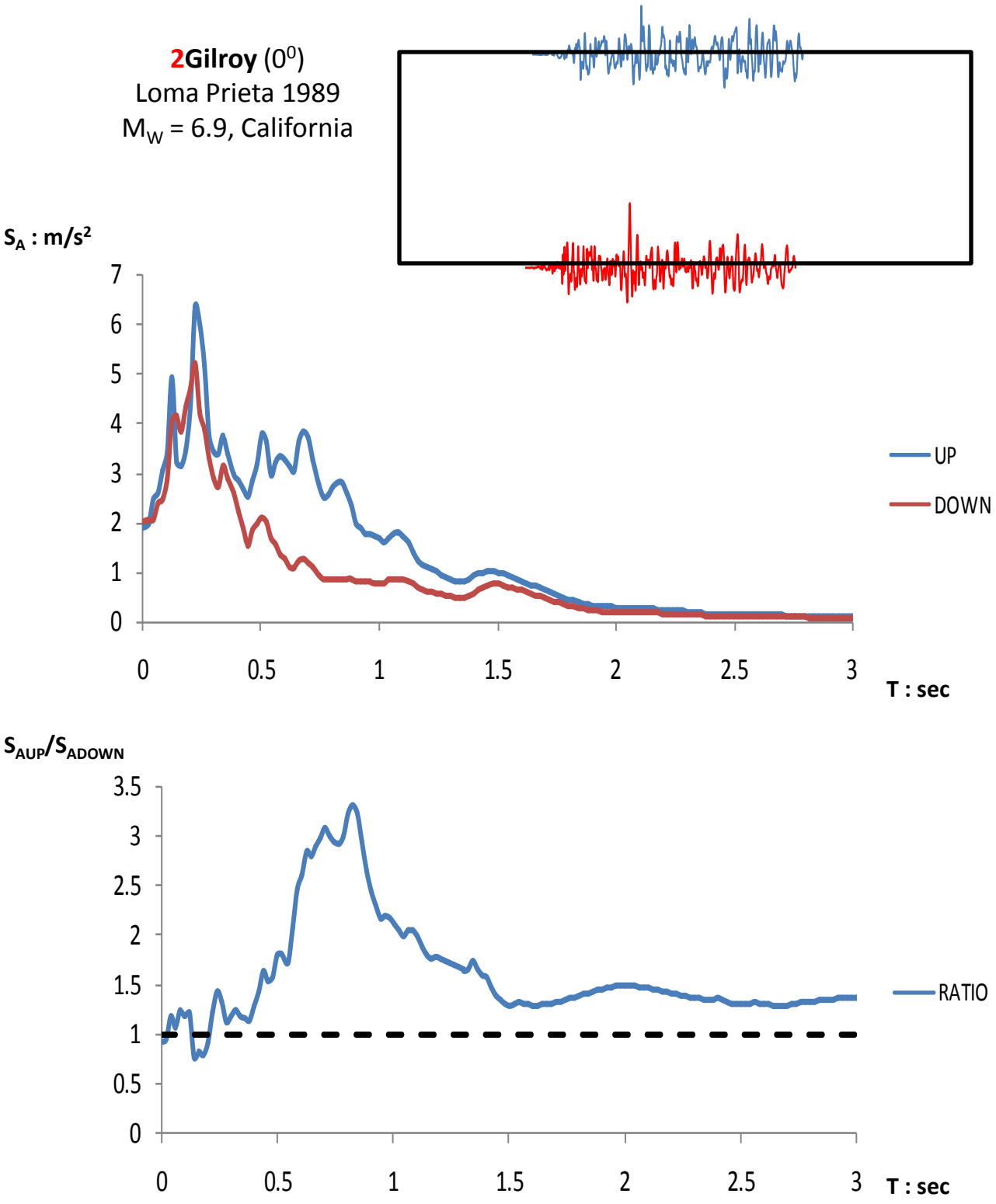

Figure 2.22 Elastic Response Spectra (ξ = 5 %) Free Field UP and DOWN for 2Gilroy (0 °)

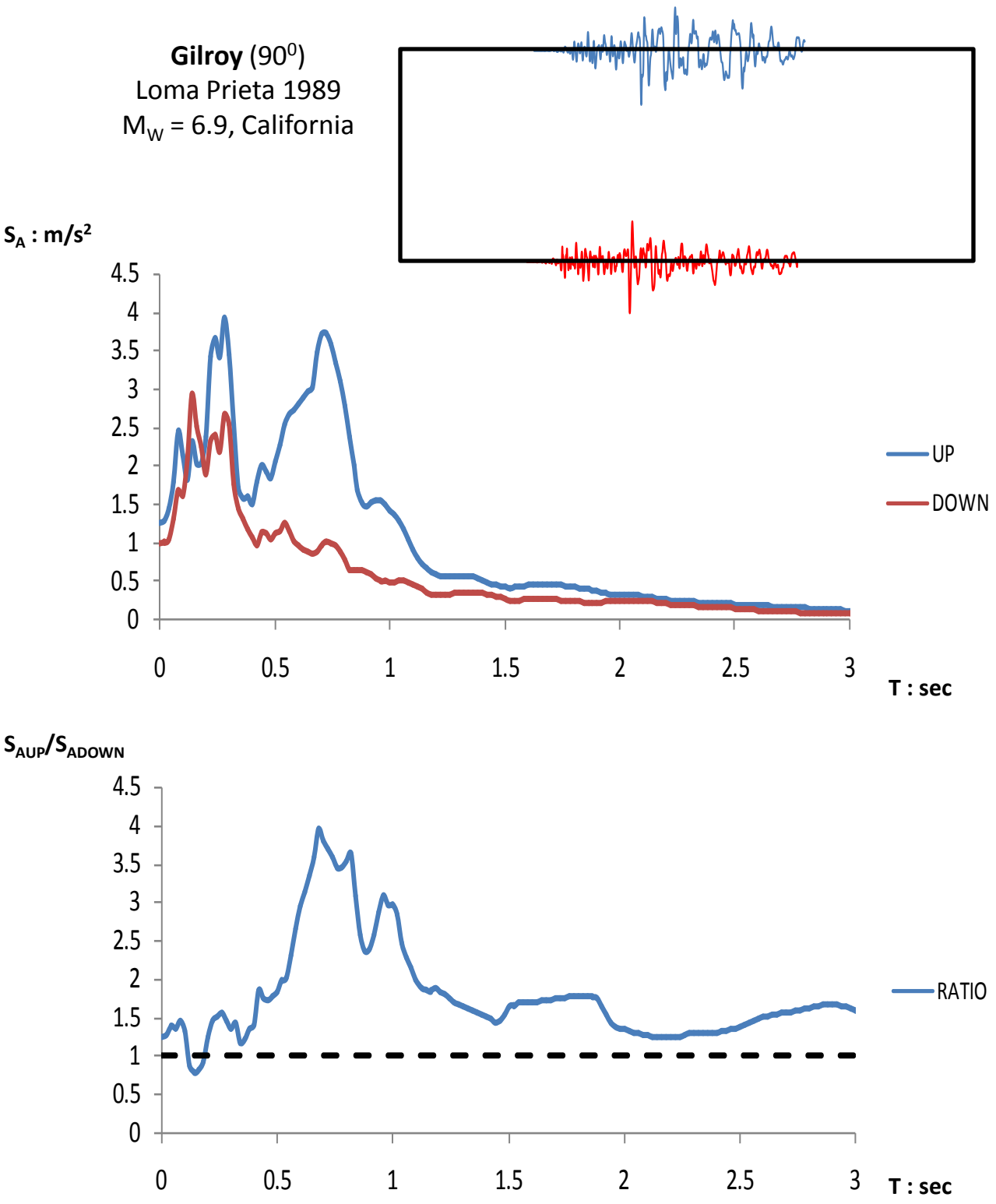

Figure 2.23 Elastic Response Spectra (ξ = 5 %) Free Field UP and DOWN for Gilroy (90 °)

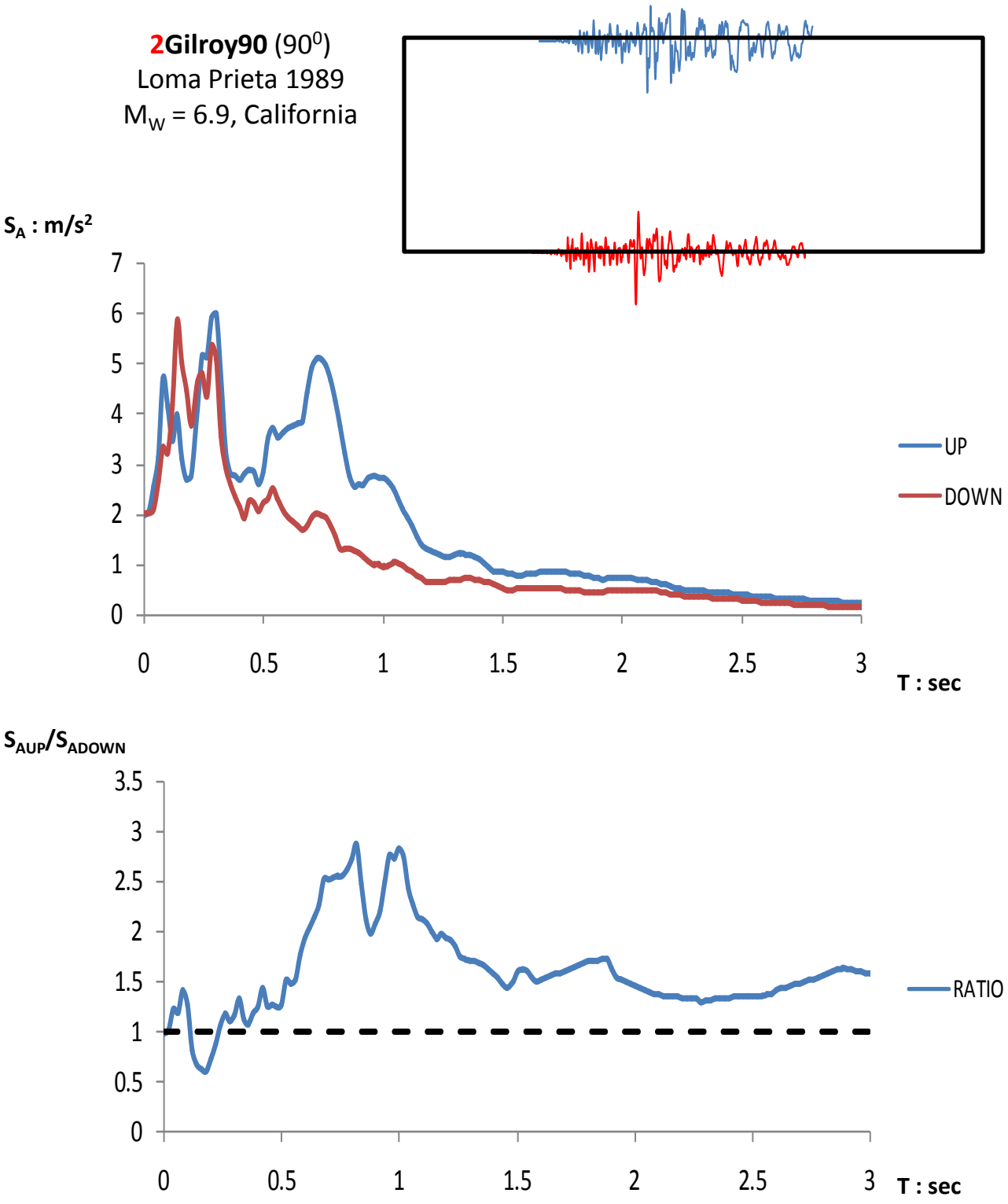

Figure 2.24 Elastic Response Spectra (ξ = 5 %) Free Field UP and DOWN for 2Gilroy (90 ^{o})

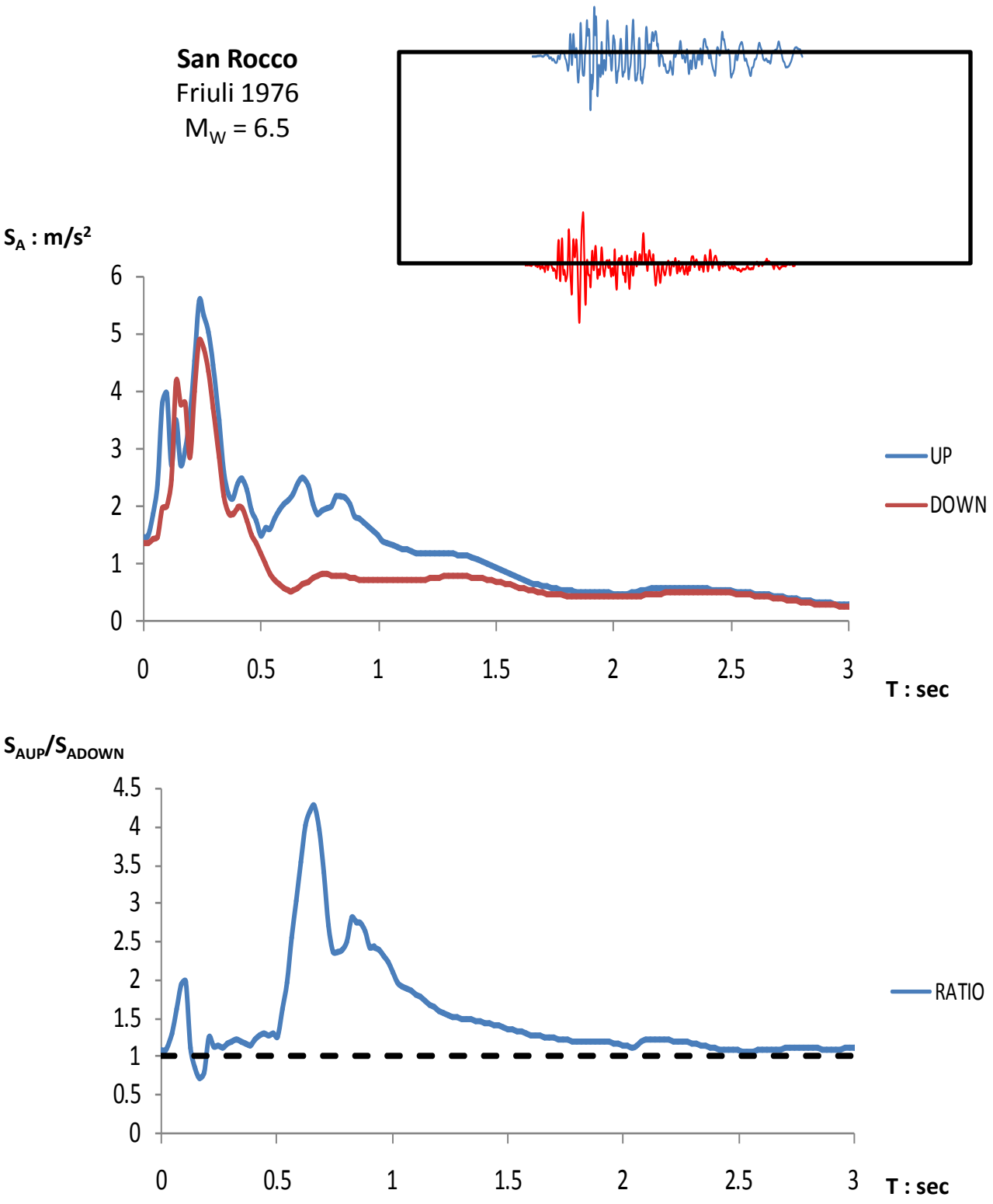

Figure 2.25 Elastic Response Spectra (ξ = 5 %) Free Field UP and DOWN for San Rocco

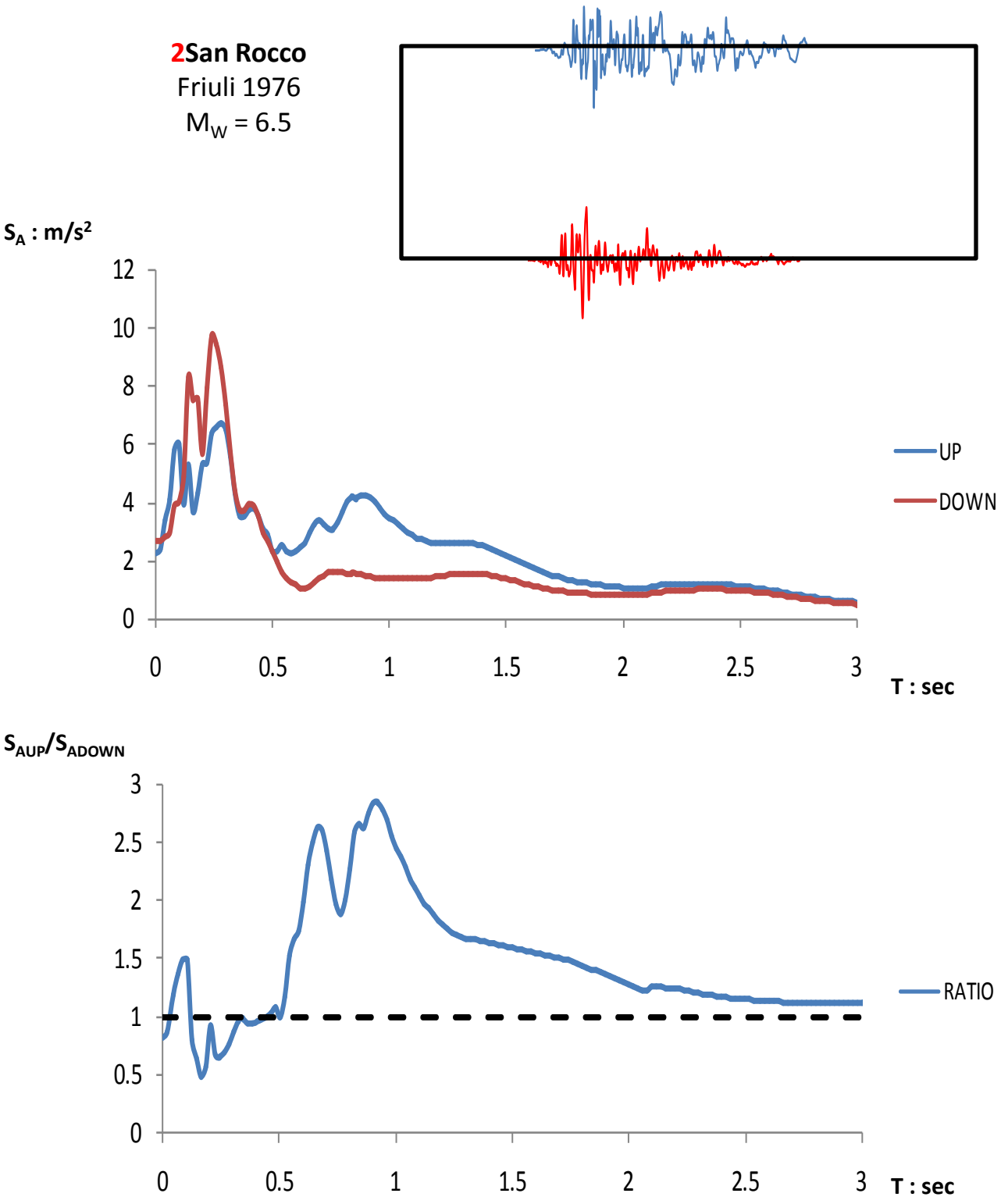

Figure 2.26 Elastic Response Spectra (ξ = 5 %) Free Field UP and DOWN for 2San Rocco

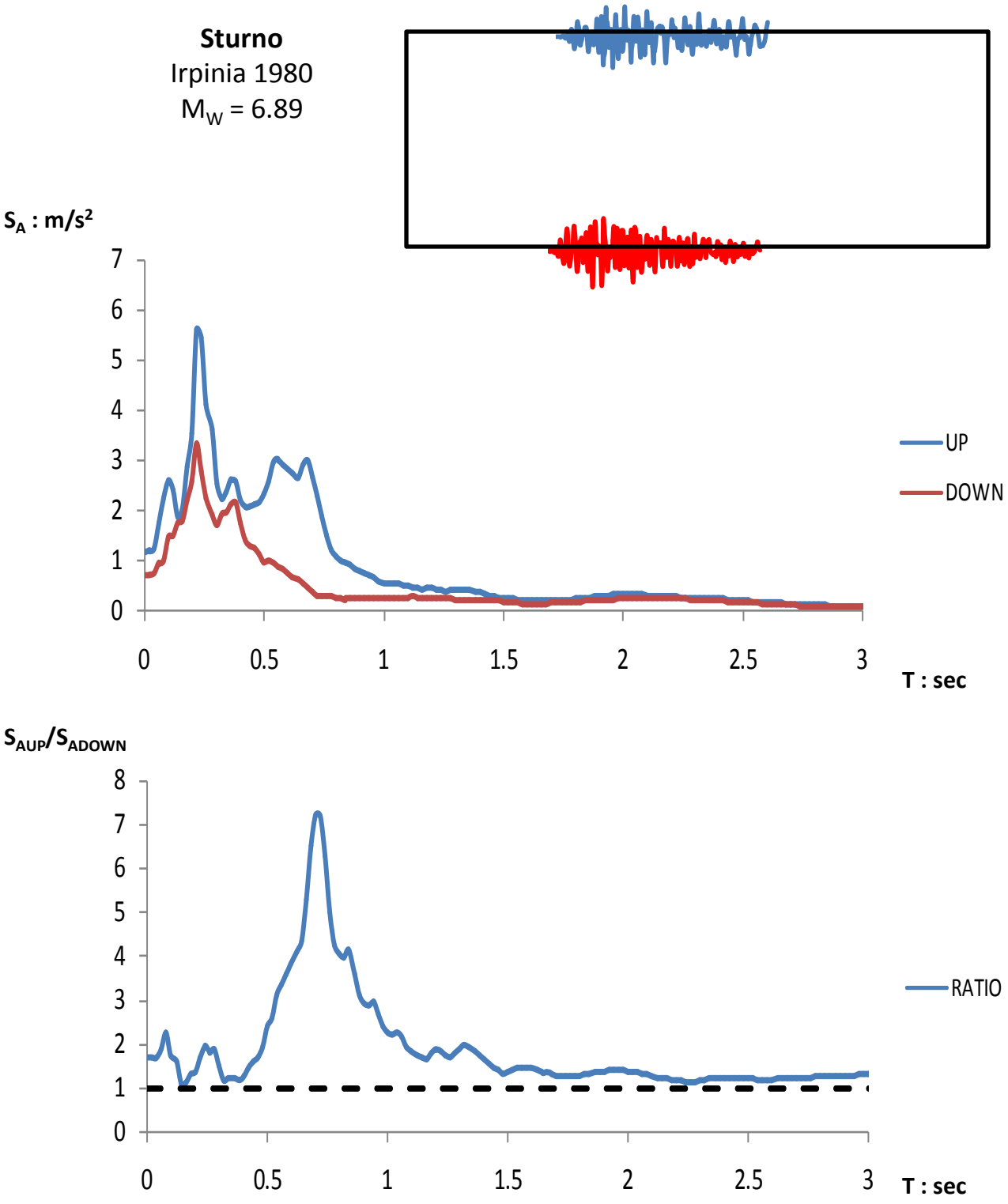

Figure 2.27 Elastic Response Spectra (ξ = 5 %) Free Field UP and DOWN for Sturno

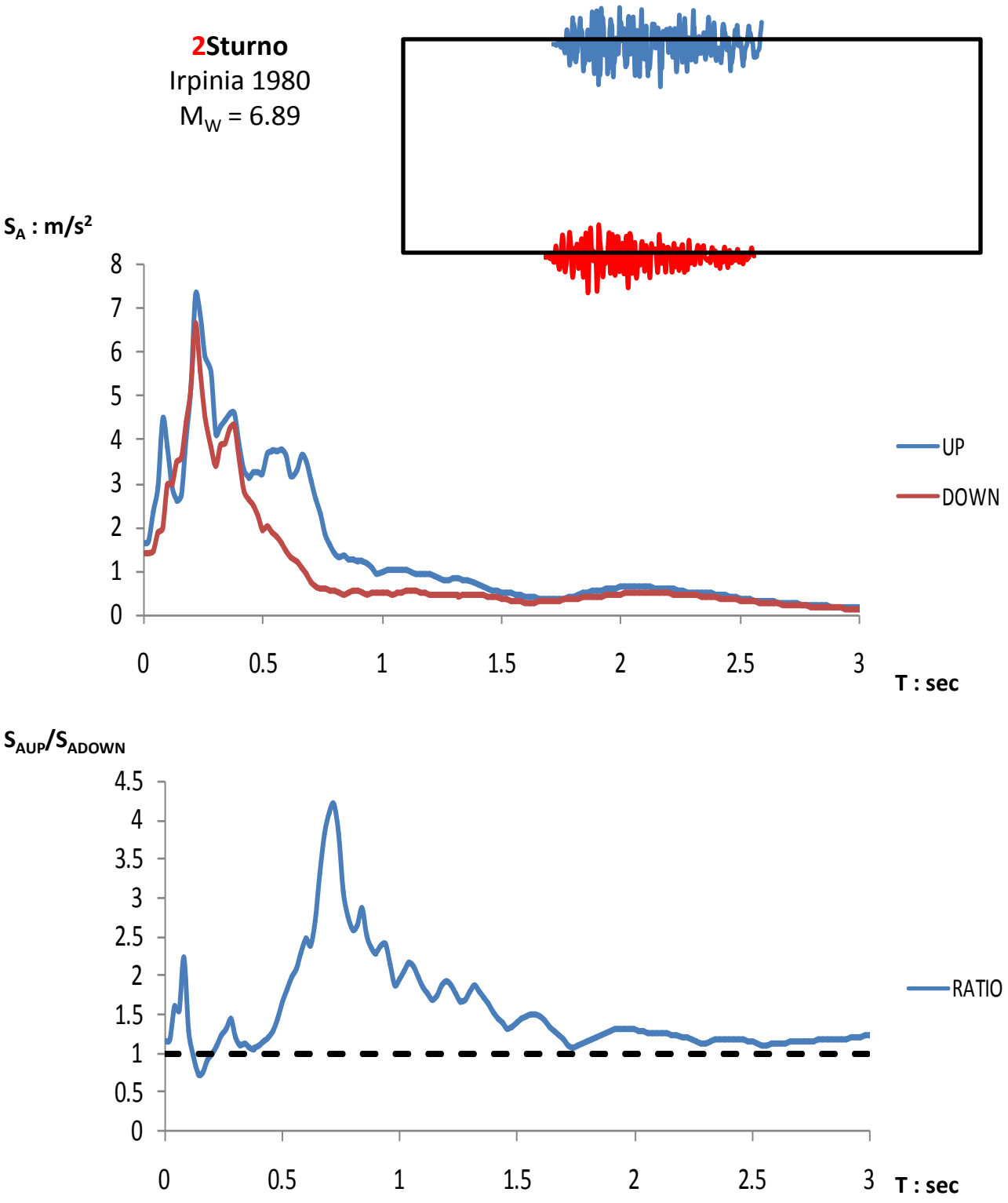

Figure 2.28 Elastic Response Spectra (ξ = 5 %) Free Field UP and DOWN for 2Sturno

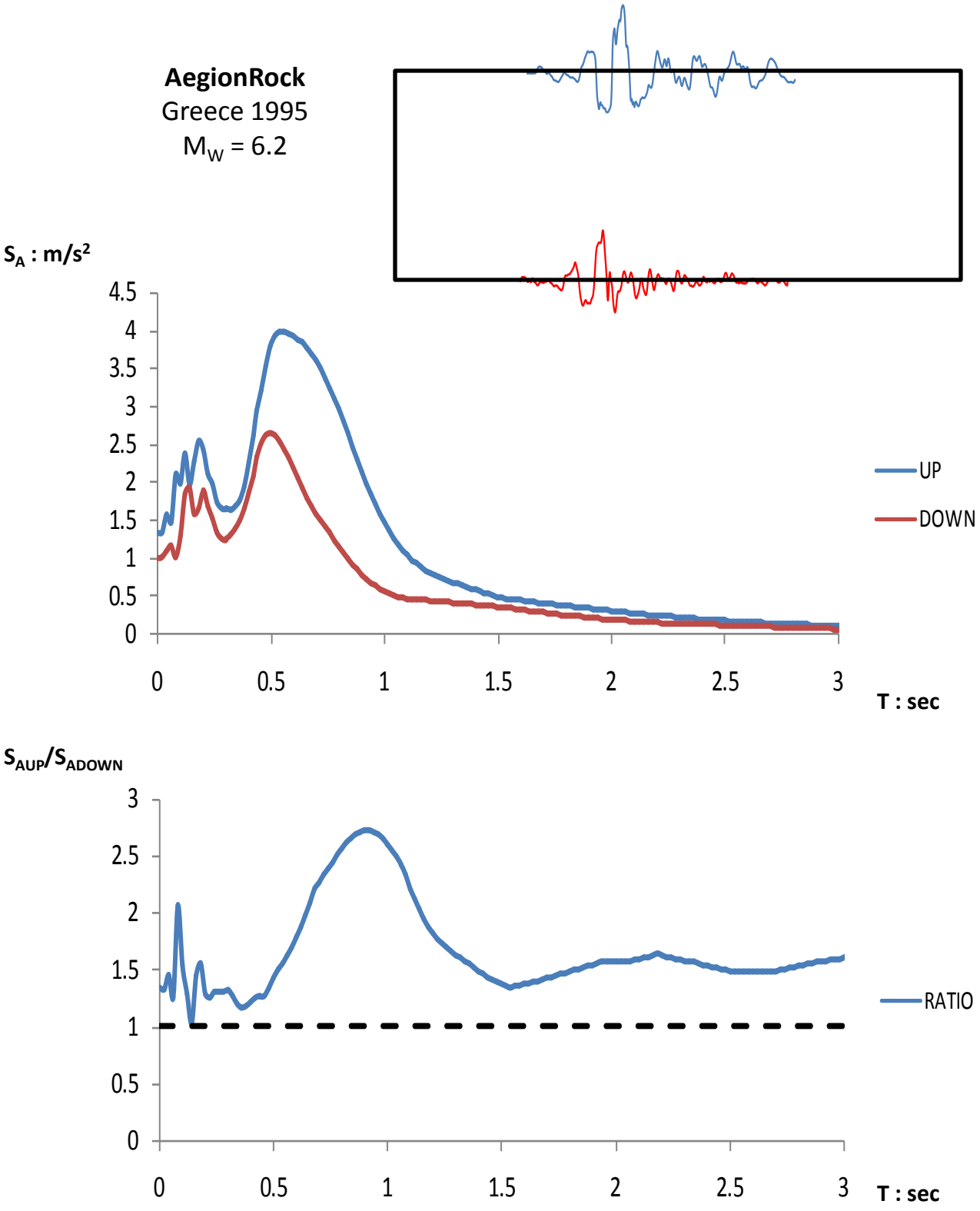

Figure 2.29 Elastic Response Spectra (ξ = 5 %) Free Field UP and DOWN for AegionRock

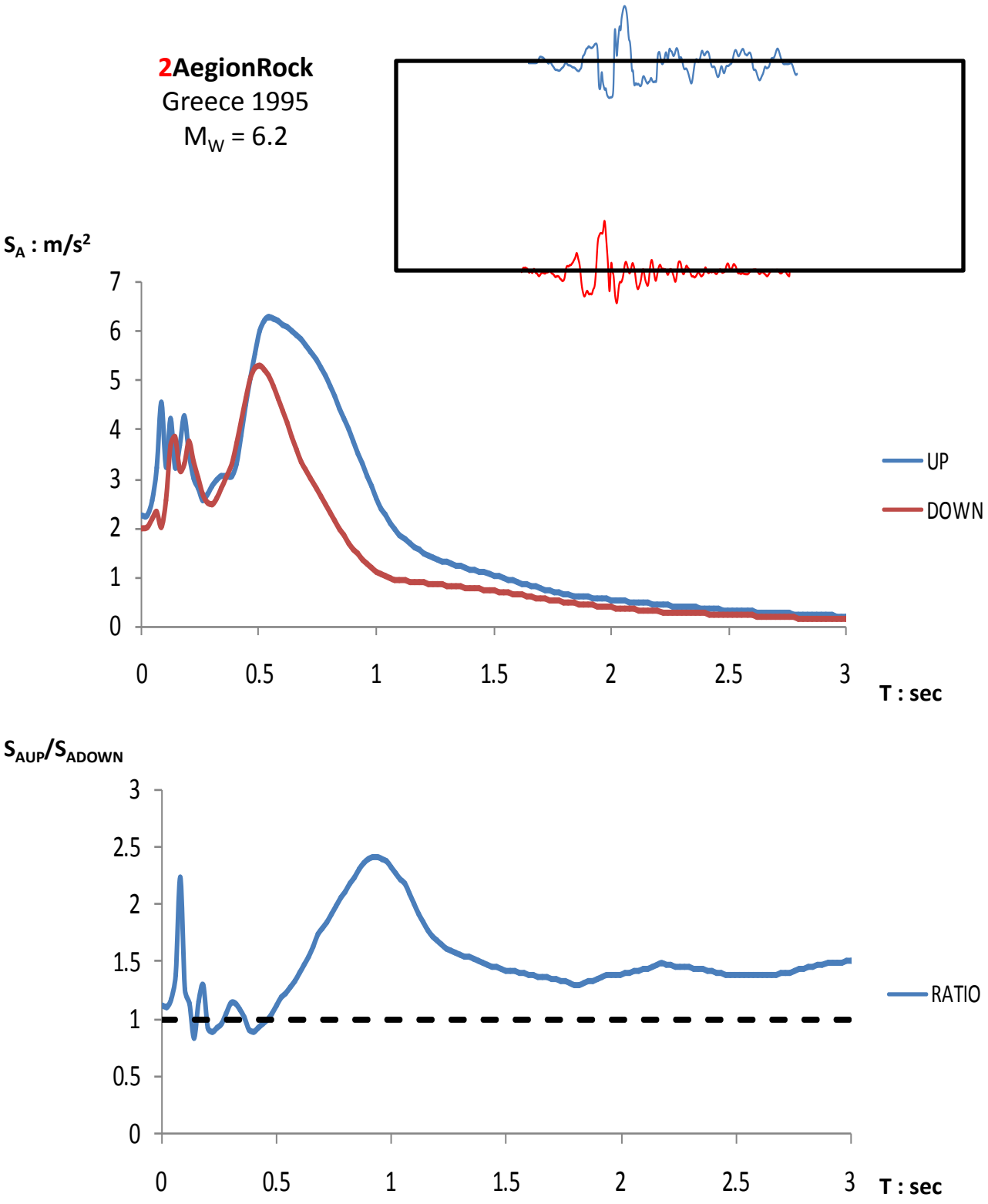

Figure 2.30 Elastic Response Spectra (ξ = 5 %) Free Field UP and DOWN for 2AegionRock

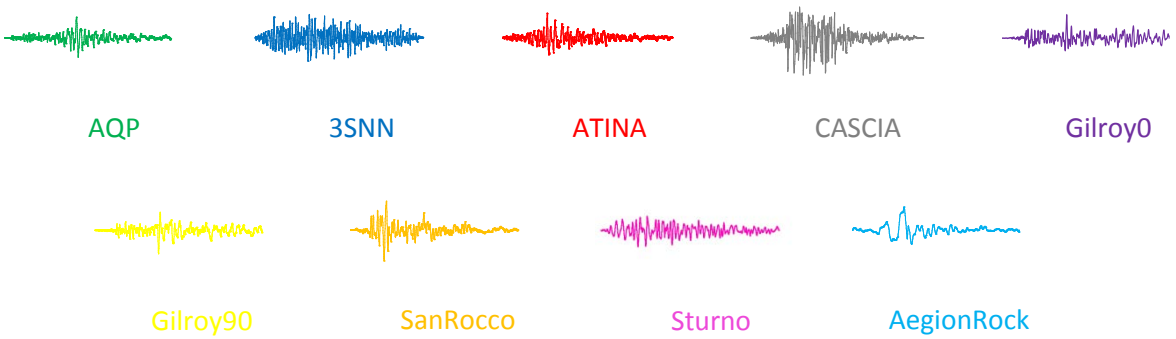

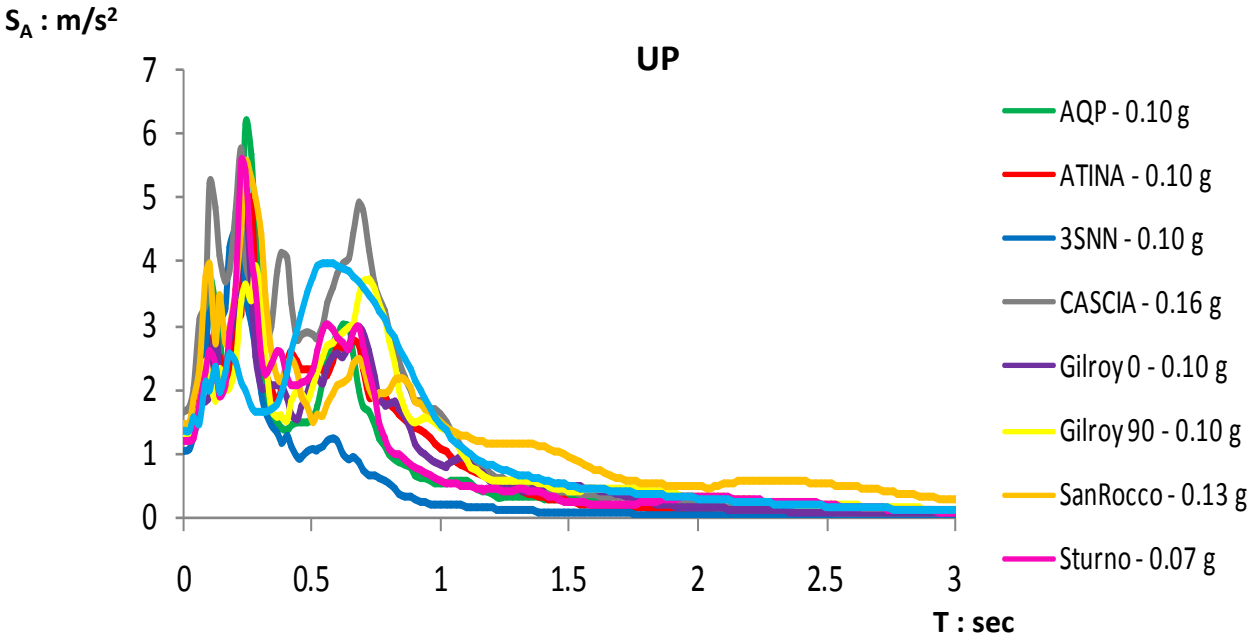

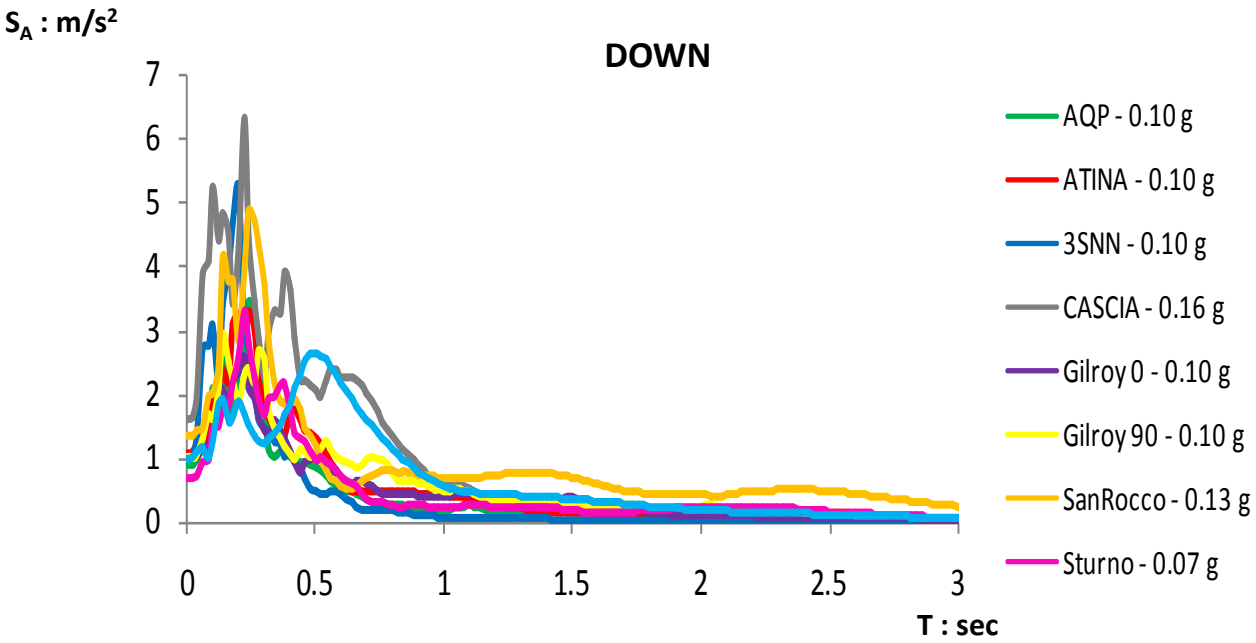

Figure 2.31 Comparison of Elastic Response Spectra (ξ = 5 %) Free Field UP and DOWN for excitations with peak ground acceleration between 0.07 g and 0.16 g.

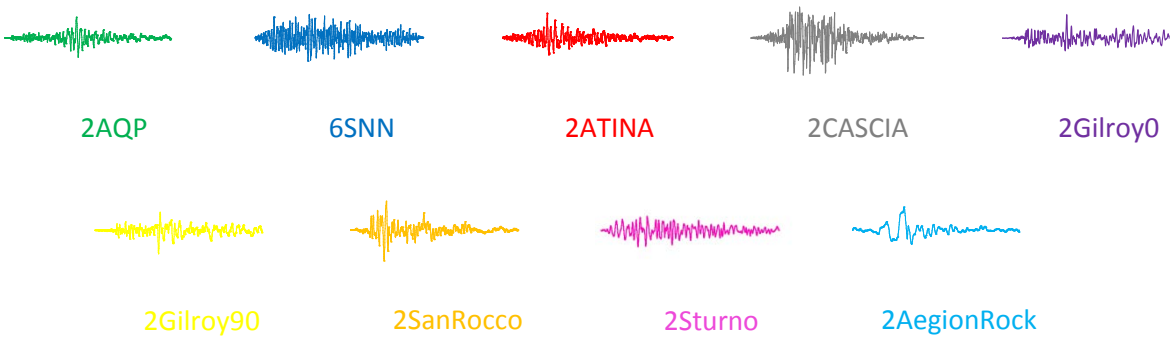

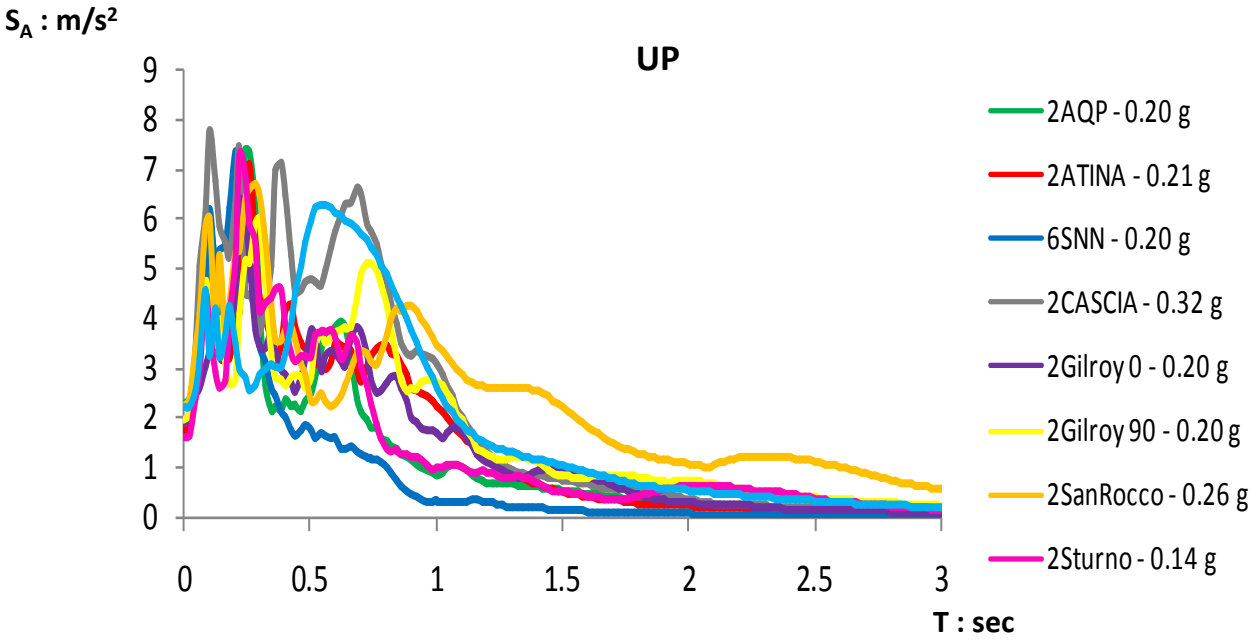

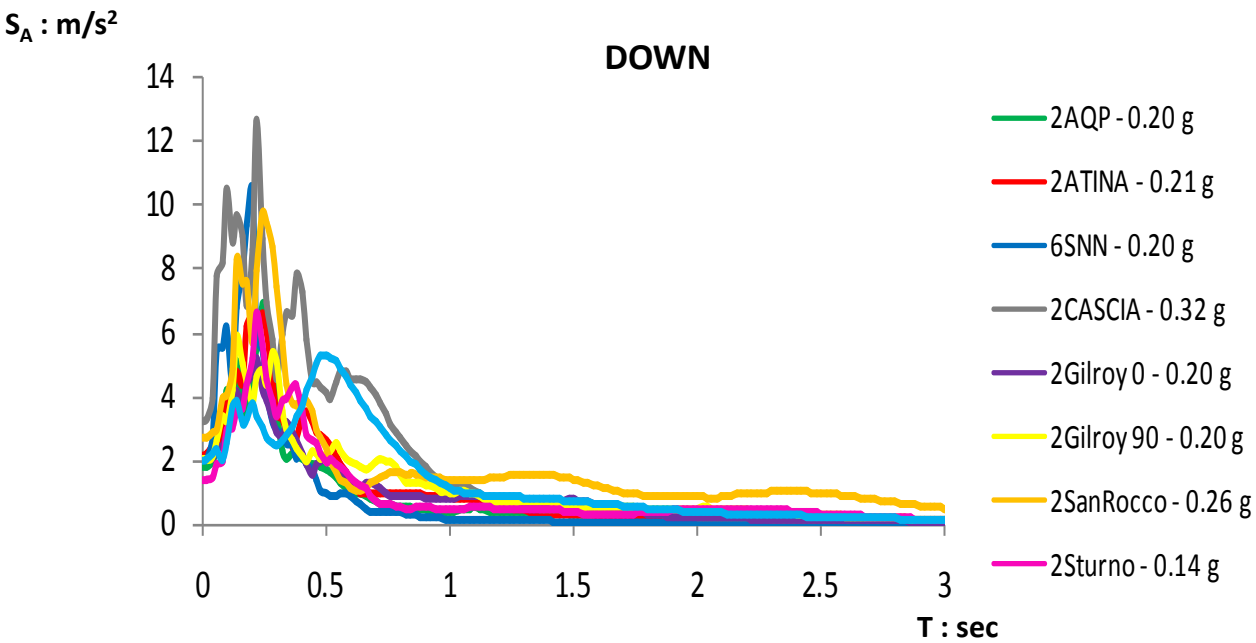

Figure 2.32 Comparison of Elastic Response Spectra (ξ = 5 %) Free Field UP and DOWN for excitations with peak ground acceleration between 0.14 g and 0.32 g.

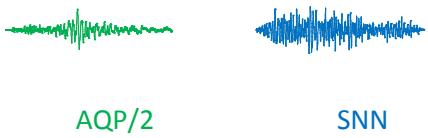

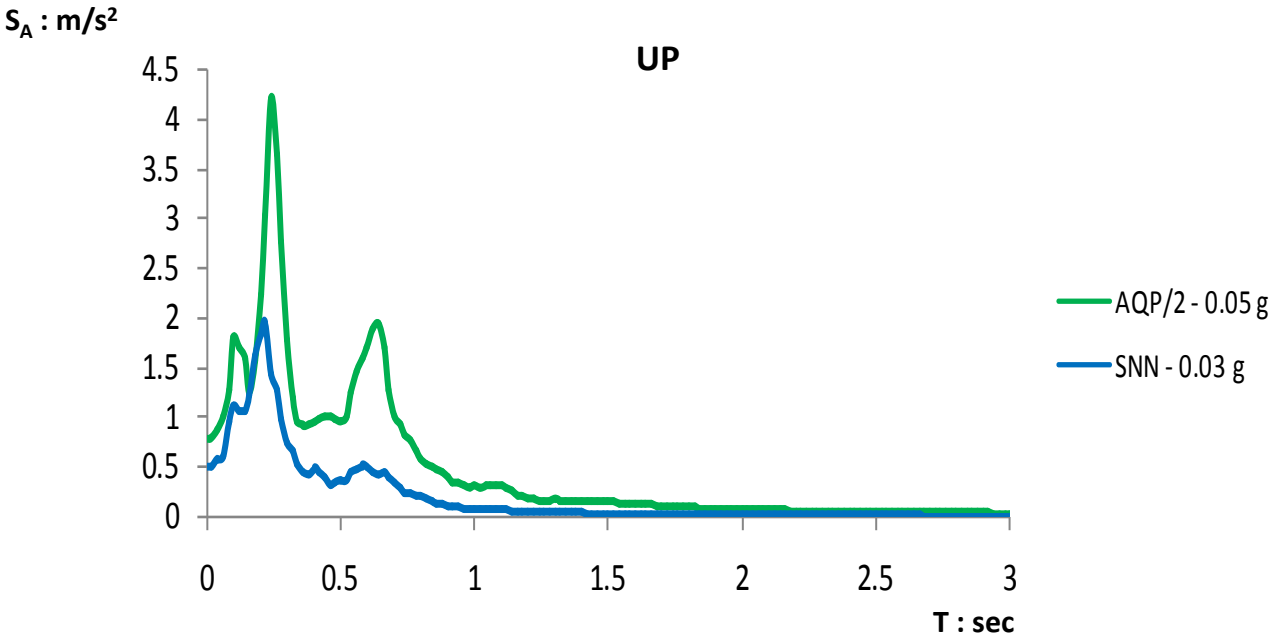

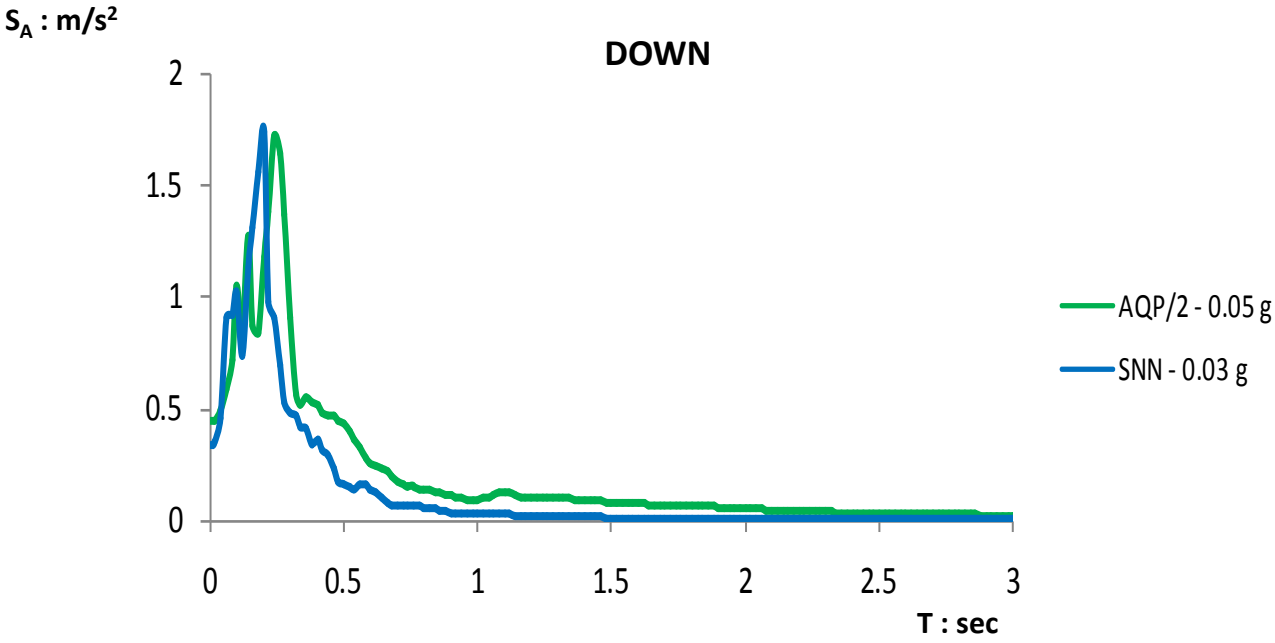

Figure 2.33 Comparison of Elastic Response Spectra (ξ = 5 %) Free Field UP and DOWN for excitations with peak ground acceleration between 0.03 g and 0.05 g.

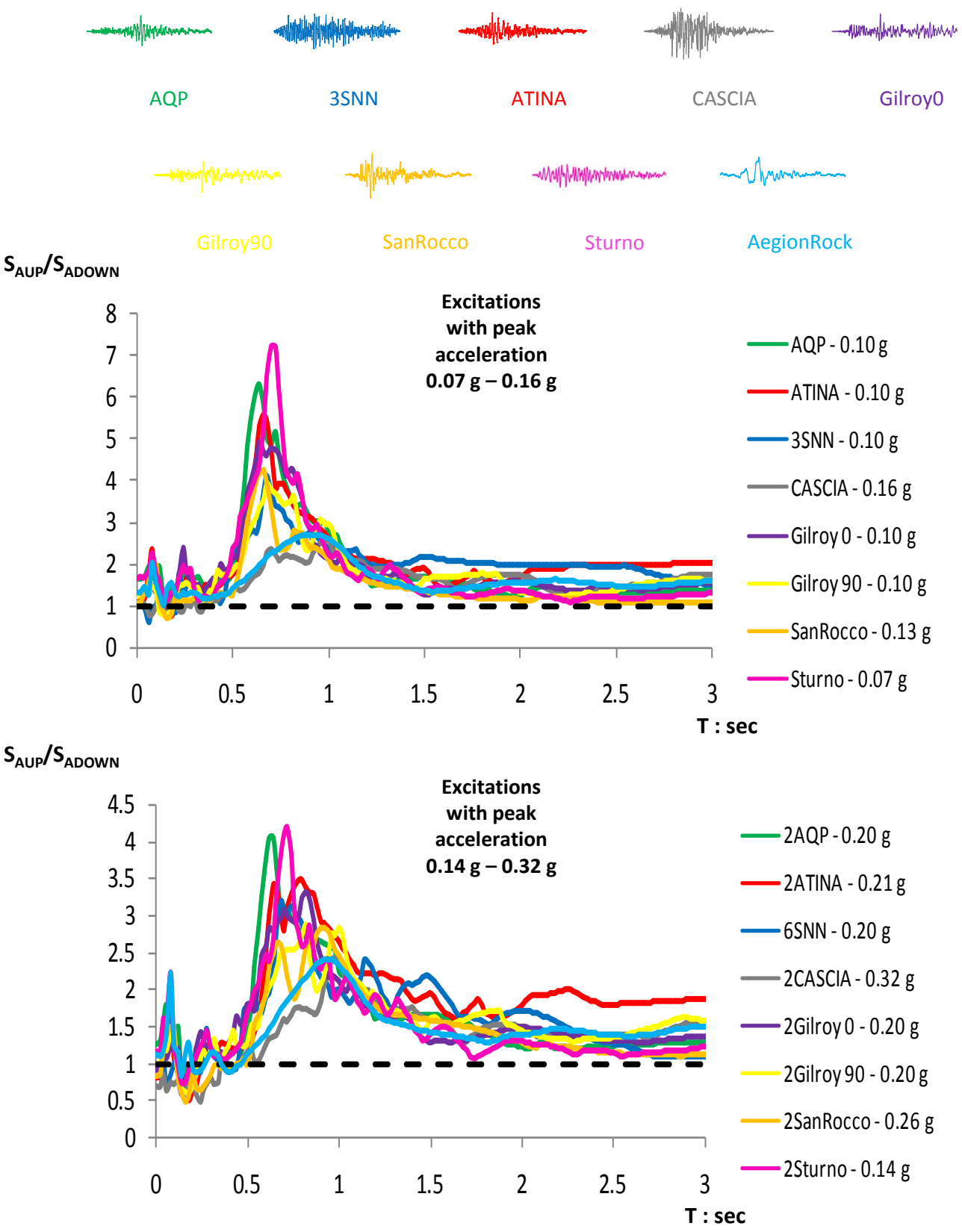

Figure 2.34 Comparison of Ampliication Free Field UP and DOWN for excitations with peak ground acceleration between 0.07 g and 0.32 g

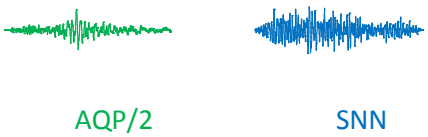

AQP/2 SNN

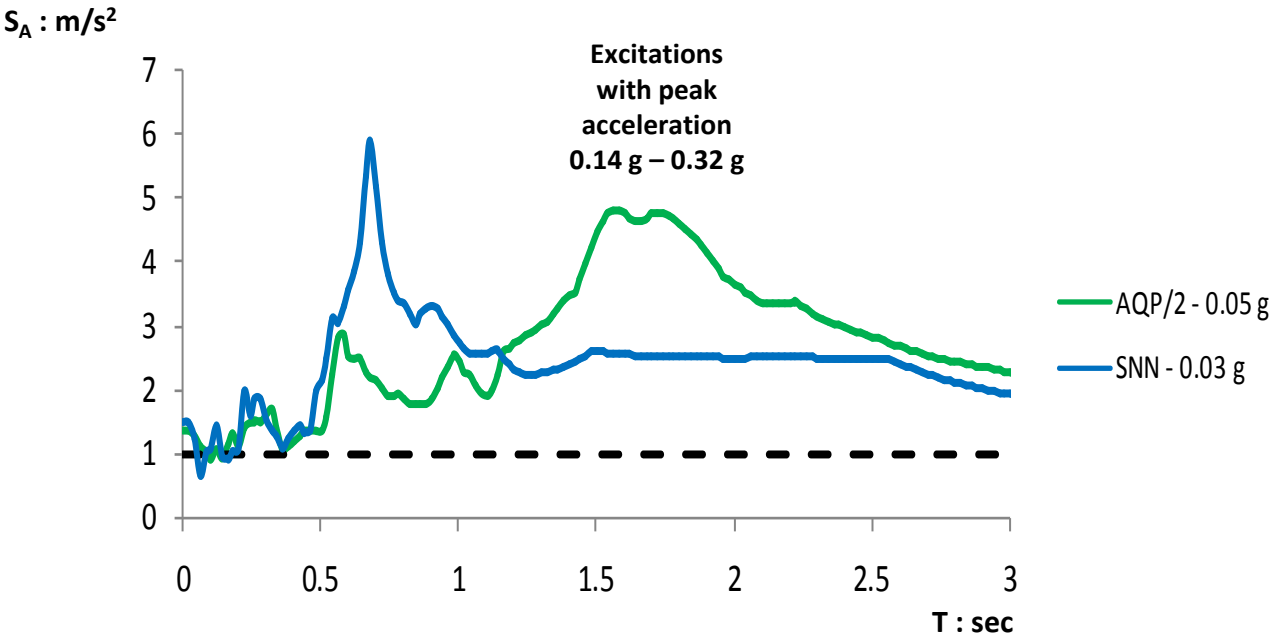

Figure 2.35 Comparison of Ampliication Free Field UP and DOWN for excitations with peak ground acceleration between 0.03 g and 0.05 g

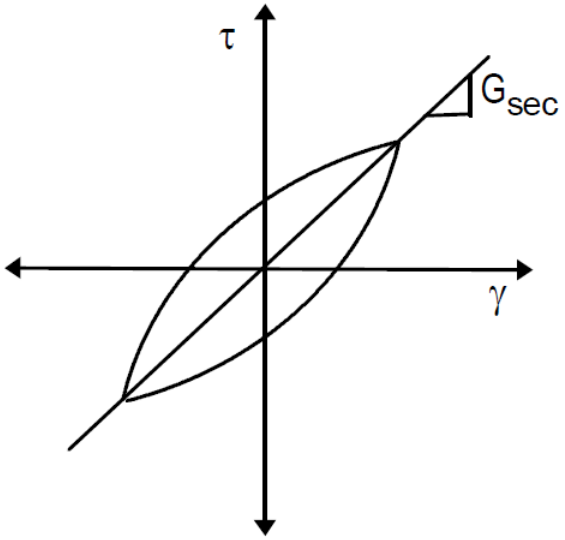

Figure 2.36 Secant shear modulus G over an entire cycle of loading

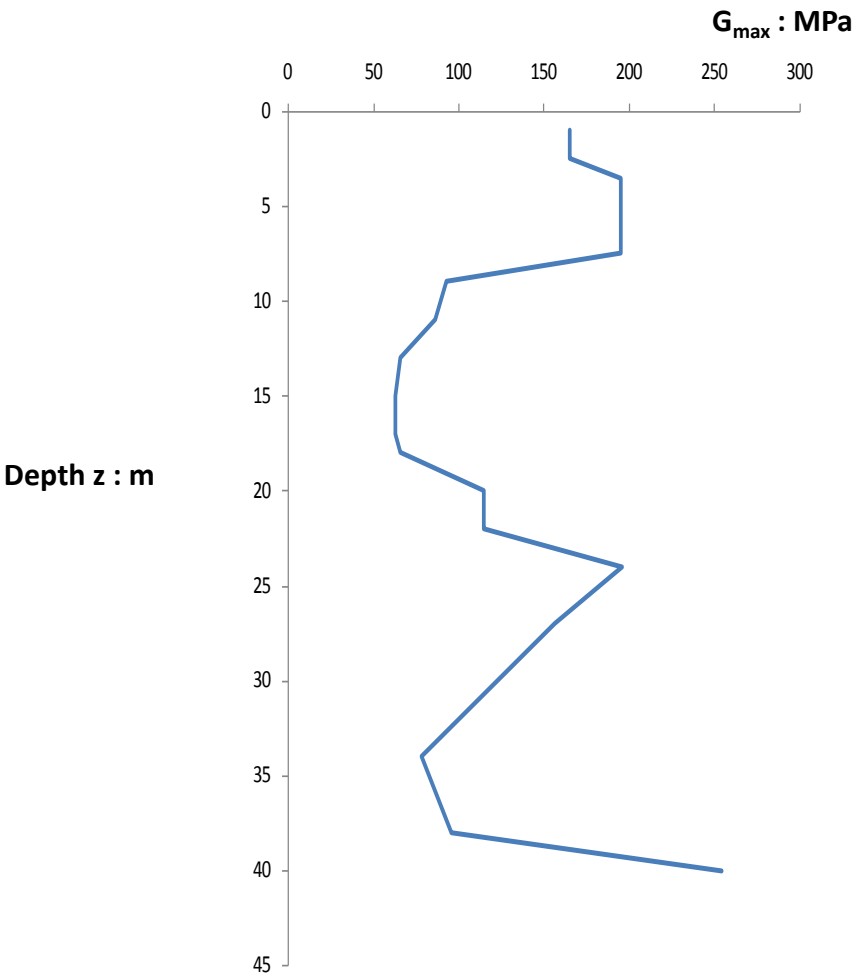

Figure 2.37 Maximum shear modulus G_{max} for the soil underneath the Tower of Pisa

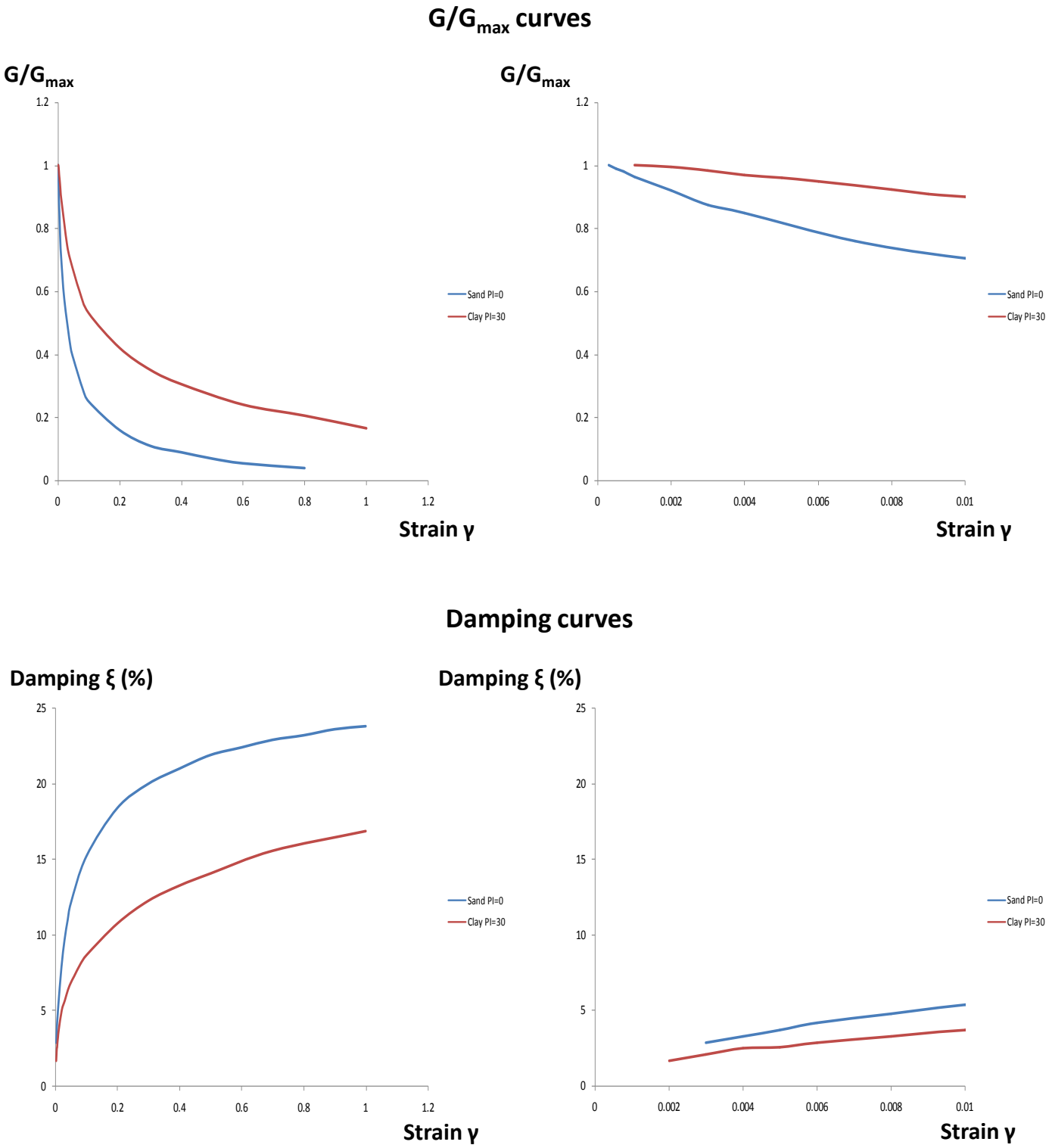

Figure 2.38 Vucetic and Dobry curves for sand PI = 0 and clay PI = 15

G/G_{max} curves

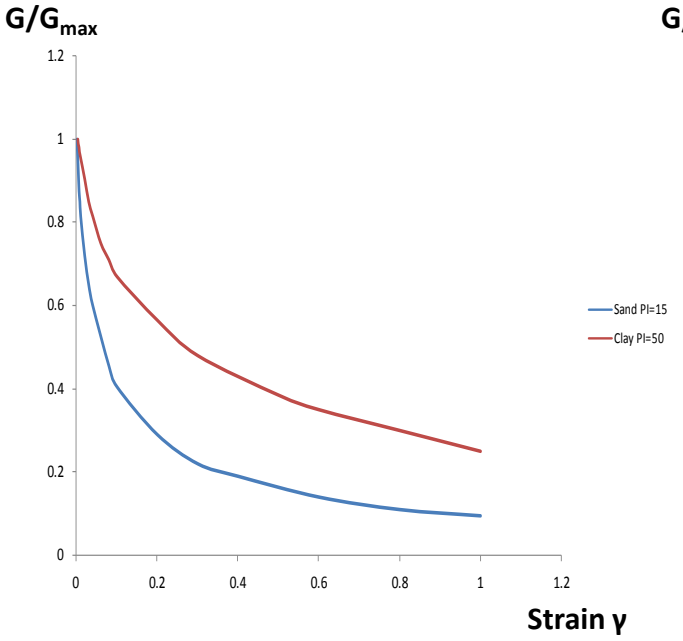

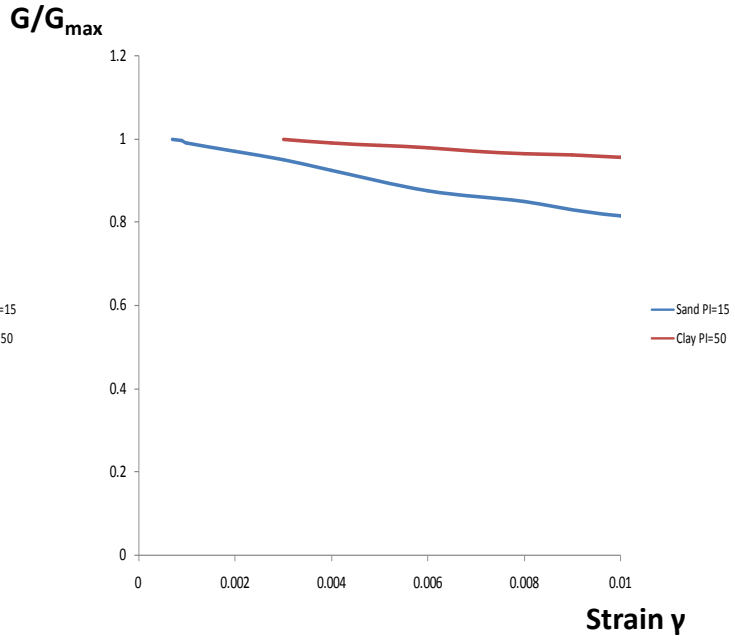

Damping curves

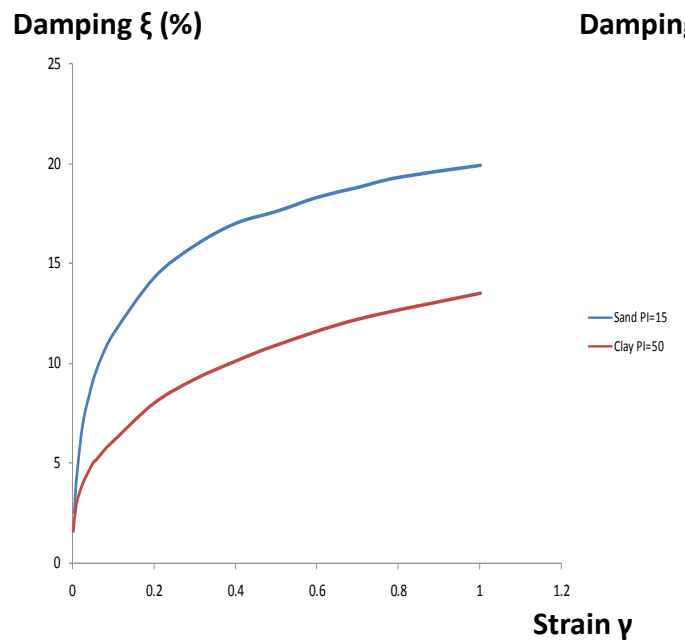

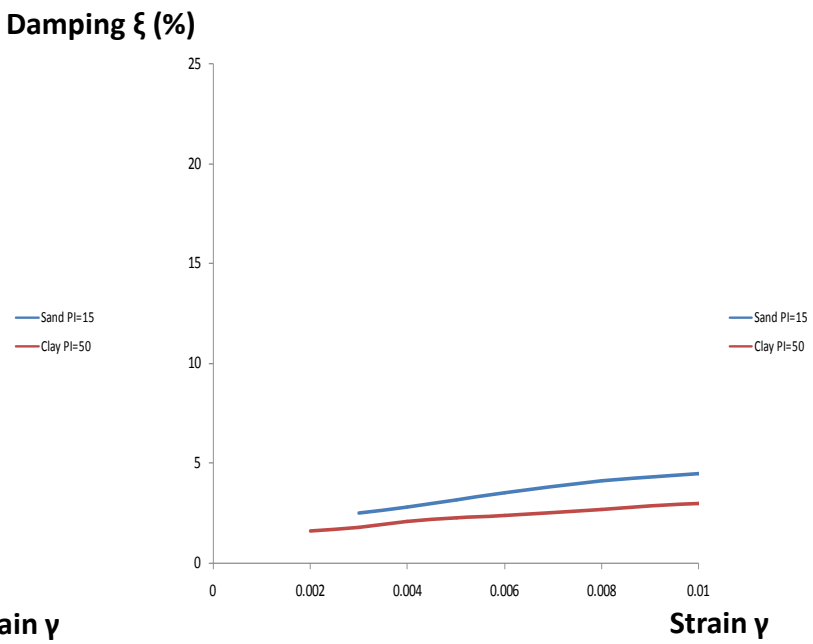

Figure 2.39 Vucetic and Dobry curves for sand PI = 15 and clay PI = 50

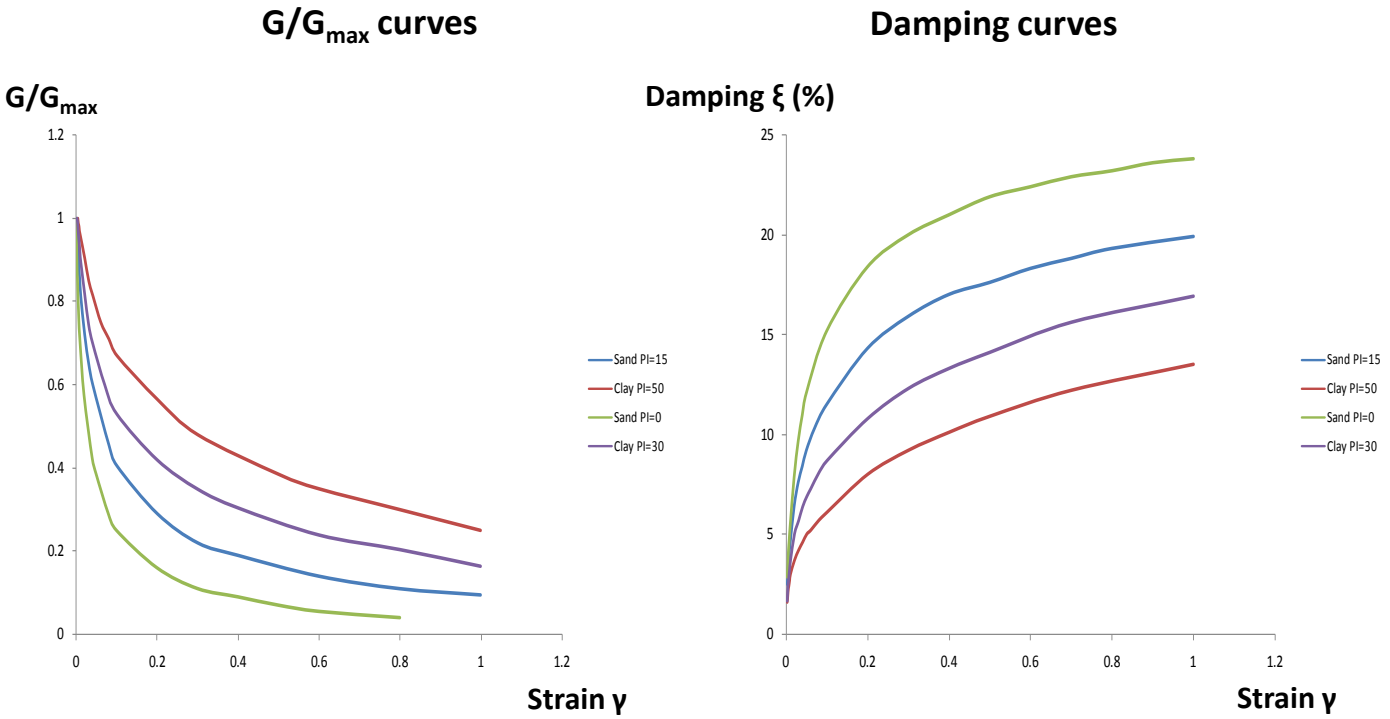

Figure 2.40 Vucetic and Dobry curves for various plasticity indexes PI = 0 -15 -30 - 50

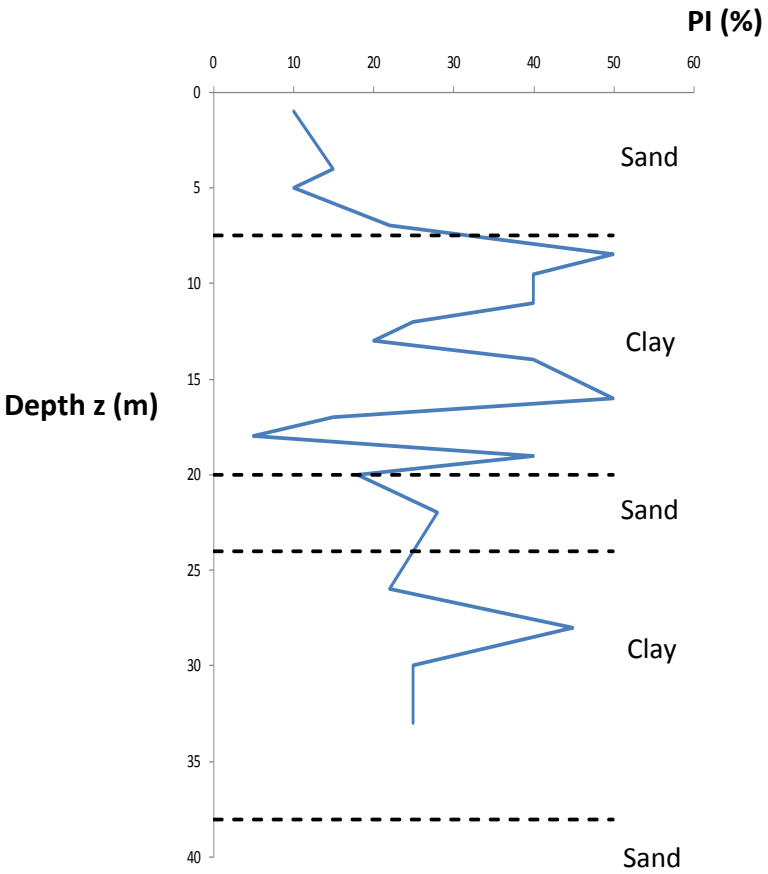

Figure 2.41 PI for the soil underneath the Tower of Pisa

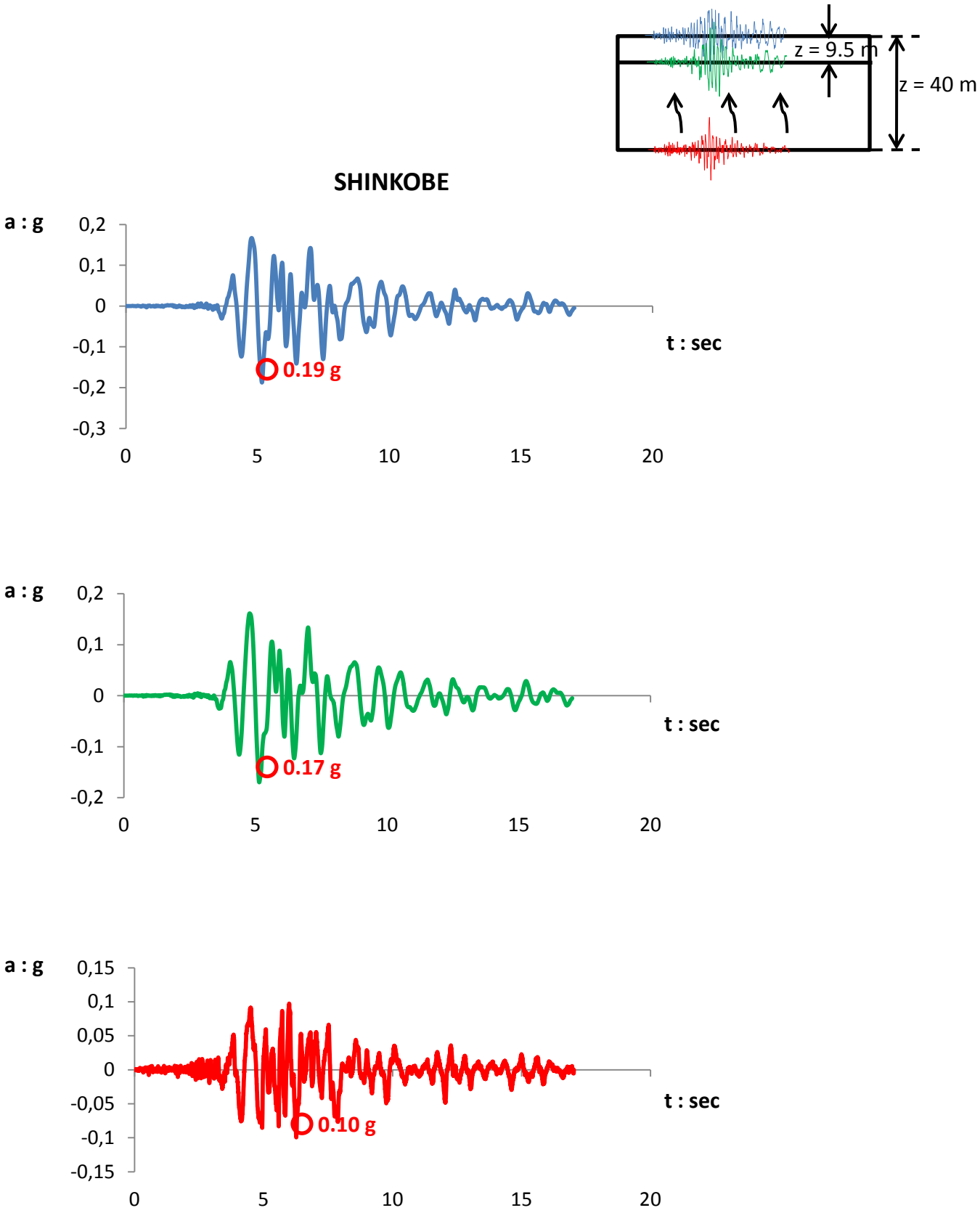

Figure 2.42 Accelerograms at depths 0 – 9.5 – 40 m from SHAKE for Shinkobe (Peak acceleration 0.10 g)

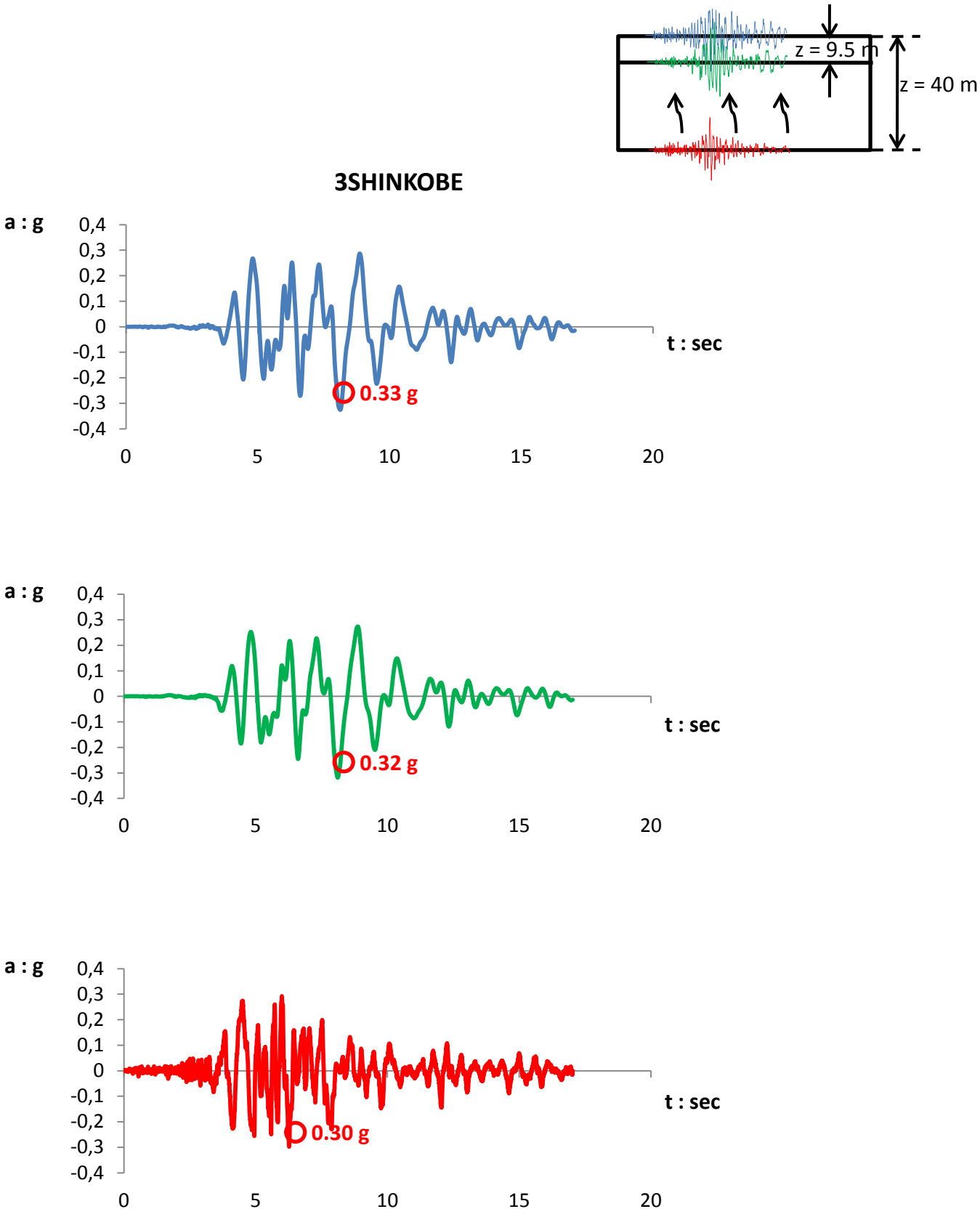

Figure 2.43 Accelerograms at depths 0 – 9.5 – 40 m from SHAKE for 3Shinkobe (Peak acceleration 0.30 g)

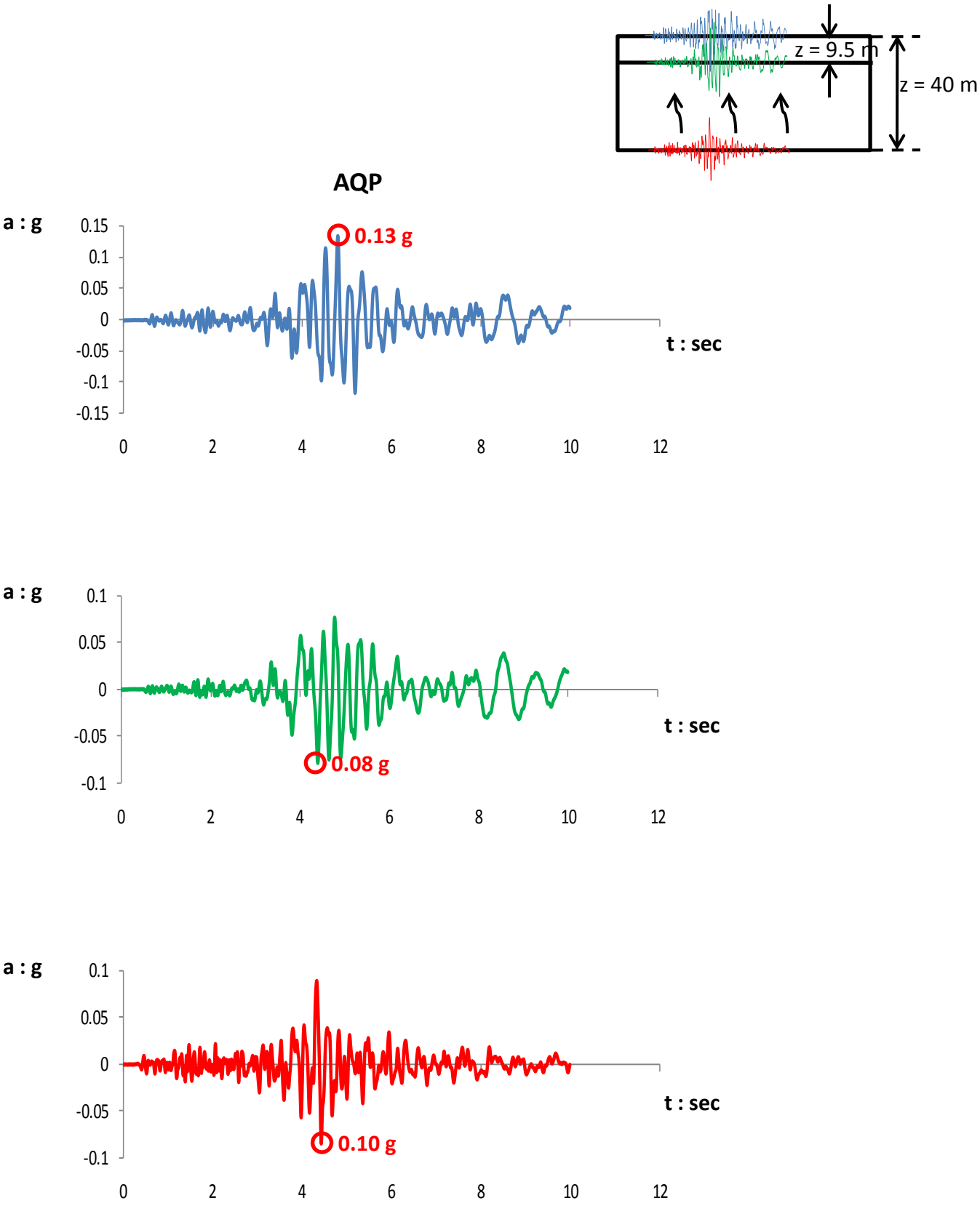

Figure 2.44 Accelerograms at depths 0 – 9.5 – 40 m from SHAKE for AQP (Peak acceleration 0.10 g)

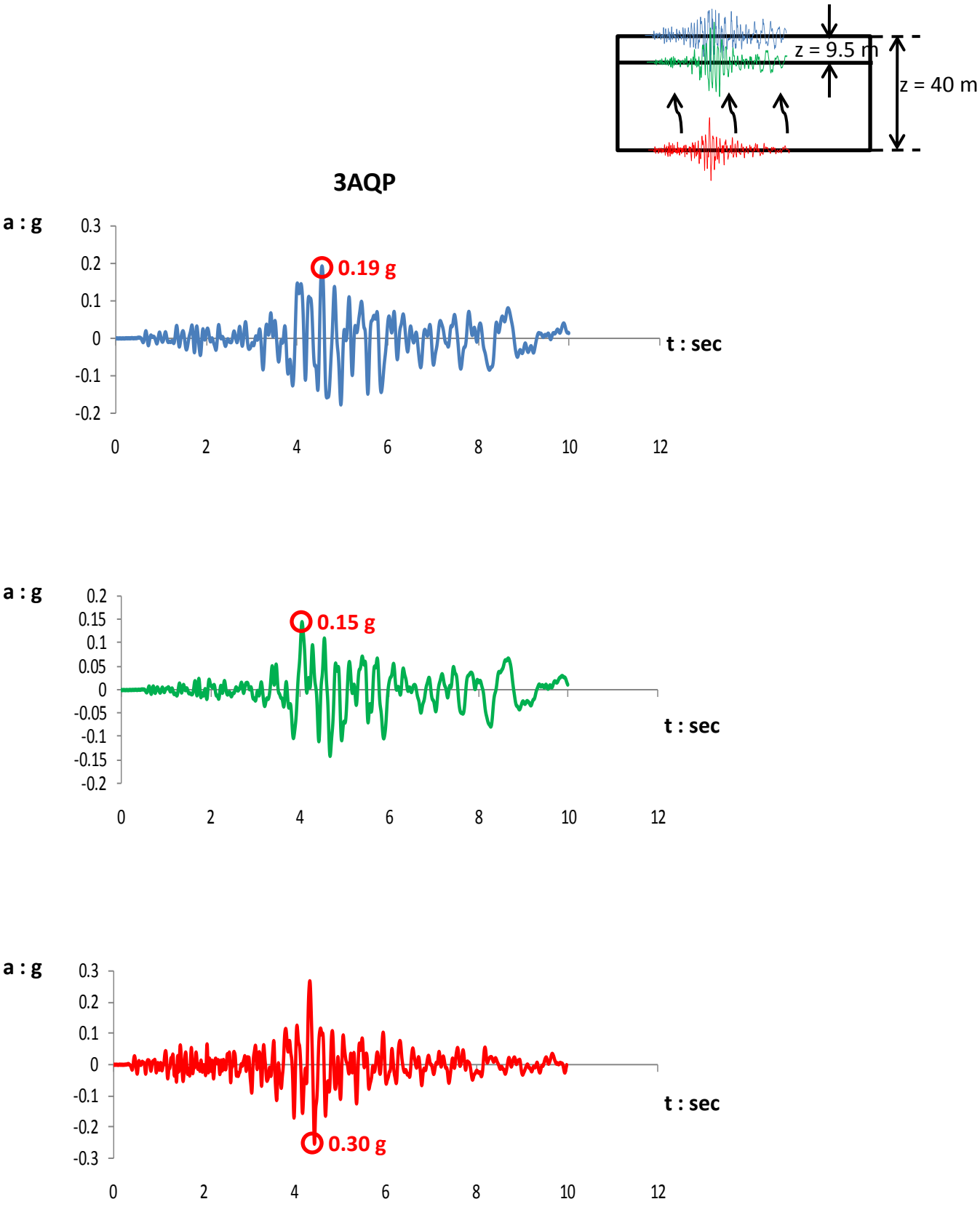

Figure 2.45 Accelerograms at depths 0 – 9.5 – 40 m from SHAKE for 3AQP (Peak acceleration 0.30 g)

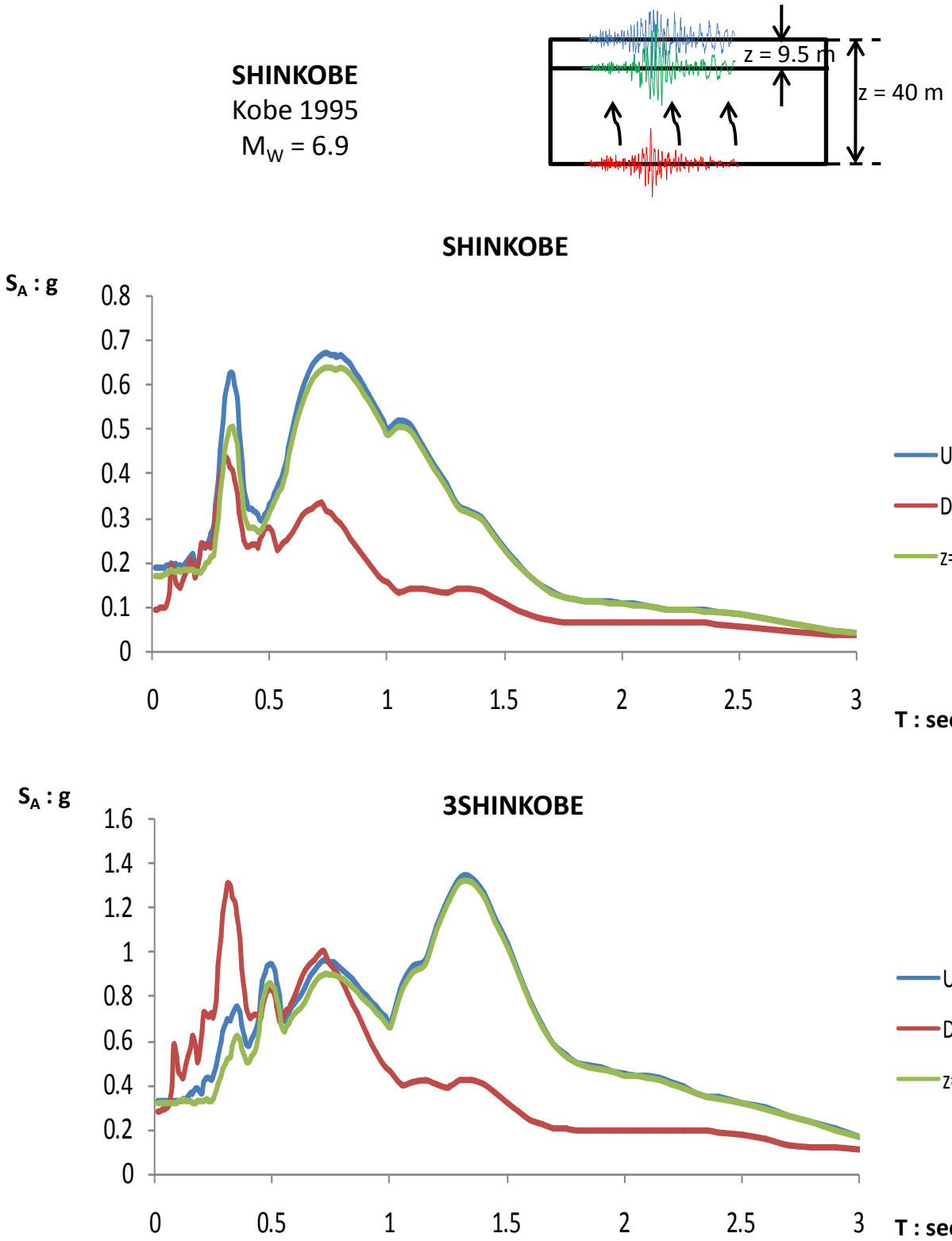

Figure 2.46 Elastic Response Spectra (ξ = 5 %) Free Field UP and DOWN for Shinkobe (Peak acceleration 0.10 g) and 3Shinkobe (Peak acceleration 0.30 g)

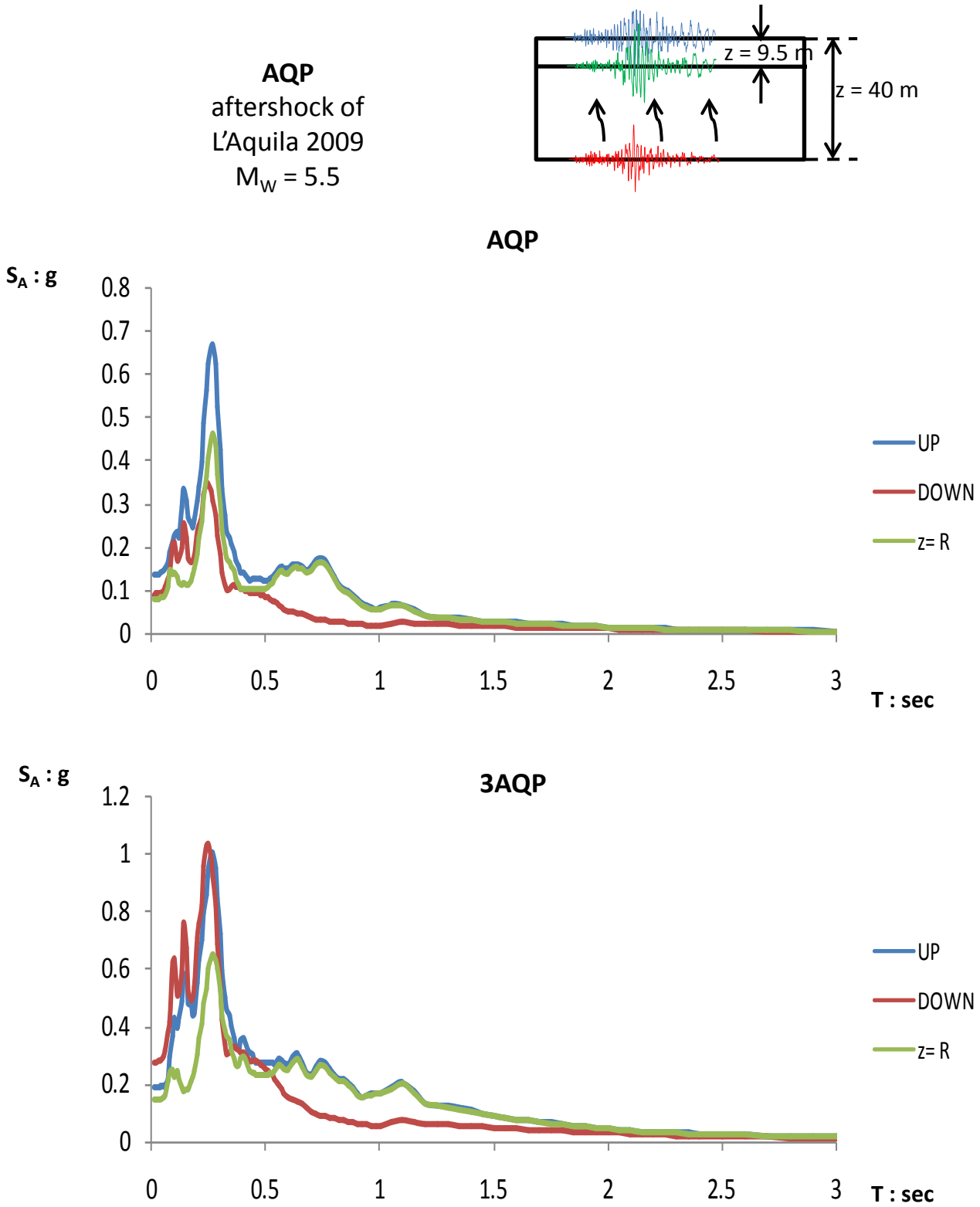

Figure 2.47 Elastic Response Spectra (ξ = 5 %) Free Field UP and DOWN for AQP (Peak acceleration 0.10 g) and 3AQP (Peak acceleration 0.30 g)

SHINKOBE

AQP

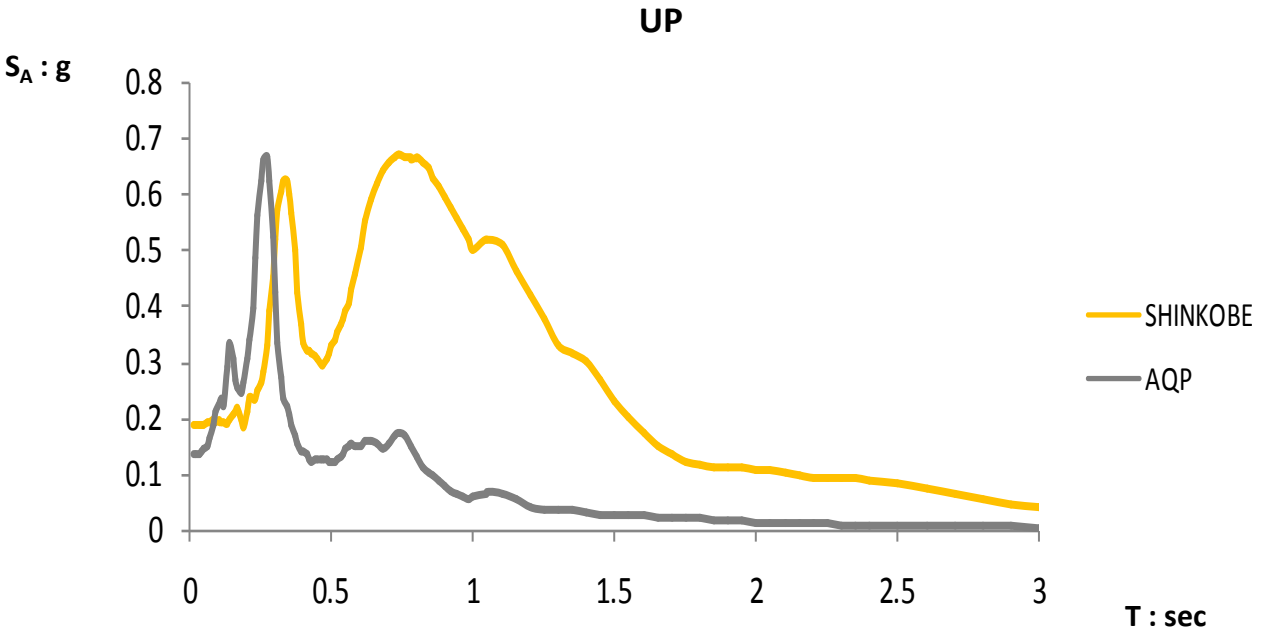

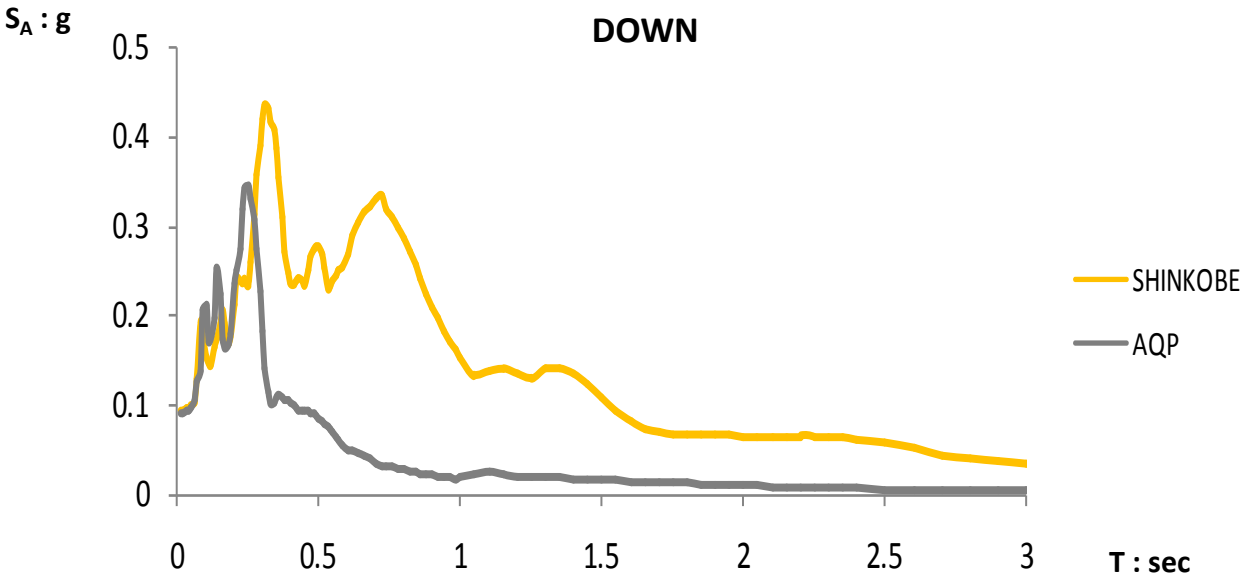

Figure 2.48 Comparison of Elastic Response Spectra (ξ = 5 %) Free Field UP and DOWN between AQP and SHINKOBE (Peak acceleration 0.10 g for both exitations)

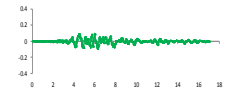

SHINKOBE – 0.10 g

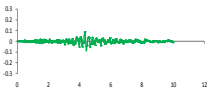

AQP – 0.10 g

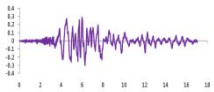

3SHINKOBE – 0.30 g

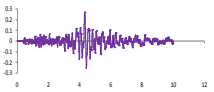

3AQP – 0.30 g

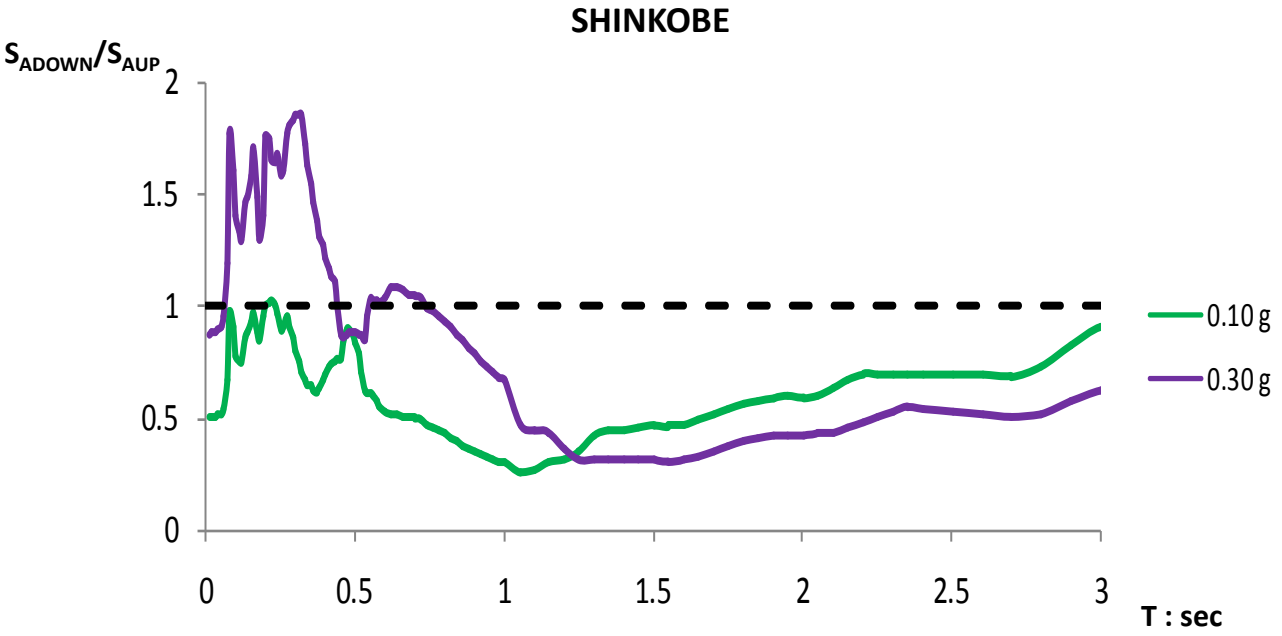

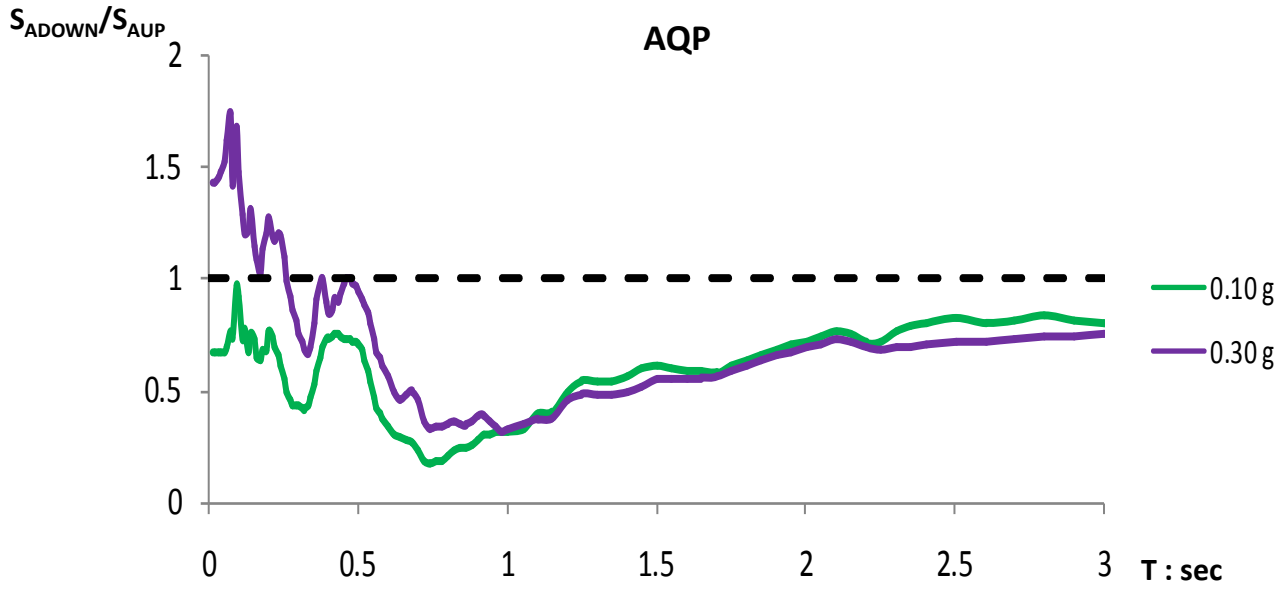

Figure 2.49 Amplification function for AQP - SHINKOBE (Peak acceleration 0.10 g) and 3AQP - 3SHINKOBE (Peak acceleration 0.30 g)

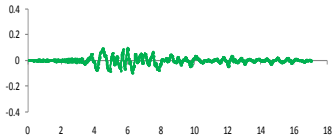

SHINKOBE – 0.10 g

3SHINKOBE – 0.30 g

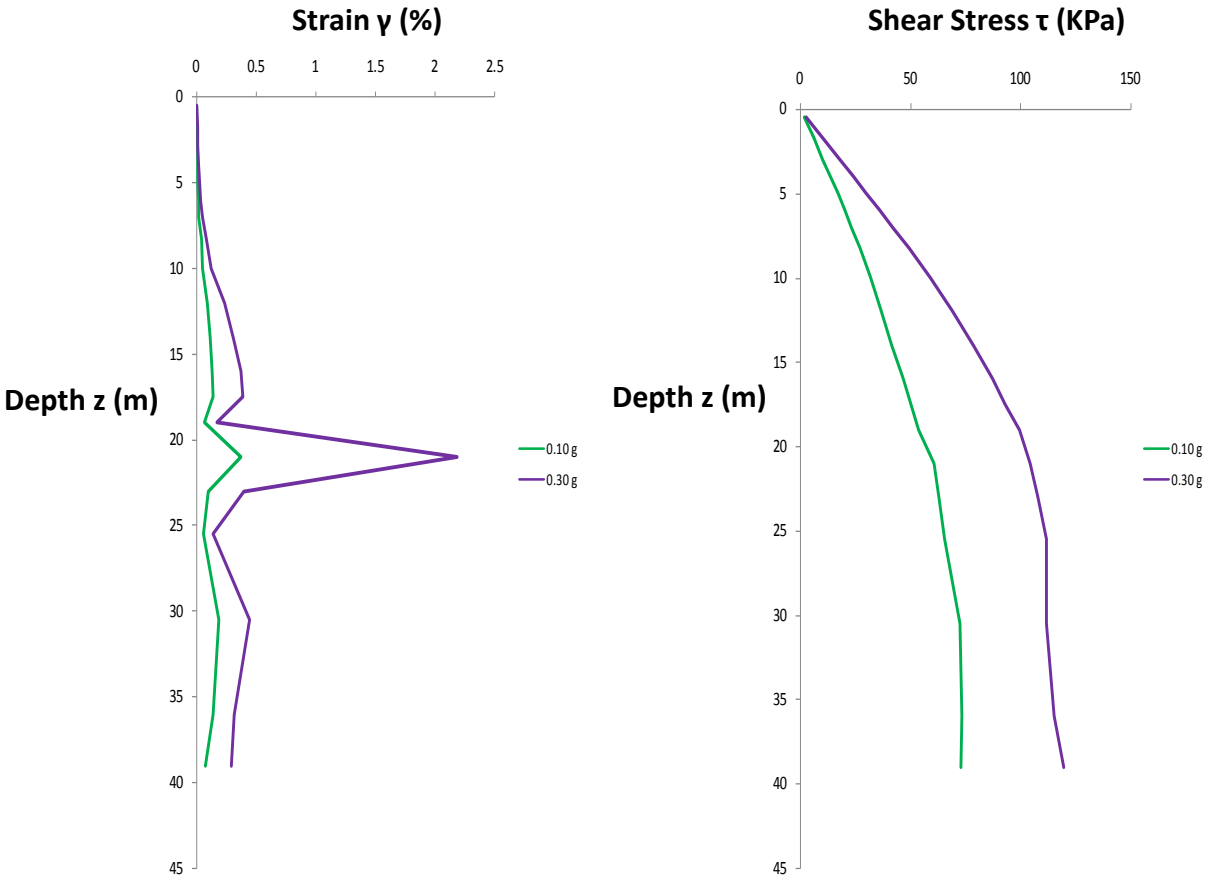

Figure 2.50 Distribution of peak shear stress and strain with depth for SHINKOBE and 3SHINKOBE (Peak acceleration 0.10 g - 0.30 g respectively)

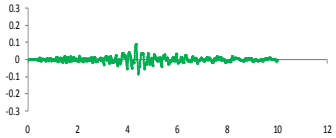

AQP – 0.10 g

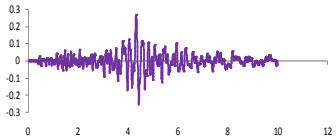

3AQP – 0.30 g

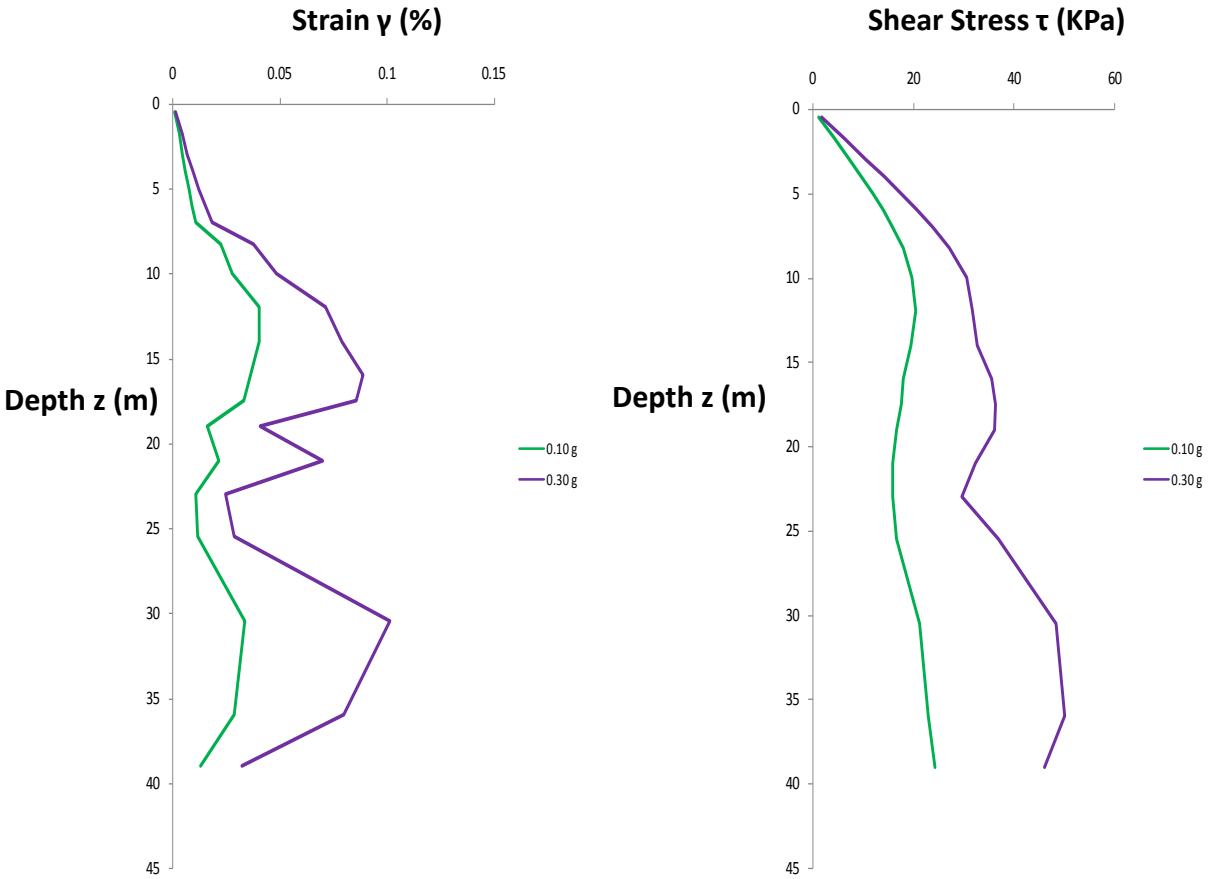

Figure 2.51 Distribution of peak shear stress and strain with depth for AQP and 3AQP (Peak acceleration 0.10 g - 0.30 g respectively)

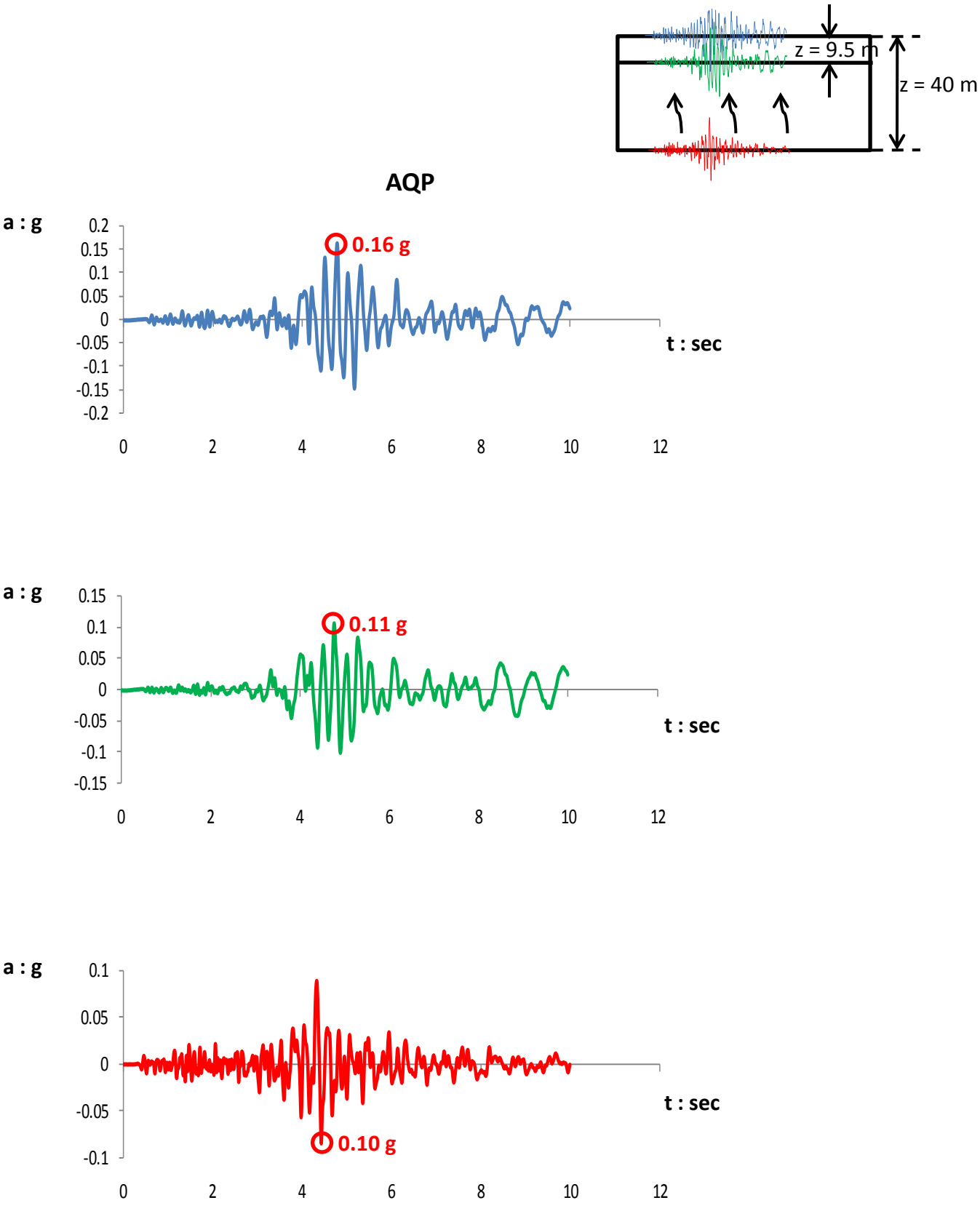

Figure 2.52 Accelerograms at depths 0 – 9.5 – 40 m from SHAKE for AQP – Calibration (New curves)

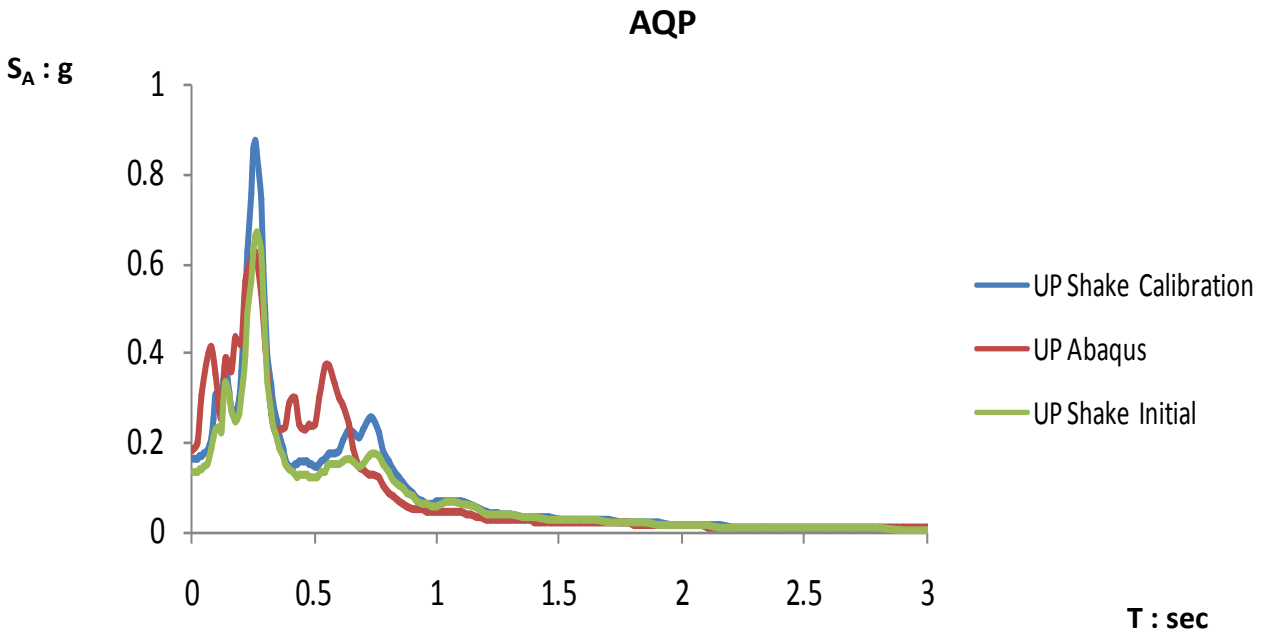

Figure 2.53 Comparison of Elastic Response Spectra (ξ = 5 %) Free Field UP between a non-linear method (Abaqus) and a linear elastic method (SHAKE)

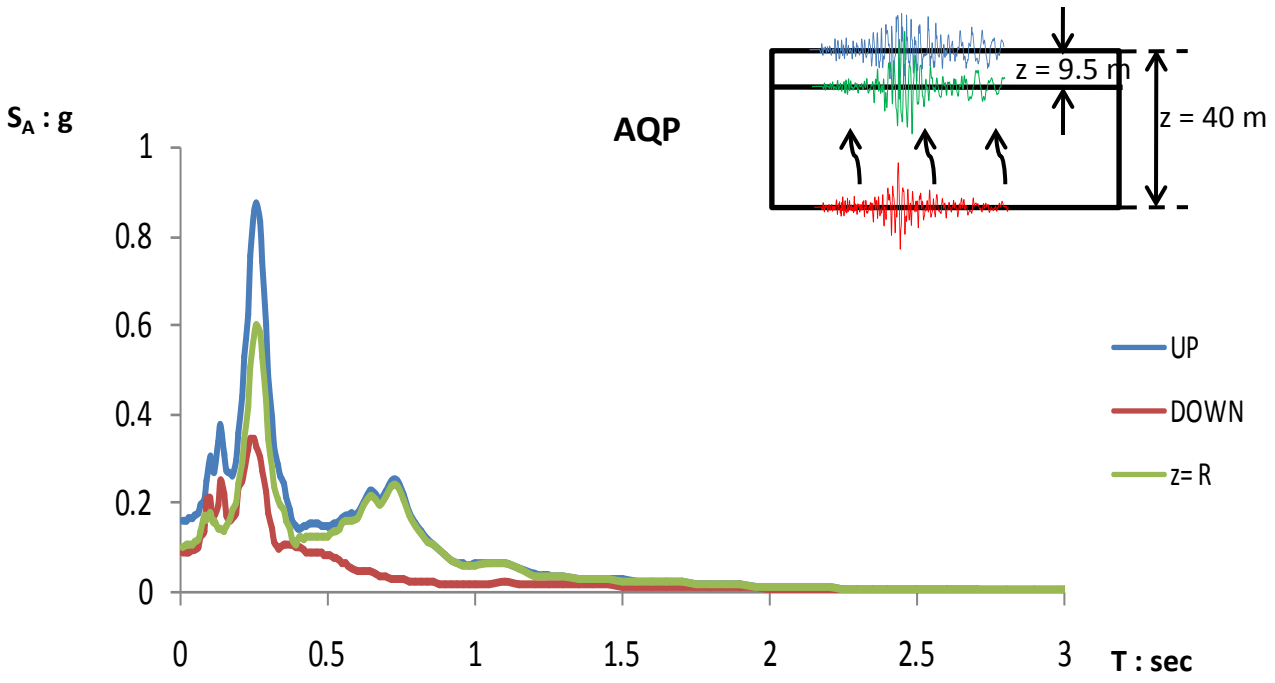

Figure 2.54 Elastic Response Spectra (ξ = 5 %) Free Field UP and DOWN for AQP – Calibration (Peak acceleration 0.10 g)

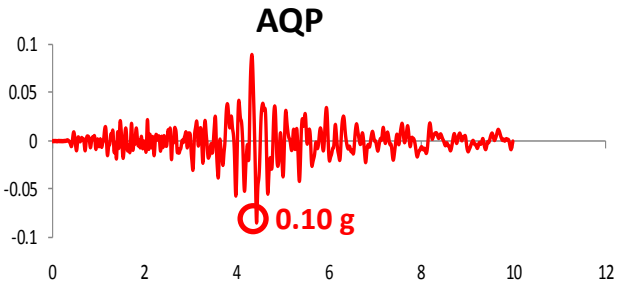

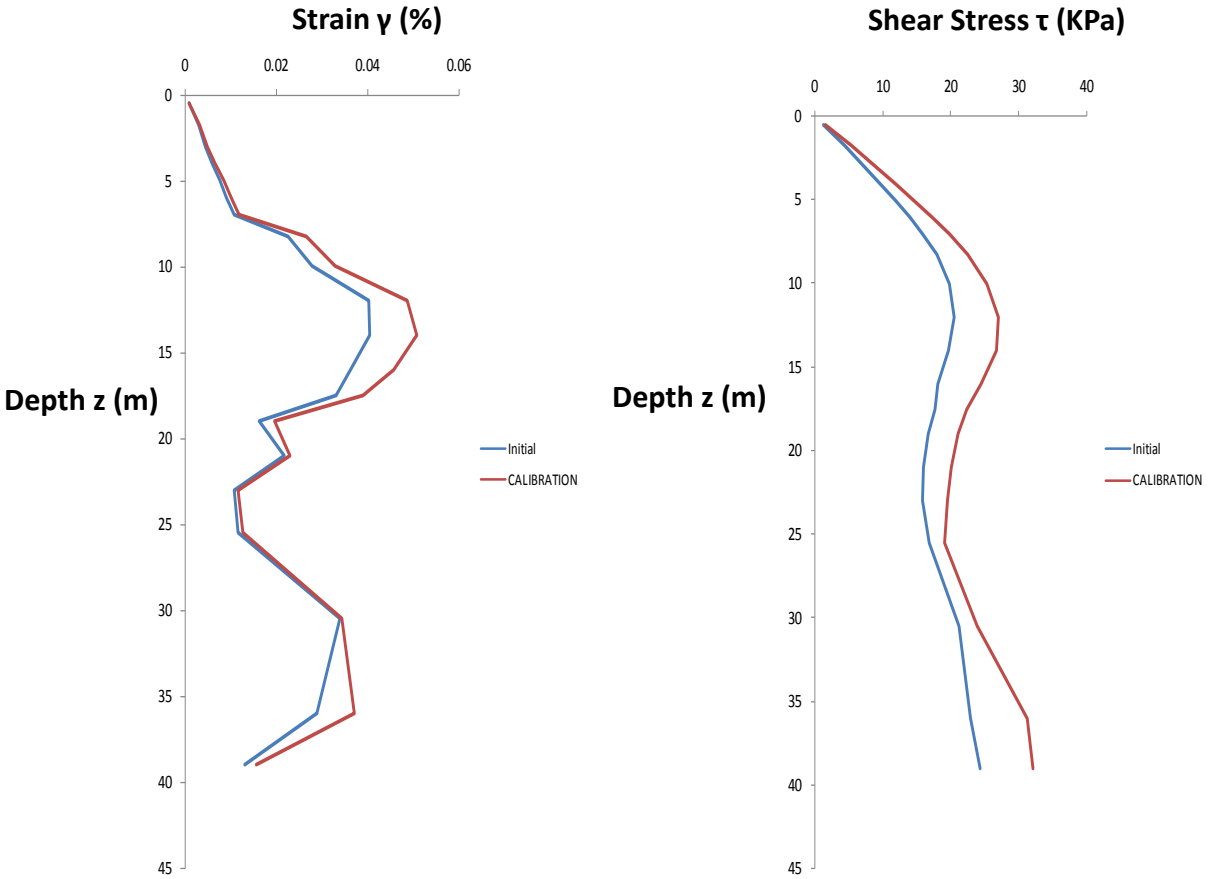

Figure 2.55 Comparsion of Distribution of peak shear stress and strain with depth for AQP (Peak acceleration 0.10) for different curves